6-2020

Cosyntropin as a Therapeutic Intervention following Traumatic Brain Injury

Lorraine C. Siebold

LOMA LINDA UNIVERSITY
School of Behavioral Health
in conjunction with the
Faculty of Graduate Studies

Cosyntropin as a Therapeutic Intervention following Traumatic Brain Injury

by

Lorraine C. Siebold

A Dissertation submitted in partial satisfaction of
the requirements for the degree
Doctor of Philosophy in Physiology

June 2020

Each person whose signature appears below certifies that this dissertation in his/her opinion is adequate, in scope and quality, as a dissertation for the degree of Doctor of Philosophy.

_____, Chairperson

Christopher G. Wilson, Professor of Physiology

_____

Stephen Ashwal, Pediatric Neurologist

_____

Barbara Holshouser, Professor of Radiology

_____

Brenda Bartnik-Olson, Associate Professor of Radiology

_____

Johnny D. Figueroa, Assistant Professor of Physiology

ACKNOWLEDGEMENTS

Completing the PhD program and writing my dissertation was not only the result of the training I received during my graduate studies at Loma Linda University but is an extension of my years of previous growth, mentorship and support. This dissertation represents a moment of time in which I am given the opportunity and privilege to demonstrate my intellectual growth and express my deepest gratitude. I am humbled by the extent of encouragement and feedback I have received.

First, I would like to thank my parents for always encouraging my curiosity and allowing me to engage with my tenacious, project-based lifestyle. Thank you for inspiring me to be a life-long learner and defender of those in need. Mom, you were my first teacher and are my biggest cheerleader. Thank you for demonstrating commitment to a mission and for intentionally developing my talents. Dad, thank you for the many talks on leadership, philosophies of education and the process of learning. I am daily learning to embrace the process and not just the product.

To my dissertation writing motivation team, Jill Buller and Tiffany Siebold, thank you for helping me meet my deadlines and maintain motivation during the Coronavirus quarantine. Thank you for rewarding my little successes along the way.

To my amazing siblings and sibling-in-laws – Jill, Jesse, Jayson, Stephanie, Kristina, Keaton, and Fredy – thank you for pushing me towards excellence.

Thank you for holding me accountable, going on adventures when I needed a break and reminding me that there is more to life than books and pipettes.

To my Grandpa Finkbeiner, thank you for fostering an environment of learning and encouraging me to be intentional, even in the small tasks. Thank you for giving me a tremendous amount of autonomy and showing me that no single individual is the sole keeper of good ideas. We were a team, always striving for something better. Even at 13-years-old, I could bring something to the table and felt as though I contributed.

To my committed and supportive network and my "Team Science" avengers, John Tan, Perla Ontiveros Angel and Jonathan Abdala. Thank you for all your emotional, psychological, spiritual and technical help. You made this journey one of thriving and not just surviving. You held on to hope when I doubted and you cheered me on as I pushed forward in the midst of uncertainty.

To my committee members, I remember the day that I joined the team with great awe and appreciation. You were an answer to a prayer I didn't know how to verbalize in a time of great uncertainty. Dr. Ashwal, you always pointed me to clinical relevance and lead with humble confidence. Thank you for providing clear, frank and timely feedback that always elevated my writing and thinking. Dr. Bartnik-Olson, thank you for taking me under your wing and answering my many technical questions. Your authentic enthusiasm and passion for research in the midst of the difficulties is inspiring. Dr. Holshouser, thank you for taking the time to brainstorm ideas and plan for the future. You are an

amazing example of a life-long learner and always pushed me to have clearer thinking and broader objectives. Dr. Figueroa, I remember sitting in your Neurobiology of Stress class and thinking: “This is why I came to grad school!”. I was so excited. You pushed me to be clear, concise and professional. I took notes not only on your content but also your teaching style. Your commitment to high-quality science and the development of your students is cherished and admired. Dr. Wilson, I could write a thesis on my acknowledgments for you alone. In two years, we went through a lot. Thank you for providing an environment for me to grow, experiment and lead. Thank you for allowing me to extend past the expected and for the many hours of discussion on the multi-faceted role of a scientist. Thank you.

To all those who allowed me the opportunity to mentor them, thank you. Specifically, Sam Vander Dussen and Camille Krueger. I demanded much and you rose to the occasion. Thank you for exceeding my expectations, providing feedback on how to be a better mentor, and being patient with me as I learned along with you.

I will end my acknowledgements with two words of encouragement that I received when I was hesitant in my conclusions during a manuscript revision:

“Be brave” - *Brenda Bartnik-Olson*

To all those who stood by my side in times of uncertainty, hardship, and triumph, thank you for helping me “be brave”.

CONTENT

FIGURES

Chapter 4

TABLES

Tables Page

Chapter 1

Chapter 4

Chapter 5

ABBREVIATIONS

α-MSH	Alpha-melanocyte stimulating hormone
ACTH	Adrenocorticotropic hormone
AHRQ	Agency for Healthcare Research and Quality
BBB	Blood brain barrier
CCI	Controlled cortical impact
CCL2	C-C Chemokine Ligand 2
CCR2	C-C Motif Chemokine Receptor 2
CDC	Center for Disease Control
CNS	Central nervous system
CoSyn	Long-acting cosyntropin
CRF	Corticotrophin-releasing hormone
CSF	Cerebral spinal fluid
DAMPs	Damage-associated molecular patterns
DoD	Department of Defense
DPI	Day post injury
ELISA	Enzyme-linked immunosorbent assay
GC	Glucocorticoid
GCS	Glasgow Coma Scale
GFAP	Glial fibrillary acidic protein
GM-CSF	Granulocyte-monocyte colony stimulating factor

Iba1	Ionized calcium binding adaptor molecule 1
ICP	Intracranial pressure
IHC	Immunohistochemistry
IL1	Interleukin-1
IL1β	Interleukin-1-beta
IL4	Interleukin-4
IL10	Interleukin-10
MBP	Myelin basic protein
MC	Melanocortins
MC4R	Melanocortin receptor 4
MCP-1	Monocyte chemoattractant protein 1
MDC	Macrophage derived chemoattractant
MP	Methylprednisone
MPO	Myeloperoxidase
MR	Magnetic resonance
MWM	Morris water maze
NF-H	Neurofilament heavy chain protein
NOR	Novel object recognition
NSE	Neuron-specific enolase
OF	Open field
PBS	Phosphate buffered saline
PET	Positron emission tomography

PFA	Paraformaldehyde
RFP	Red-fluorescent protein
ROI	Region of interest
TBI	Traumatic Brain Injury
TNFα	Tumor necrosis factor alpha
TSPO	Translocator protein 18 kDa
UCHL1	Ubiquitin c-terminal hydrolase L1
VA	Department of Veterans Affairs
WHO	World Health Organization

ABSTRACT OF THE DISSERTATION

Cosyntropin as a Therapeutic Intervention following Traumatic Brain Injury

by

Lorraine C. Siebold

Doctor of Philosophy, Graduate Program in Physiology
Dr. Christopher G. Wilson, Major Professor

Traumatic brain injury (TBI) is a major health concern in the United States. With over two million occurrences and approximately 50,000 deaths annually, TBI is a leading cause of death in young adults and is associated with cognitive deficits influenced by acute and persistent neuroinflammation. Melanocortins, such as adrenocorticotropic hormone (ACTH), are agonists for melanocortin receptors located in the adrenal glands and peripheral immune cells as well as throughout the central nervous system. Melanocortins ameliorate inflammation and provide a novel therapeutic approach for TBI. The focus of this dissertation was to describe and quantify effects of cosyntropin, a synthetic ACTH analog and melanocortin receptor agonist, on the early inflammatory response and functional outcome in a murine TBI model. We used the controlled-cortical impact model of TBI to induce injury followed by subcutaneous saline or cosyntropin administration. We investigated the effect of cosyntropin on the early inflammatory response through quantification of cytokine expression in contused cortical and hippocampal tissue following injury. Immune cell response was evaluated through immunohistochemical staining and quantification of

microglia/macrophage and neutrophil density as well as microglia/macrophage response through morphological feature quantification. Additionally, we assessed and compared the behavioral outcomes through open field, novel object recognition, and Morris water maze (MWM) testing. Cosyntropin reduced the inflammatory response by attenuation of injury-induced increases in IL-1ß, IL-6, and MIP-1□ and increased MCP-1 and IL-12 expression in injured cortical tissue. Furthermore, cosyntropin administration reduced accumulation of microglia/macrophages and neutrophils in perilesional cortex and hippocampal regions. Additionally, cosyntropin administration attenuated injury-induced microglia/macrophage morphological changes, suggesting that cosyntropin reduced the activation state of microglia/macrophages. Cosyntropin administration also decreased latency to find the hidden platform during the training period of the MWM compared to saline-treated mice, suggesting improved spatial memory. Reduced immune cell response in conjunction with improved spatial learning in our cosyntropin-treated TBI mice suggests a beneficial anti-inflammatory effect of cosyntropin following TBI. A better understanding of the mechanisms driving the anti-inflammatory and immune modulatory effect of melanocortins in the central nervous system could lead to novel therapeutics providing treatment options for millions suffering from the consequences of TBI and other CNS disorders.

CHAPTER ONE

MELANOCORTINS AS MODULATORS OF INFLAMMATION AND FUNCTIONAL OUTCOME FOLLOWING TRAUMATIC BRAIN INJURY

Lawrence D. Longo, MD Center for Perinatal Biology
Department of Basic Sciences
Division of Physiology
Loma Linda University School of Medicine
Loma Linda, California 92350

Adapted from Siebold, L. et al., Criteria to Define Mild, Moderate, and Severe Traumatic Brain Injury in the Mouse Controlled Cortical Impact Model. Experimental Neurology 310 (December 2018): 48–57.

Introduction

Traumatic brain injury (TBI) is a major health concern in the United States resulting in a substantial number of hospitalizations and a broad spectrum of symptoms and disabilities. TBI is not only a personal tragedy due to chronic motor, cognitive, and emotional deficits but also results in a familial and economic burden. With over two million occurrences and approximately 50,000 deaths annually, TBI is the leading cause of death in young adults (< 45 years of age) and is associated with $76.5 billion in direct and indirect medical costs[1–3]. Of importance, TBI can result in lifelong complications and at present the therapeutic options limited in scope and effectiveness. Heightened public awareness of the devastating impact of TBI along with advances in neuroimaging and other diagnostic tools has led to an increase in studies investigating the mechanisms underlying these deleterious effects with the goal of developing effective therapeutic options.

Traumatic Brain Injury in the Clinical Setting

In the clinical setting, TBI is classified into mild, moderate, and severe injury using clinical practice guidelines. A number of guides have been developed including, Department of Veterans Affairs and the Department of Defense (VA/DoD), Center for Disease Control (CDC), Agency for Healthcare Research and Quality (AHRQ) and World Health Organization (WHO)[4–6]. All aforementioned clinical practice guidelines incorporate structural imaging, duration of loss of consciousness and post-traumatic amnesia, and the Glasgow

Coma Scale (GCS) in their criteria for classifying injury severity. The GCS is a 15-point behavioral observation scale that defines severity based on eye, verbal, and motor response [7]. Individuals with a score of 3 – 8 are classified as severe, 9 – 12 as moderate, and those between 13 and 15 as mild TBI. Mild TBIs are defined as momentary changes in consciousness as a result of an external force to the skull and contribute to over 70% of reported brain injuries and include concussions[8]. Most individuals experience complete symptom resolution within three months after mild TBI despite evidence for chronic pathological changes in brain tissue[8]. In contrast to mild, severe TBI is associated with sustained loss of consciousness (> 24 h) and a 24% mortality rate with 43% of surviving patients exhibiting chronic physical and emotional disabilities[9,10]. Along with neurological symptoms and structural imaging, there is ongoing research evaluating the prognostic and diagnostic potential of blood and cerebrospinal fluid biomarkers[11]. In 2018 the FDA approved a blood test detecting glial fibrillary acidic protein (GFAP) and ubiquitin c-terminal hydrolase L1 (UCHL1) in patients with head injuries as an indicator of potential intracranial lesions and the necessity of neuroimaging[12]. S100- beta[13], neuron-specific enolase (NSE)[14,15], myelin basic protein (MBP)[16], tau[17], H-FABP[18] and neurofilament heavy chain protein (NF-H)[19] continue to be potential candidates in the evaluation of acute injury severity and progression.

Treatment of Traumatic Brain Injury

Present clinical interventions, including drug, device-based or surgical options, are limited—particularly for long-term consequences. While limited, clinical interventions are available in response to the primary insult and several clinical trials are underway to evaluate potential therapeutic interventions. Immediately following the primary insult, brain edema results in increased intracranial pressure (ICP). Increased ICP is associated with poor outcome in clinical cases of severe TBI and is the main cause of preventable death[20,21]. ICP is often a required monitoring measure in the management of severe TBI and, when elevated and deemed pathological, treatment options include ventricular drainage, neuromuscular blockade, mild hyperventilation, hyperosmolar/hypertonic therapy and decompressive craniectomy [22]. The largest TBI clinical trial conducted to date evaluated high-dose methylprednisone[24]. Results from this study indicate that high-dose methylprednisolone increases mortality following significant head injury and therefore suggests that synthetic glucocorticoids should not be used for the treatment of TBI[25]. While the mechanism underlying the increased mortality is unknown, current explanations include the use of high dosage and uncontrolled hyperglycemia[26].

Along with treatments to address complications arising from the primary injury, drug intervention clinical trials have been conducted for the treatment of secondary sequelae resulting from trauma. These include optic neuropathy,

cognitive dysfunction and dementia, psychiatric disorders, post-traumatic vascular headaches, muscular spasticity, epilepsy and other nervous system disorders with varying degrees of effectiveness (Table 1, clinicaltrials.gov). Interestingly, in the past decade, there has been a reduction in the percentage and number of drug intervention studies initiated for the treatment of TBI and post-traumatic symptoms (Figure 1). No studies in this selection of clinical trials reported evaluation of inflammation as a primary or secondary outcome through quantification of cytokines/chemokines following injury. However, involved in inflammation and oxidative stress, one study did evaluate the effect of a Probenecid/N-acetylcysteine combination study on pediatric TBI and showed a treatment-induced alteration in the metabolomic signature [27]. Following injury, treatment increased glutathione levels and biochemical pathways involved in glutathione processing[27]. However, this study was only in Phase 1 and therefore did not have sufficient power to evaluate morbidity or mortality or evaluate association between metabolomic signature and outcomes. Outside the selected clinical trials, a phase II study evaluating the treatment effect of Anakinra, a recombinant human interleukin-1 receptor antagonist, published work showing treatment-induced alterations in cytokine signature[28,29]. Principal component analysis (PCA) of cytokines and chemokines showed a bias towards the M1 microglial phenotype following Anakinra exposure, as evidenced by increased interleukin-1 (IL1) and granulocyte-monocyte colony stimulating factor (GM-CSF) and a reduction in interleukin-4 (IL4), interleukin-10 (IL10) and

Table 1. Examples of clinical trial drug interventions for TBI-induced conditions

Drug Intervention	Possible Mechanism / Drug Class
Memory Deficits	
Memantine	Low affinity uncompetitive NMDA receptor antagonist
Methylphenidate	Blocking reuptake of norepinephrine and dopamine into presynaptic neurons
Huperzine, Rivastigmine	Reversible inhibitor of acetylcholinesterase
Prognenolone	Precursor to neurosteroids, modulation of NMDA receptors [30]
Optic Neuropathy	
Recombinant human EPO	Stimulates erythrocyte production [31]
Cerebral Edema	
Diphenhydramine	Competes with histamine for cell receptor sites, anticholinergic effects
Post-traumatic Headaches	
OnabotulimuntoxinA	Inhibits acetylcholine release
Amitriptyline	Inhibits membrane pump mechanism for uptake of norepinephrine and serotonin
Sumatriptan	Selective agonist for vascular 5-hydroxytryptamine1 receptor
Muscle Spasms	
Botulinum toxin Type A	Inhibits release of acetylcholine
Epilepsy	
Allopregnanolone	Modulation of $GABA_A$ receptor
Lacosamide	Modulation of voltage-gated sodium channels
Psychiatric Disorders	
Nuedexta	Sigma-1 receptor agonist and uncompetitive antagonist for NDMA receptors
Escitalopram	Serotonin-selective reuptake inhibitor

Unless otherwise indicated, proposed mechanisms of action are based on U.S. Food and Drug Administration documentation

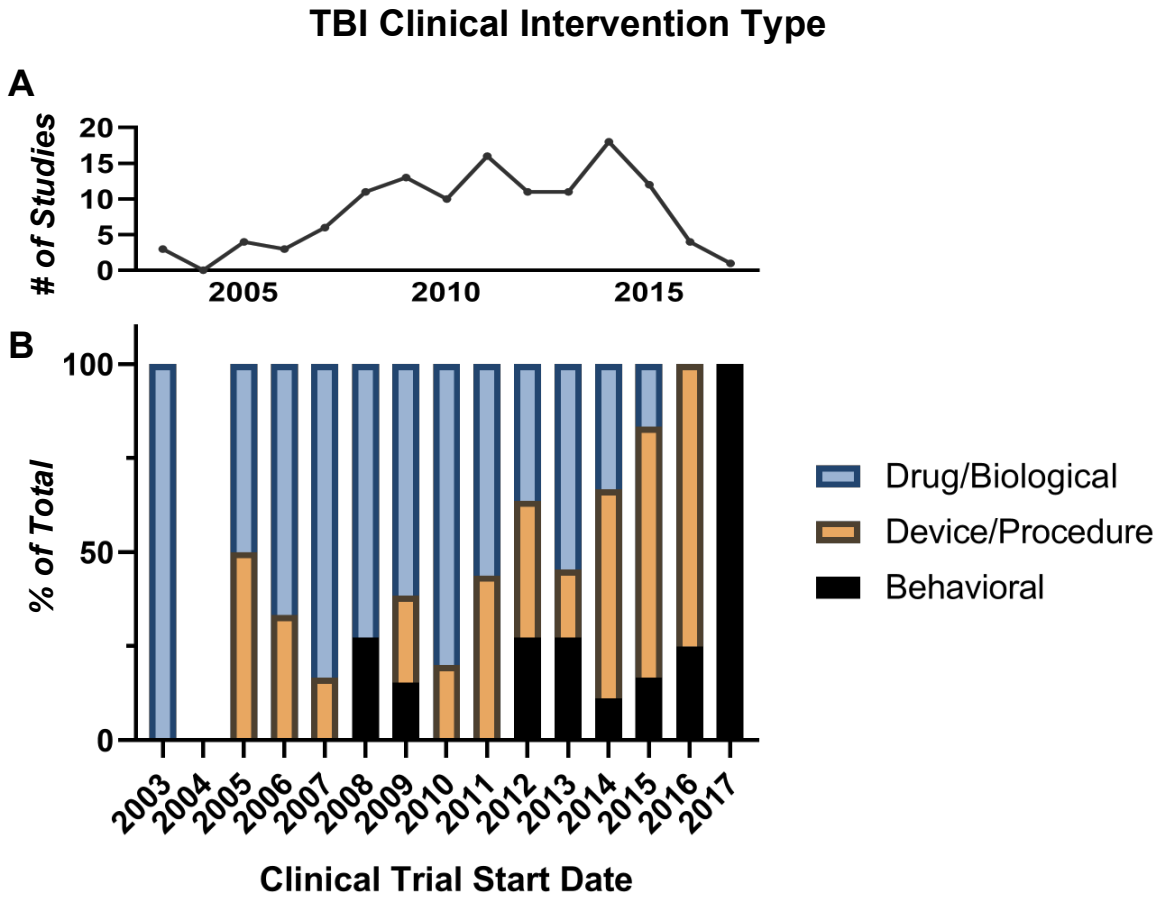

Figure 1. Interventional TBI clinical trials according to NIH clinical trial database. A) Total number of interventional TBI studies started and reported. B) Percent of total studies classified as behavior, device or drug based intervention. Clinical trial selection parameters: Clinical trials were selected on 05/04/2020 and were filtered according to TBI interventional studies that had documented results, had a recruiting, enrolling, suspended, terminated or completed status and was in any phase of their study. Dates indicate the year in which the clinical trial was started and values are reported as percent of total number of trials started that year.

macrophage derived chemoattractant (MDC)[28]. Similar to the metabolomics study, the IL1R-antagonist studies did not correlate CSF data to functional outcomes. Current limitations in clinical treatment and lack of quantification of inflammatory status in clinical trials emphasize the need for novel pharmaceutical approaches and expanded clinical outcome measurements.

Neuroinflammation following Traumatic Brain Injury

TBI results from an initial insult to the brain referred to as the primary injury. The primary injury can be produced by a penetrating, blast injury or an impact of the brain against the skull as a result of falls and motor vehicle collisions. The heterogeneous primary injury is then followed by a complex secondary response. This includes changes in cell proliferation and differentiation[32–34], neuronal cell death[35,36], mitochondrial dysfunction[37,38], multifaceted immune responses[39–41], glutamate-induced excitotoxicity[42–45], and cerebrovascular dysfunction and repair[46–48]. The secondary injury response is initiated seconds after the primary insult and can last for decades after the insult. Several studies show persistent neuroinflammation following TBI, lasting as long as 17 years after injury[49–51]. However, it is not clear which components of the inflammatory response are indicators of repair and which continue to drive pathology and brain vulnerability[51]. Clinically, neuroinflammation following TBI is associated with increased intracranial pressure, increased mortality, poor functional outcomes[52], reduced processing speed[49], and increased risk of epilepsy and neurodegenerative disorders[51,53,54]. These findings illustrate the imperative

need for a more thorough understanding of the multifaceted endogenous neuroinflammatory response to TBI and the therapeutic mechanisms of immunomodulatory compounds.

TBI is associated with a rapid and robust neuroinflammatory response followed by chronic microglia activation and inflammation[49,50]. Under physiologically normal conditions, the brain parenchyma is isolated from the periphery by the blood brain barrier (BBB). However, this immune privilege is severely undermined following TBI resulting in a robust local and peripheral immune response within the injured CNS. As the tissue-resident macrophage, microglia are key players in the inflammatory process following brain injury resulting in regenerative, phagocytic, and pro-/anti-inflammatory phenotypes corresponding to two polarization states, M1 and M2[55]. The M1/M2 classification provides a simplified framework to assess the spectrum of phenotypes contributing to degenerative and regenerative processes[56]. As demonstrated by several recent microglia depletion studies, microglia are neuroprotective following brain injury[57–60]. Microglia depleted at 4 weeks post-injury and allowed to re-populate resulted in improved cognitive functioning and increased neuronal density in the dentate gyrus[58]. Interestingly, acutely depleted microglia impaired learning ability[59]. Furthermore, microglia can also exaggerate the inflammatory response through TLR4 activation and NFκB signaling[61,62]. The aforementioned studies suggest a multifaceted microglia response emphasizing the need for identification of not only the presence of microglia but the dynamic,

time-dependent microglia changes in phenotypes following injury. When classifying microglia in preclinical TBI studies, phenotype is often designated by quantifying overall activation (CD68) or distinguishing between M1 (CD86) and M2 (Arg-1, CD206) phenotypes through the use of specific cellular markers[63]. MG also exhibit dramatic and rapid morphological changes following brain injury[64]. Along with tissue resident-macrophages, peripheral monocyte and neutrophil invasion into the brain parenchyma also occur[63]. Peripheral monocyte and neutrophil infiltration is associated with increased edema, exaggerated inflammatory responses, and poorer functional outcomes[65]. Enhancement of the beneficial response of tissue-resident MG through enhancement of the M2 phenotype with concurrent reduction in infiltrating neutrophils may be neuroprotective following TBI.

Melanocortins as Modulators of Central Nervous System Functioning

Melanocortins (MCs) are a family of peptides endogenously derived from pro-opiomelanocortin precursors [66]. MCs include compounds such as adrenocorticotropic hormone (ACTH) and alpha-melanocyte stimulating hormone (α-MSH), both of which are agonists for melanocortin receptors [66,67]. There are five MC receptor subtypes with tissue-specific expression, including melanocytes (MC1R), peripheral immune cells (MC1,3,5R), endothelial cells (MC1R), the adrenal cortex (MC2R) and the central nervous system (MC3-4R). In the CNS, MC receptor distribution is ubiquitous, showing expression in cortex, hippocampus, arcuate nucleus of the hypothalamus, limbic system and

thalamus[68]. The Human Protein Atlas has documented MC4R expression throughout the human CNS, including cerebral cortex, thalamus, hypothalamus, amygdala and hippocampus (www.proteinatlas.org)[69]. Furthermore, MC receptors are expressed in neural and glial cells, contributing to their multifaceted functions (Table 2)[68,70,71]. Of particular interest, MCs have been shown to have glucocorticoid-independent immune modulatory and neuroprotective effects following brain insult[72–74]. Independent of MC2R activation which results in glucocorticoid production, MC1, MC3 and MC4 receptor signaling have all demonstrated neuroprotective effects following brain insult[70,72,75,76]. In these studies, MC1R, MC3R, and MC4R-agonist treatment all reduced inflammation, brain contusion and cell death and resulted in overall improvements in behavioral outcomes[75–77]. Furthermore, MC1R and MC3R-agonists reduce peripheral immune cell invasion[75]. While the mechanisms are still unclear and are subtype- and injury-dependent, *in vitro* studies show that MC4R agonists reduce NFκB translocation and therefore downstream pro-inflammatory cascades, promote an M2 MG phenotype via inhibition of TLR2 and TLR4-induced MG activation, and protect oligodendrocytes from inflammation-related damage[78]. MC1/3R agonists also regulate the neuroinflammatory response by reducing expression of adhesion molecules and chemoattractants resulting in subsequent reduction in peripheral immune cell infiltration[75,79,80]. Along with the ability to stimulate the GC-independent anti-inflammatory responses of MC1R, MC3R, and MC4R signaling, ACTH is the

Table 2. Brain effects and potential benefits of melanocortin signaling following traumatic brain injury

Modulation	*Model*	*Summary of Results*	
Synaptic Plasticity			
MC4R knockdown, HS024, [D-tyr^4]-MTII	Alzheimer's model with APP/PS1 mice	Rescues long-term potentiation impairment	81
a-MSH	IL1β-induced neuroinflammation	Modulates AMPAR function through stimulation of surface GluA1 trafficking	82
shMC4R, [D-tyr^4]-MTII	Cultured hippocampal neurons	Maturity of dendritic spines and functional synapses, enhancement of LTP	83
MC4R knockdown[1], HS024, [D-tyr^4]-MTII	Alzheimer's model with APP/PS1 mice	Regulation of dendritic spine morphology	81
Stretching and Grooming Behavior			
ACTH, MSH	Intracisternal injection in dogs	Excessive stretching and yawning	84
ACTH	Intraventricular injections into rats	Excessive grooming	85
Cognition and Behavior			
α-MSH	IL1β-induced neuroinflammation	Recovered contextual fear learning	82
MC4R genetic manipulation	Drd1a-cre / MC4R-TB mice	Required for procedural learning in D1R neurons	86
NDP-MSH, HSO24	Traumatic Brain Injury, Weight-drop	Reduced escape latency in MWM	77

MC4R genetic manipulation, MTII	MC4R mutation	Reduced ambulatory activity and grooming, MTII increased grooming	[87]
R027-3225, NDP-α-MSH, HS024	Cerebral Ischemia	Reduced escape latency in MWM	[88]
Inflammation			
α-MSH (11-13)	Traumatic Brain Injury, CCI	No change in TNFα or IL1β at 24 hpi	[76]
NDP-MSH, HSO24	Traumatic Brain Injury, Weight-drop	Decreased TNFα, IL6, HMGB1 and increased IL10	[77]
α-MSH	LPS-induced neuroinflammation	Inhibits NF-kB activation	[89]
ACTH (1-39)	Glutamate-mediated toxicity, In vitro neurons	Reduced cell death, reduced apoptosis	[71]
ACTH	Clinical, Pediatric opsoclonus–myoclonus, CSF	Reduces CCR4-agonist CCL22	[90]
NDP-MSH, HSO24	Common carotid artery occlusion	Decreased TNFα and IL6 at 2 hpi	[91]
α-MSH, HSO24	LPS/INFɣ exposure in astrocyte cultures	Reduced iNOS and COX-2 at 24 hrs	[92]
R027-3225, NDP-α-MSH, HS024	Cerebral Ischemia	Decreased TNFα	[88]
α-MSH, ACTH (1–24)	N9 microglial culture	Decreased TNFα, IL6 and nitric oxide	[93]

Microglial Response

α-MSH (11-13)	Traumatic Brain Injury, CCI	Microglia showed less activated morphology	76
Synthetic α-MSH, [Nle^4, D-Phe^7]-α-MSH	Primary microglia cultures	Increased expression of Arg1 and reduced TLR4 and IL-4rα, decreased Pam_3CSK_4-induced phagocytosis	78
RO27-3225, HS024	Intracerebral hemorrhage	Decreased Iba1-Positive cells and	70

Glucocorticoids

Methylprednisolone	Clinical	Reduces vasogenic edema and swelling secondary to damage	94
Sphingosine 1-phosphate	Traumatic Brain Injury, CCI	Reduces circulating and infiltrating T-cells	95
CORT, Adrenolectomy	Traumatic Brain Injury, FPI	Decreased BDNF	96
CORT, Adrenolectomy	Traumatic Brain Injury, FPI	Increased NGF	97

Neuroprotection

α-MSH (11-13)	Traumatic Brain Injury, CCI	Reduced activated caspase-3-positive neurons and brain contusion volume	76
NDP-MSH, HSO24	Traumatic Brain Injury, Weight-drop	Increased viable neurons and decreased axonal damage	77
R027-3225, NDP-α-MSH, HS024	Cerebral Ischemia	Decreased caspase-3	88

Neurogenesis

R027-3225, NDP-α-MSH, HS024	Cerebral Ischemia	Upregulation of Wnt-3a/β-catenin and Shh signaling pathways	[88]
NDP-MSH, HS024	Cerebral Ischemia	Increases mature neurons in DG	[91]
MC4R knockdown, HS024, [D-tyr^4]-MTII	Alzheimers model with APP/PS1 mice	Increased neurogenesis, prevented cognitive decline	[81]

Peripheral Immune Cells

Mc3r Knockdown	Mc3r$^{-/-}$ mice	Reduced leukocyte adhesion and emigration	[98]
RO27-3225, HS024	Intracerebral hemorrhage	Decreased neutrophil infiltration	[70]

only endogenous MC that can activate MC2R in the adrenal cortex, stimulating glucocorticoid (GC) production. ACTH has been shown to be superior to GC in the treatment of multiple sclerosis and infantile spasms with hypsarrhythmia suggesting that stimulation of endogenously produced GCs do not fully explain the immune modulatory effect of ACTH [99]. Furthermore, a head-to-head comparison of clinical dosages of ACTH and methylprednisolone indicates that the cortisol exposure from ACTH is significantly lower than methylprednisolone (MP)[100]. According to the Lal et al. study, 80U of an ACTH analog equates to 30 mg of IVMP while 1g of IVMP is required for effective treatment. This suggests that cortisol levels alone do not explain the mechanism of action for ACTH and adds to the evidence supporting a glucocorticoid-independent effect. Dual activation of GC-dependent and independent responses through a synthetic ACTH analog may result in a more controlled and thorough resolution of the complex inflammatory response following TBI.

Long-Acting Cosyntropin for the Treatment of Traumatic Brain Injury

Current acute management following TBI includes intracranial pressure monitoring, hypertonic saline, surgical intervention and seizure monitoring[101]. While chronic inflammation is well documented in TBI patients[49–51], limited pharmaceutical interventions directly target the inflammatory response. Synthetic ACTH analogs could be such a compound and is an attractive pharmaceutical for its multifaceted immuno-modulatory capacity. The most common indications for the use ACTH include adrenocortical testing and the

treatment of multiple sclerosis and infantile spasms[102]. Cosyntropin, also referred to as *tetracosactide*, is a synthetic ACTH analog composed of the first 24 amino acids of the full-length ACTH. ACTH was originally FDA approved in 1952 and, currently, two forms of ACTH have *Food and Drug Administration* approval for use in diagnostic testing of adrenal functioning including cosyntropin and H.P. Acthar Gel Repository Injection (Questcor Pharmaceuticals), the 39 amino acid natural form of the peptide[102]. Both the natural and synthetic variants stimulate all subtypes of the melanocortin receptors resulting in stimulation of the adrenal cortex to secrete glucocorticoids[72]. Due to a half-life of approximately 20 minutes in humans, several compounds have been developed to increase length of activity for the natural or synthetic variants of ACTH through the use of gels or zinc suspensions[103]. One such compound, Long-acting Cosyntropin (CoSyn), a 24 amino acid ACTH analog (ACTH 1–24) [104], was developed by West Therapeutics with the use of a zinc suspension to extend activity. The most effective dosage and length of treatment for the synthetic and natural variants of ACTH remains uncertain. Evaluation of previous literature on the use of ACTH in experimental rodent studies shows regimens of multiple-day administration varying between 0.4 – 0.6 mg/kg/day (Table 3).

There is limited research investigating neuroprotective effects of melanocortin signaling following TBI and no research has been conducted investigating CoSyn as a post-TBI therapeutic. To address this gap in research, this study aimed to evaluate the effect of CoSyn administration following an

experimental model of TBI. Functional outcomes included behavioral assessment of anxiety-like behavior, spontaneous locomotor activity and cognitive performance. Along with behavioral outcomes, inflammatory response was evaluated through the quantification of microglia/macrophage density, neutrophil infiltration and cytokine expression in perilesional and hippocampal regions. Additionally, this study includes an analysis of current methods for evaluation of cell counting and morphological quantification. Both cell counts and morphology are tools for evaluating inflammatory response following injury and treatment. Our findings support the continued investigation of CoSyn and the other melanocortin receptors agonists for the treatment of acquired brain injuries. Furthermore, melanocortin receptor agonists may have therapeutic potential not only in treatment of traumatic brain injury but may extend to other CNS disorders including Alzheimer's disease and chronic traumatic encephalopathy.

Table 3. Mouse studies with ACTH analog administration

Drug	*Dosage mg/kg*	*Mode/Frequency*	*Purpose*	
ACTH	1.1	Subcutaneous, once daily, 14 days	Depression-like symptoms.	[105]
Cortrosyn	0.450	Subcutaneous, once daily, 14 days	Animal model of depression	[106]
ACTH	0.450	Subcutaneous,15 days	Animal model of depression	[107]
ACTH	0.450	Subcutaneous,14 days	Chronic activation of the HPA axis caused anxiogenic responses in mice.	[108]
Acthar Gel	1.200	Subcutaneous, every other day, 12 or 21 days	Treatment of EAE.	[109]
ACTH, 1-24	0.002	Intraperitoneal, 3/week, 3-weeks	Regulation of plasma cytokines and IgE	[110]
ACTH	0.096	Subcutaneous, 2 weeks	ACTH-induced hypertension	[111]
Synacthen	0.1	Osmotic pump, 14 days	Steroid assessment	[112]
Synacthen	1.100	Subcutaneous, 10 days	Adrenal morphology and glucocorticoid production	[113]
Synacthen	0.104	Subcutaneous, 4 days	Effect on sodium appetite	[114]
ACTH	0.450	Subcutaneous, 14 days	Animal model of depression	[115]
ACTH	0.450	Subcutaneous, 14 days	Animal model of depression	[116]
Acthar Gel	0.800	Subcutaneous, very other day, 18 weeks	Treatment for proteinuria, SLE	[117]
Acthar Gel	0.6-1.2	Subcutaneous, every other day	Treatment of ALS	[118]

Dosage Statistics: Mean = 0.57 mg/kg/day, Median = 0.45 mg/kg/day

References

1. Finkelstein, E., Corso, P. S. & Miller, T. R. The Incidence and Economic Burden of Injuries in the United States. (Oxford University Press, 2006).

2. Faul, M. & Coronado, V. Epidemiology of traumatic brain injury. Handb Clin Neurol 127, 3–13 (2015).

3. Patel, H. C. et al. Trends in head injury outcome from 1989 to 2003 and the effect of neurosurgical care: an observational study. 366, 7 (2005).

4. Report to Congress on Traumatic Brain Injury in the United States: Epidemiology and Rehabilitation. (2015).

5. Brasure, M. et al. in Multidisciplinary Postacute Rehabilitation for Moderate to Severe Traumatic Brain Injury in Adults (2012).

6. Holm, L., Cassidy, J. D., Carroll, L. J. & Borg, J. Summary of the WHO collaborating centre for neurotrauma task force on mild traumatic brain injury. J Rehabil Med 37, 137–141 (2005).

7. Gomez, D. et al. Inclusion of Highest Glasgow Coma Scale Motor Component Score in Mortality Risk Adjustment for Benchmarking of Trauma Center Performance. Journal of the American College of Surgeons 225, 755–762 (2017).

8. Cassidy, J. D. et al. Incidence, risk factors and prevention of mild traumatic brain injury: results of the who collaborating centre task force on mild traumatic brain injury. Journal of Rehabilitation Medicine 36, 28–60 (2004).

9. Steppacher, I., Kaps, M. & Kissler, J. Against the odds: a case study of recovery from coma after devastating prognosis. Ann Clin Transl Neurol 3, 61–65 (2016).

10. Selassie, A. W. et al. Incidence of Long-term Disability Following Traumatic Brain Injury Hospitalization, United States, 2003: Journal of Head Trauma Rehabilitation 23, 123–131 (2008).

11. Agoston, D. V., Shutes-David, A. & Peskind, E. R. Biofluid biomarkers of traumatic brain injury. Brain Injury 31, 1195–1203 (2017).

12. FDA authorizes marketing of first blood test to aid in the evaluation of concussion in adults. FDA News Release (2018).

13. Egea-Guerrero, J. J. et al. Accuracy of the S100beta protein as a marker of brain damage in traumatic brain injury. Brain Inj 26, 76–82 (2012).

14. Costine, B. A. et al. Neuron-specific enolase, but not S100B or myelin basic protein, increases in peripheral blood corresponding to lesion volume after cortical impact in piglets. J Neurotrauma 29, 2689–95 (2012).

15. Zurek, J. & Fedora, M. The usefulness of S100B, NSE, GFAP, NF-H, secretagogin and Hsp70 as a predictive biomarker of outcome in children with traumatic brain injury. Acta Neurochir (Wien) 154, 93–103; discussion 103 (2012).

16. Beers, S. R., Berger, R. P. & Adelson, P. D. Neurocognitive outcome and serum biomarkers in inflicted versus non-inflicted traumatic brain injury in young children. J Neurotrauma 24, 97–105 (2007).

17. Gabbita, S. P. et al. Cleaved-tau: a biomarker of neuronal damage after traumatic brain injury. J Neurotrauma 22, 83–94 (2005).

18. Lagerstedt, L. et al. H-FABP: A new biomarker to differentiate between CT-positive and CT-negative patients with mild traumatic brain injury. PLoS One 12, e0175572 (2017).

19. Gatson, J. W. et al. Detection of neurofilament-H in serum as a diagnostic tool to predict injury severity in patients who have suffered mild traumatic brain injury. J Neurosurg 121, 1232–8 (2014).

20. Coronado, V. G. et al. Trends in Traumatic Brain Injury in the U.S. and the public health response: 1995–2009. Journal of Safety Research 43, 299–307 (2012).

21. Thurman, D. J., Alverson, C., Dunn, K. A., Guerrero, J. & Sniezek, J. E. Traumatic Brain Injury in the United States: A Public Health Perspective: Journal of Head Trauma Rehabilitation 14, 602–615 (1999).

22. Juul, N. Intracranial hypertension and cerebral perfusion pressure: influence on neurological deterioration and outcome in severe head injury. J. Neurosurg. 92, 6 (2000).

23. Moon, J. W. & Hyun, D. K. Decompressive Craniectomy in Traumatic Brain Injury: A Review Article. Korean J Neurotrauma 13, 1 (2017).

24. Roberts, I, Yates, D & Sandercock, P. Effect of intravenous corticosteroids on death within 14 days in 10008 adults with clinically significant head injury (MRC CRASH trial): randomized placebo-controlled trial.

25. Edwards, P., Arango, M., Balica, L., Cottingham, R. & El-Sayed, H. Final results of MRC CRASH, a randomised placebo-controlled trial of intravenous corticosteroid in adults with head injury—outcomes at 6 months. The Lancet 365, 1957–1959 (2005).

26. Douglas, Ivor S. Possible explanations for the results of CRASH. The Lancet 365, (2005).

27. Hagos, F. T. et al. Exploratory Application of Neuropharmacometabolomics in Severe Childhood Traumatic Brain Injury*: Critical Care Medicine 46, 1471–1479 (2018).

28. Helmy, A. et al. Recombinant human interleukin-1 receptor antagonist promotes M1 microglia biased cytokines and chemokines following human traumatic brain injury. J Cereb Blood Flow Metab 36, 1434–1448 (2016).

29. Helmy, A. et al. Recombinant Human Interleukin-1 Receptor Antagonist in Severe Traumatic Brain Injury: A Phase II Randomized Control Trial. J Cereb Blood Flow Metab 34, 845–851 (2014).

30. Marx, C. E. et al. Proof-of-Concept Trial with the Neurosteroid Pregnenolone Targeting Cognitive and Negative Symptoms in Schizophrenia. Neuropsychopharmacol 34, 1885–1903 (2009).

31. Inoue, N., Takeuchi, M., Ohashi, H. & Suzuki, T. The production of recombinant human erythropoietin. in Biotechnology Annual Review vol. 1 297–313 (Elsevier, 1995).

32. Gao, X. & Chen, J. Moderate traumatic brain injury promotes neural precursor proliferation without increasing neurogenesis in the adult hippocampus. Experimental Neurology 239, 38–48 (2013).

33. Susarla, B. T., Villapol, S., Yi, J. H., Geller, H. M. & Symes, A. J. Temporal patterns of cortical proliferation of glial cell populations after traumatic brain injury in mice. ASN neuro 6, 159–70 (2014).

34. Bye, N. et al. Neurogenesis and glial proliferation are stimulated following diffuse traumatic brain injury in adult rats. J. Neurosci. Res. 89, 986–1000 (2011).

35. Clark, R. S. et al. Apoptosis-suppressor gene bcl-2 expression after traumatic brain injury in rats. J Neurosci 17, 9172–82 (1997).

36. Sabirzhanov, B. et al. miR-711 upregulation induces neuronal cell death after traumatic brain injury. Cell Death & Differentiation 23, 654–668 (2016).

37. Miller, D. M., Singh, I. N., Wang, J. A. & Hall, E. D. Nrf2-ARE activator carnosic acid decreases mitochondrial dysfunction, oxidative damage and neuronal cytoskeletal degradation following traumatic brain injury in mice. Experimental neurology 264, 103–10 (2015).

38. Wu, Q. et al. Mitochondrial division inhibitor 1 (Mdivi-1) offers neuroprotection through diminishing cell death and improving functional outcome in a mouse model of traumatic brain injury. Brain Res 1630, 134–43 (2016).

39. Scherbel, U. et al. Differential acute and chronic responses of tumor necrosis factor-deficient mice to experimental brain injury. Proc Natl Acad Sci U S A 96, 8721–6 (1999).

40. Laird, M. D. et al. High mobility group box protein-1 promotes cerebral edema after traumatic brain injury via activation of toll-like receptor 4. Glia 62, 26–38 (2014).

41. Weaver, L. C. et al. CD11d integrin blockade reduces the systemic inflammatory response syndrome after traumatic brain injury in rats. Exp Neurol 271, 409–22 (2015).

42. Amorini, A. M. et al. Severity of experimental traumatic brain injury modulates changes in concentrations of cerebral free amino acids. J. Cell. Mol. Med. 21, 530–542 (2017).

43. Katayama, Y., Becker, D. P., Tamura, T. & Hovda, D. A. Massive increases in extracellular potassium and the indiscriminate release of glutamate following concussive brain injury. J Neurosurg 73, 889–900 (1990).

44. Bullock, R. et al. Factors affecting excitatory amino acid release following severe human head injury. J Neurosurg 89, 507–18 (1998).

45. Hinzman, J. M., Thomas, T. C., Quintero, J. E., Gerhardt, G. A. & Lifshitz, J. Disruptions in the regulation of extracellular glutamate by neurons and glia in the rat striatum two days after diffuse brain injury. J Neurotrauma 29, 1197–208 (2012).

46. Jullienne, A. et al. Chronic cerebrovascular dysfunction after traumatic brain injury: Cerebrovascular Dysfunction After TBI. Journal of Neuroscience Research 94, 609–622 (2016).

47. Salehi, A. et al. Up-regulation of Wnt/β-catenin expression is accompanied with vascular repair after traumatic brain injury. J Cereb Blood Flow Metab 38, 274–289 (2018).

48. Obenaus, A. et al. Traumatic brain injury results in acute rarefication of the vascular network. Sci Rep 7, 239 (2017).

49. Ramlackhansingh, A. F. et al. Inflammation after trauma: Microglial activation and traumatic brain injury. Annals of Neurology 70, 374–383 (2011).

50. Johnson, V. E. et al. Inflammation and white matter degeneration persist for years after a single traumatic brain injury. Brain 136, 28–42 (2013).

51. Cherry, J. D. et al. Microglial neuroinflammation contributes to tau accumulation in chronic traumatic encephalopathy. Acta Neuropathologica Communications 4, (2016).

52. Lindolfo da Silva Meirelles, Daniel Simon & Andrea Regner. Neurotrauma: The Crosstalk between Neurotrophins and Inflammation in the Acutely Injured Brain. International Journal of Molecular Sciences 18, 1082 (2017).

53. Appleton, R. E. Post-traumatic epilepsy in children requiring inpatient rehabilitation following head injury. Journal of Neurology, Neurosurgery & Psychiatry 72, 669–672 (2002).

54. Faden, A. I. & Loane, D. J. Chronic Neurodegeneration After Traumatic Brain Injury: Alzheimer Disease, Chronic Traumatic Encephalopathy, or Persistent Neuroinflammation? Neurotherapeutics 12, 143–150 (2015).

55. Xu, H. et al. The Polarization States of Microglia in TBI: A New Paradigm for Pharmacological Intervention. Neural Plasticity 2017, 1–11 (2017).

56. Turtzo, L. et al. Macrophagic and microglial responses after focal traumatic brain injury in the female rat. Journal of Neuroinflammation 11, 82 (2014).

57. Jin, W.-N. et al. Depletion of microglia exacerbates postischemic inflammation and brain injury. Journal of Cerebral Blood Flow & Metabolism 37, 2224–2236 (2017).

58. Henry, R. J. et al. Microglial depletion with CSF1R inhibitor during chronic phase of experimental traumatic brain injury reduces neurodegeneration and neurological deficits. J. Neurosci. 2402–19 (2020) doi:10.1523/JNEUROSCI.2402-19.2020.

59. Hanlon, L. A., Raghupathi, R. & Huh, J. W. Depletion of microglia immediately following traumatic brain injury in the pediatric rat: Implications for cellular and behavioral pathology. Experimental Neurology 316, 39–51 (2019).

60. Wang, C. et al. Depletion of Microglia Attenuates Dendritic Spine Loss and Neuronal Apoptosis in the Acute Stage of Moderate Traumatic Brain Injury in Mice. Journal of Neurotrauma 37, 43–54 (2020).

61. Ahmad, A. et al. Absence of TLR4 reduces neurovascular unit and secondary inflammatory process after traumatic brain injury in mice. PLoS One 8, e57208 (2013).

62. Yao, X. et al. TLR4 signal ablation attenuated neurological deficits by regulating microglial M1/M2 phenotype after traumatic brain injury in mice. Journal of neuroimmunology 310, 38–45 (2017).

63. Jin, X., Ishii, H., Bai, Z., Itokazu, T. & Yamashita, T. Temporal Changes in Cell Marker Expression and Cellular Infiltration in a Controlled Cortical Impact Model in Adult Male C57BL/6 Mice. PLoS ONE 7, e41892 (2012).

64. Davalos, D. et al. ATP mediates rapid microglial response to local brain injury in vivo. Nature Neuroscience 8, 752–758 (2005).

65. Kenne, E., Erlandsson, A., Lindbom, L., Hillered, L. & Clausen, F. Neutrophil depletion reduces edema formation and tissue loss following traumatic brain injury in mice. Journal of Neuroinflammation 9, (2012).

66. Gallo-Payet, N. 60 YEARS OF POMC: Adrenal and extra-adrenal functions of ACTH. Journal of Molecular Endocrinology 56, T135–T156 (2016).

67. Bertolini, A., Tacchi, R. & Vergoni, A. Brain effects of melanocortins☆. Pharmacological Research 59, 13–47 (2009).

68. Kishi, T. et al. Expression of melanocortin 4 receptor mRNA in the central nervous system of the rat. The Journal of Comparative Neurology 457, 213–235 (2003).

69. Uhlen, M. et al. Tissue-based map of the human proteome. Science 347, 1260419–1260419 (2015).

70. Chen, S. et al. Activation of melanocortin receptor 4 with RO27-3225 attenuates neuroinflammation through AMPK/JNK/p38 MAPK pathway after intracerebral hemorrhage in mice. Journal of Neuroinflammation 15, (2018).

71. Lisak, R. P., Nedelkoska, L., Bealmear, B. & Benjamins, J. A. Melanocortin receptor agonist ACTH 1–39 protects rat forebrain neurons from apoptotic, excitotoxic and inflammation-related damage. Experimental Neurology 273, 161–167 (2015).

72. Catania, A. Targeting Melanocortin Receptors as a Novel Strategy to Control Inflammation. Pharmacological Reviews 56, 1–29 (2004).

73. Catania, A. Neuroprotective actions of melanocortins: a therapeutic opportunity. Trends in Neurosciences 31, 353–360 (2008).

74. Montero-Melendez, T. ACTH: The forgotten therapy. Seminars in Immunology 27, 216–226 (2015).

75. Holloway, P. M. et al. Both MC $_1$ and MC $_3$ Receptors Provide Protection From Cerebral Ischemia-Reperfusion–Induced Neutrophil Recruitment. Arterioscler Thromb Vasc Biol. 35, 1936–1944 (2015).

76. Schaible, E.-V. et al. Single Administration of Tripeptide α-MSH(11–13) Attenuates Brain Damage by Reduced Inflammation and Apoptosis after Experimental Traumatic Brain Injury in Mice. PLoS ONE 8, e71056 (2013).

77. Bitto, A. et al. Protective effects of melanocortins on short-term changes in a rat model of traumatic brain injury*. Critical Care Medicine 40, 945–951 (2012).

78. Carniglia, L. et al. [Nle4, D-Phe7]-α-MSH Inhibits Toll-Like Receptor (TLR)2- and TLR4-Induced Microglial Activation and Promotes a M2-Like Phenotype. PLOS ONE 11, e0158564 (2016).

79. Scholzen, T. E. et al. α-Melanocyte Stimulating Hormone Prevents Lipopolysaccharide-Induced Vasculitis by Down-Regulating Endothelial Cell Adhesion Molecule Expression. Endocrinology 144, 360–370 (2003).

80. Harazin, A. et al. Protection of cultured brain endothelial cells from cytokine-induced damage by α-melanocyte stimulating hormone. PeerJ 6, e4774 (2018).

81. Shen, Y. et al. Stimulation of the Hippocampal POMC/MC4R Circuit Alleviates Synaptic Plasticity Impairment in an Alzheimer's Disease Model. Cell Reports 17, 1819–1831 (2016).

82. Machado, I., Schiöth, H. B., Lasaga, M. & Scimonelli, T. IL-1β reduces GluA1 phosphorylation and its surface expression during memory reconsolidation and α-melanocyte-stimulating hormone can modulate these effects. Neuropharmacology 128, 314–323 (2018).

83. Shen, Y., Fu, W.-Y., Cheng, E. Y. L., Fu, A. K. Y. & Ip, N. Y. Melanocortin-4 Receptor Regulates Hippocampal Synaptic Plasticity through a Protein Kinase A-Dependent Mechanism. Journal of Neuroscience 33, 464–472 (2013).

84. Ferrari, W., Gessa, G. L. & Vargiu, L. BEHAVIORAL EFFECTS INDUCED BY INTRACISTERNALLY INJECTED ACTH AND MSH. Annals of the New York Academy of Sciences 104, 330–345 (2006).

85. Cools, A. R., Wiegant, V. M. & Hendrik Gispen, W. Distinct dopaminergic systems in ACTH-induced grooming. European Journal of Pharmacology 50, 265–268 (1978).

86. Cui, H. et al. Melanocortin 4 receptor signaling in dopamine 1 receptor neurons is required for procedural memory learning. Physiology & Behavior 106, 201–210 (2012).

87. Mul, J. D. et al. Melanocortin Receptor 4 Deficiency Affects Body Weight Regulation, Grooming Behavior, and Substrate Preference in the Rat. Obesity 20, 612–621 (2012).

88. Spaccapelo, L. et al. Melanocortin MC4 receptor agonists counteract late inflammatory and apoptotic responses and improve neuronal functionality after cerebral ischemia. European Journal of Pharmacology 670, 479–486 (2011).

89. Ichiyama, T. et al. Systemically administered a-melanocyte-stimulating peptides inhibit NF-kB activation in experimental brain inflammation. 7 (1999).

90. Pranzatelli, M. R., Tate, E. D., McGee, N. R., Colliver, J. A. & Ransohoff, R. M. CCR4 Agonists CCL22 and CCL17 are Elevated in Pediatric OMS Sera: Rapid and Selective Down-Regulation of CCL22 by ACTH or Corticosteroids. J Clin Immunol 33, 817–825 (2013).

91. Giuliani, D. et al. Treatment of cerebral ischemia with melanocortins acting at MC4 receptors induces marked neurogenesis and long-lasting functional recovery. Acta Neuropathol 122, 443–453 (2011).

92. Caruso, C. et al. Activation of Melanocortin 4 Receptors Reduces the Inflammatory Response and Prevents Apoptosis Induced by Lipopolysaccharide and Interferon-γ in Astrocytes. Endocrinology 148, 4918–4926 (2007).

93. Delgado, R. et al. Melanocortin peptides inhibit production of proinflammatory cytokines and nitric oxide by activated microglia. Journal of Leukocyte Biology 63, 740–745 (1998).

94. Hoshide, R., Cheung, V., Marshall, L., Kasper, E. & Chen, C. Do corticosteroids play a role in the management of traumatic brain injury? Surgical Neurology International 7, 84 (2016).

95. Dong, T., Zhi, L., Bhayana, B. & Wu, M. X. Cortisol-induced immune suppression by a blockade of lymphocyte egress in traumatic brain injury. Journal of Neuroinflammation 13, (2016).

96. Grundy, P. L., Patel, N., Harbuz, M. S., Lightman, S. L. & Sharples, P. M. Glucocorticoids modulate BDNF mRNA expression in the rat hippocampus after traumatic brain injury: NeuroReport 11, 3381–3384 (2000).

97. Grundy, P. L., Patel, N., Harbuz, M. S., Lightman, S. L. & Sharples, P. M. Glucocorticoids modulate the NGF mRNA response in the rat hippocampus after traumatic brain injury. Brain Research 892, 386–390 (2001).

98. Patel, H. B., Montero-Melendez, T., Greco, K. V. & Perretti, M. Melanocortin Receptors as Novel Effectors of Macrophage Responses in Inflammation. Frontiers in Immunology 2, (2011).

99. Ross, A. P., Ben-Zacharia, A., Harris, C. & Smrtka, J. Multiple Sclerosis, Relapses, and the Mechanism of Action of Adrenocorticotropic Hormone. Frontiers in Neurology 4, (2013).

100. Lal, R. et al. Pharmacodynamics and tolerability of repository corticotropin injection in healthy human subjects: A comparison with intravenous methylprednisolone. The Journal of Clinical Pharmacology 56, 195–202 (2016).

101. Vella, M. A., Crandall, M. L. & Patel, M. B. Acute Management of Traumatic Brain Injury. Surgical Clinics of North America 97, 1015–1030 (2017).

102. Gettig, J., Cummings, J. P. & Matuszewski, K. H.P. Acthar Gel and Cosyntropin Review. 8 (2009).

103. Veldhuis, J. D. et al. Corticotropin Secretory Dynamics in Humans under Low Glucocorticoid Feedback. 10.

104. Tao, Y.-X. The Melanocortin-4 Receptor: Physiology, Pharmacology, and Pathophysiology. Endocrine Reviews 31, 506–543 (2010).

105. Srikumar, B. N. et al. Characterization of the adrenocorticotrophic hormone - induced mouse model of resistance to antidepressant drug treatment. Pharmacology Biochemistry and Behavior 161, 53–61 (2017).

106. Sasaki-Hamada, S. et al. Antidepressant-like effects exerted by the intranasal administration of a glucagon-like peptide-2 derivative containing cell-penetrating peptides and a penetration-accelerating sequence in mice. Peptides 87, 64–70 (2017).

107. Antunes, M. S. et al. Neuropeptide Y administration reverses tricyclic antidepressant treatment-resistant depression induced by ACTH in mice. Hormones and Behavior 73, 56–63 (2015).

108. Iwai, T. et al. Glucagon-like peptide-2-induced memory improvement and anxiolytic effects in mice. Neuropeptides 49, 7–14 (2015).

109. Cusick, M. F., Libbey, J. E., Oh, L., Jordan, S. & Fujinami, R. S. Acthar gel treatment suppresses acute exacerbations in a murine model of relapsing-remitting multiple sclerosis. Autoimmunity 48, 222–230 (2015).

110. Hashimoto, M. et al. Role of Adrenocorticotropic Hormone in the Modulation of Pollinosis Induced by Pollen Antigens. Neuroimmunomodulation 22, 256–262 (2014).

111. Bailey, M. A., Mullins, J. J. & Kenyon, C. J. Mineralocorticoid and Glucocorticoid Receptors Stimulate Epithelial Sodium Channel Activity in a Mouse Model of Cushing Syndrome. Hypertension 54, 890–896 (2009).

112. Al-Dujaili, E. A. S., Mullins, L. J., Bailey, M. A., Andrew, R. & Kenyon, C. J. Physiological and pathophysiological applications of sensitive ELISA methods for urinary deoxycorticosterone and corticosterone in rodents. Steroids 74, 938–944 (2009).

113. Coll, A. P. Peripheral administration of the N-terminal pro-opiomelanocortin fragment 1-28 to Pomc-/- mice reduces food intake and weight but does not affect adrenal growth or corticosterone production. Journal of Endocrinology 190, 515–525 (2006).

114. Denton, D. A. et al. Effect of adrenocorticotrophic hormone on sodium appetite in mice. American Journal of Physiology-Regulatory, Integrative and Comparative Physiology 277, R1033–R1040 (1999).

115. Sasaki-Hamada, S., Yuri, Y., Hoshi, M. & Oka, J.-I. Immunohistochemical determination of the site of antidepressant-like effects of glucagon-like peptide-2 in ACTH-treated mice. Neuroscience 294, 156–165 (2015).

116. Iwai, T. et al. Glucagon-like peptide-2 but not imipramine exhibits antidepressant-like effects in ACTH-treated mice. Behavioural Brain Research 243, 153–157 (2013).

117. Decker, D. et al. Immunomodulatory effects of H.P. Acthar Gel on B cell development in the NZB/W F1 mouse model of systemic lupus erythematosus. Lupus 23, 802–812 (2014).

118. Arrat, H., Lukas, T. J. & Siddique, T. ACTH (Acthar Gel) Reduces Toxic SOD1 Protein Linked to Amyotrophic Lateral Sclerosis in Transgenic Mice: A Novel Observation. PLOS ONE 10, e0125638 (2015).

CHAPTER 2

OPEN-SOURCE METHODS FOR EVALUATION OF IMMUNE CELL COUNTS AND MORPHOLOGY FOLLOWING TRAUMATIC BRAIN INJURY IN MICE

Lorraine Siebold, Amy C. Krueger, Jonathan Abdala, Alena Grubaugh, Christopher G. Wilson

The Lawrence D. Longo, MD Center for Perinatal Biology
Department of Basic Sciences
Division of Physiology
Loma Linda University School of Medicine
Loma Linda, California 92350

Introduction

Traumatic brain injury (TBI) is a major health concern in the United States resulting in a substantial number of hospitalizations and deaths[1]. Following injury, damage-associated molecular patterns (DAMPs) and local cytokine signaling result in activation and proliferation of microglia, the neuronal tissue-resident macrophages[2–5]. Microglial activation, while rapid, can last for decades following initial injury and is associated with cognitive deficits[6,7].Corresponding with activation, microglia also undergo rapid and robust morphological changes in response to injury[4,8]. Activated microglia take on a more amoeboid shape with reduction, thickening and shortening of their ramifications (Figure 1A)[9]. Along with microglia proliferation and recruitment, blood brain barrier disruption and upregulation of chemoattractants results in infiltration of peripheral immune cells into the brain parenchyma[10,11]. The quantification of microglia and infiltrating immune cells following TBI is frequently completed in pre-clinical research through immunohistochemistry (IHC, Figure 1B) or flow cytometry techniques[12–14]. Flow cytometry allows for quantification of cell frequency as well as marker intensity but loses spatial distribution and morphology of cells. Immunohistochemistry remains the gold standard for evaluating immune cell response following injury. Following staining, quantification of cell number or total area of positive stain is often used to compare between injury or treatment groups. Quantification can be completed through manual cell selection or through automated cell counting processes. In

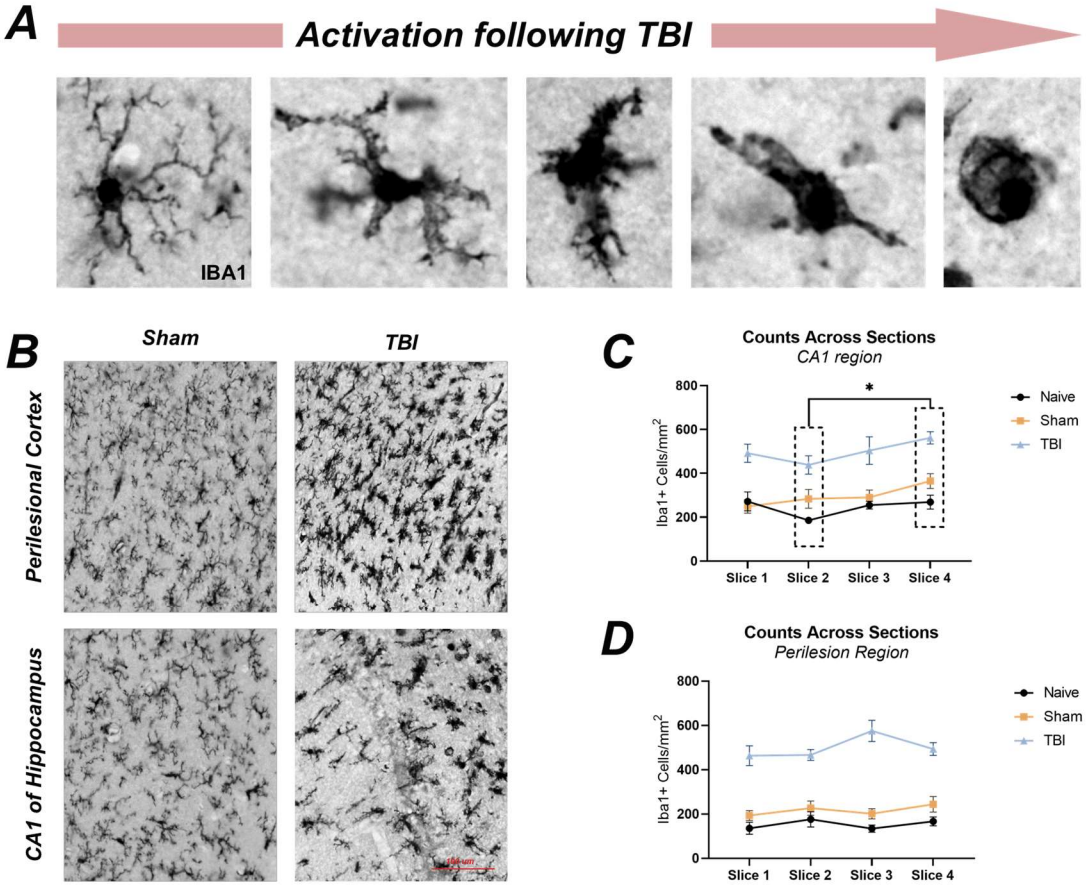

Figure 1. Microglia response to injury. A) Microglia undergo robust alterations in morphology upon injury. B) Iba1+ cells increase following injury. C,D Individual slice differences in Iba1+ cell counts in CA1 and perilesional cortex regions. Both CA1 and perilesional cortex exhibit main effect of injury (CA1 [$F(2,16)=27.90$], Perilesion [$F(2,16)=85.71$], $p<0.0001$) while only the CA1 region exhibited a main effect of slice number (CA1 main effect [$F(3,42)=3.200$, $p=0.0329$). * $p>0.01$.

this chapter, we describe and compares two open-source methods for quantification of immune cell tissue density through IHC as well as microglia/macrophage morphology in experimental TBI based on principles of unbiased counting [15].

Immune Cell Quantification

When quantifying cells using IHC, biases can be introduced. Two such biases include biased selection of tissue sections and reference region selection [16]. Our method of quantification addresses both of these biases as tissue heterogeneity is present in both brain tissue and is exaggerated following TBI.

Tissue Section Selection

Due to the heterogeneity of the injury, consistent selection of the region including tissue damage is vital. If tissue selection is based on tissue quality rather than location, bias can be introduced in the selection of regions for quantification based on tissue quality—violating the the assumption of a homogenous tissue response. This is particularly important for TBI research as the inflammatory response is graded and regionally dependent (Figure 1C). To reduce this bias, a systematic uniform method for random sampling within the injured region of tissue must be implemented. Systematic, uniform random sampling requires an initial, randomly assigned, starting point within the area to be sectioned followed by sections taken at regular sampling intervals.

Reference Region Selection

The brain has very distinct anatomical regions showing different response to injury. Furthermore, TBI results in a graded inflammatory response. For example, Iba1+ cells display a robust difference in proliferation between the CA1 and dentate gyrus in the hippocampus (Figure 1B). Additionally, the cortex alongside the lesion has a very different response than that seen in more distant cortex from the injury. Clear descriptions of the reference region should be stated and researchers should be blinded to treatment conditions when defining reference regions. Furthermore, random, or unbiased, sampling of the reference region through an unbiased 3D fractionator sampling method should be implemented (see random fractionator below, Figure 2D)[15].

Microglia Morphology

Microglia morphology changes have been widely documented following TBI. Some studies note these changes as qualitative findings with minimal or no quantification [17] while others have classified microglia based on distinct groups [18], number or length of ramifications [19,20] or more extensive morphological quantification [9,21–23]. Morphology analysis provides a method of analyzing the microglia response and is not contingent on previously described markers for microglia phenotype. The two most commonly used markers for microglia morphology are Iba1 and Cx3cr1 [5,9,24]. Because these markers for microglia do not distinguish between microglia and peripheral macrophages, morphological analysis evaluating not only microglia morphology but peripheral macrophage

morphology as well. From here forward, our use of microglia will indicate both microglia and peripheral macrophages.

Here we describe two open-source methods used to quantify microglia and neutrophils at day post injury (DPI) three following experimental TBI in mice. We also describe a method for quantifying microglia morphology with the use of *ImageJ* and *ImageJ* plug-ins (https://imagej.net/Welcome).

Methods

Animals

Three-month old male C57Bl6 (Jackson Lab) mice were used for this study. Mice were housed in Loma Linda University's Animal Care Facility (ACF) on a 12-hour light-dark cycle. Food and water were supplied *ad libitum* and food pellets were placed on the cage floor following surgery to allow access to food. All procedures were approved by the Institutional Animal Care and Use Committee at Loma Linda University, Loma Linda, California.

Controlled Cortical Impact Model

We used the controlled cortical impact model as previously described [25]. Animals were anesthetized with isoflurane (1–3%), then the surgical area was shaved and cleaned with antibacterial surgical soap, 70% isopropyl alcohol and betadine. A lidocaine injection was given prior to incision to expose the skull. After skin was retracted, we made a 5.0 mm diameter craniectomy—centered between bregma and lambda and 2.5 mm lateral to the sagittal suture—to expose underlying *dura* and cortex. The injury was induced with a 3.0 mm flat-tipped,

metal impactor. The impactor was centered within the craniectomy site and impact occurred with a velocity of 5.3 m/s, depth of 1.5 mm, and dwell time of 100 ms. Immediately following injury, the injury site was cleaned of blood and a sterile polystyrene skull-cap was placed over the craniectomy site and sealed with *VetBond* (3M, St. Paul MN). The incision was sutured and mice received an injection of saline for hydration and buprenorphine for pain prevention. Mice were placed in a heated recovery chamber and monitored for 1 hr prior to returning to their home cage. These injury parameters resulted in a moderately severe injury composed of cortical loss without overt hippocampal loss [26]. The same investigator performed all TBI and sham surgeries.

Immunohistochemistry

For immunohistochemical analysis, mice were perfused at DPI 3 with PBS followed by 4% PFA. Brains were immediately extracted and placed in 4% PFA overnight followed by PBS washes and 30% sucrose for 48 hours. Twenty-five micrometer sections separated by 400 micrometers were cut between Bregma – 3.0 and -1.0 within the lesion. Four consecutive brain sections within the lesion were used for cell count analysis. For microglia/macrophage (Iba1) and neutrophil (MPO) cell counts, staining consisted of blocking endogenous peroxide activity with quenching buffer (10% methanol, 1% hydrogen peroxide in PBS) followed by blocking with Avidin/Biotin blocking Kit (AbCam, USA) and normal serum (5% Donkey and 5% Goat serum) with 1% Triton-X in PBS. Sections were incubated overnight with a polyclonal rabbit anti-Iba1 primary

antibody (1:750, Rabbit anti-Iba1, Catalog no. 019-19741, Wako, USA) or monoclonal primary anti-MPO (1:800, Rabbit anti-Iba1, Catalog no. ab208670, Abcam, USA) and followed by secondary biotinylated antibody incubation (1:200, goat anti-rabbit IgG, Vector). The Vectastain Elite ABC HRP kit and DAB peroxidase substrate kit with nickel (Vector, Burlingame, CA) were used to visualize staining according to manufacturer instructions. Slides stained with anti-MPO were counter-stained with cresyl violet for reference region selection. Following staining, slides were dehydrated in ethanol and coverslipped with Permount Mounting Medium (Fisher Chemical).

Image Acquisition and Processing for Cell Counts

Images of Iba1 and MPO stained tissue sections were acquired using the Keyence X700 (Keyence Corporation, Osaka, Japan). Images were analyzed using *ImageJ* software (https://imagej.net/Welcome)**.** All cell counts were performed in a blinded fashion using a thresholding (method 1, Figure 2A-C) or unbiased-counting methodology (method 2, Figure 2A-B,D) [16] based on the unbiased stereology methods described in Mouton's *Principles and Practices of Unbiased Stereology* [15].

Method 1: Threshold and Particle Analysis

For Iba1+ cell counts, *ImageJ* was used to define ROIs and regions were saved in the *ROI manager*, images were smoothed to reduce detection of ramifications as independent cells, and images were manually thresholded for cells. Automated thresholding methods are available through *ImageJ*, however,

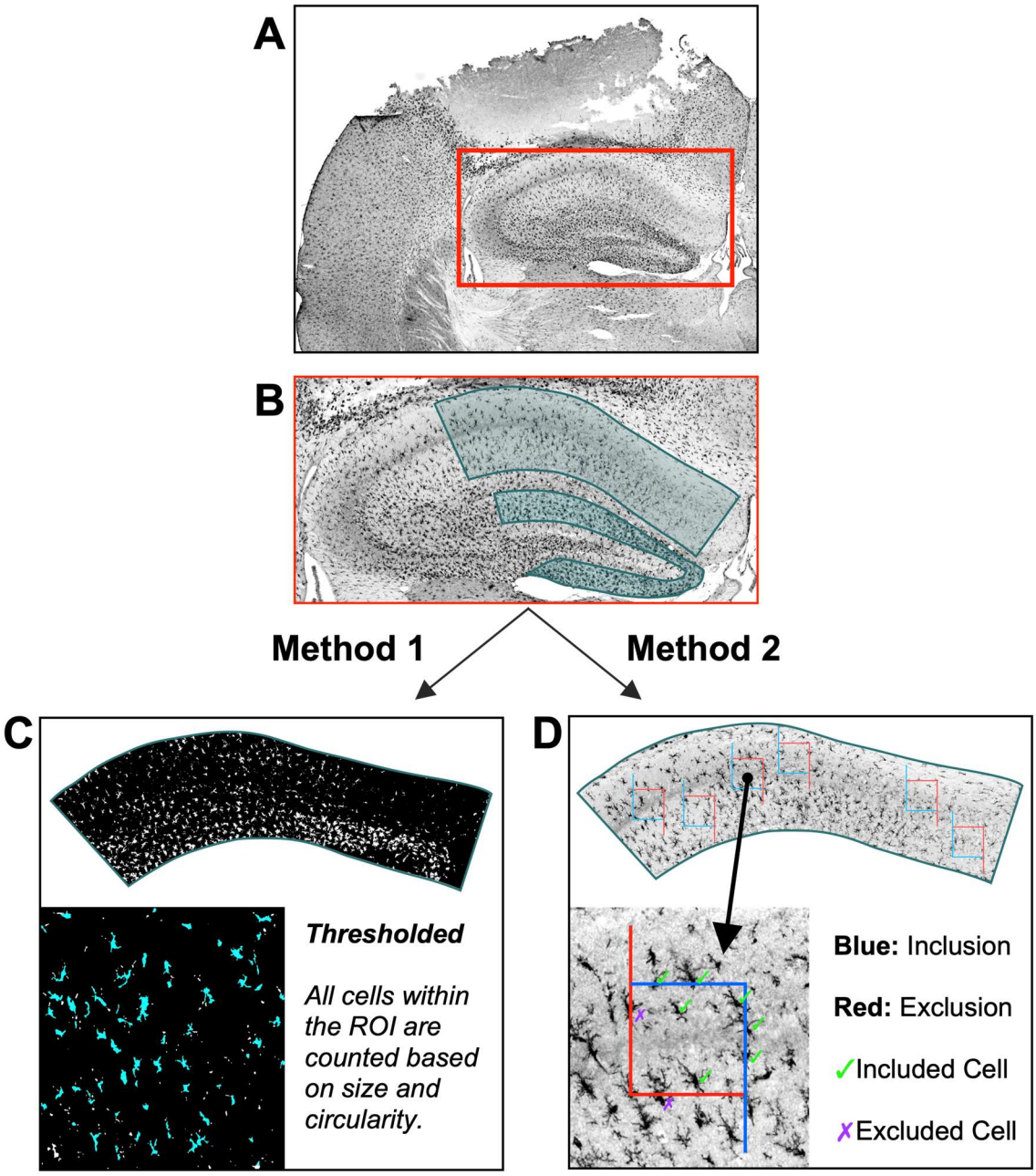

Figure 2. Illustration of counting methods**.** A,B) Both methods included identification of reference region or region of interest. C) Following thresholding, particle analysis through *ImageJ* was used to count individual cells with set pixel area and circularity. D) Disectors were randomly placed within the reference region and used for manual counting of cells.

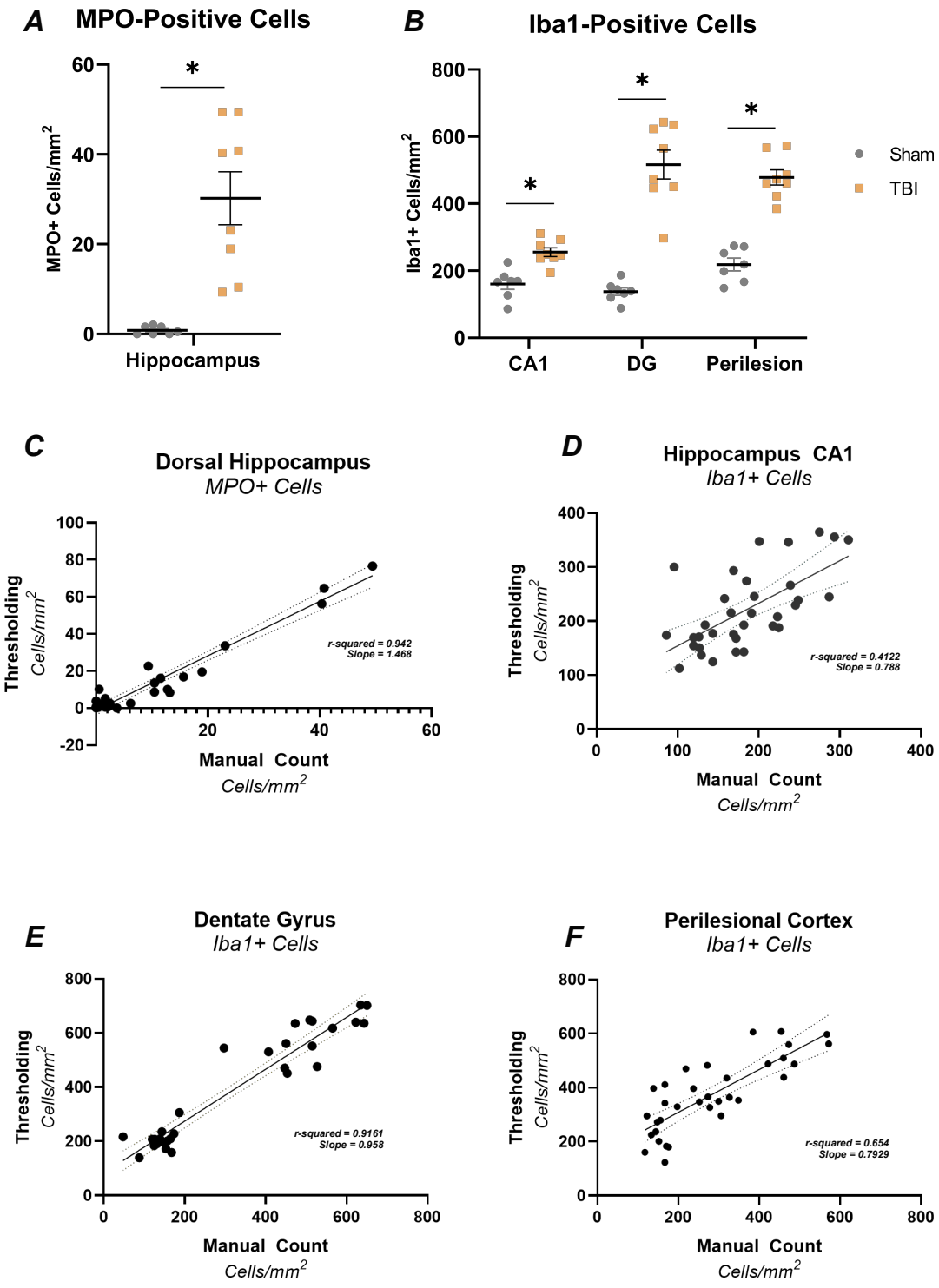

Figure 3. Immune cell counts in sham and TBI mice. A) Neutrophils (MPO+) and B) microglia (Iba1+) increase following TBI. C-F Correlation between threshold method and manual unbiased counting methods. Dotted lines indicate 95% confidence interval, * p< 0.0001

variation in IHC staining due to injury and methodology as well as the complexity of microglia morphology made automated thresholding challenging. Each brain slice had two hippocampal ROIs, one for the dentate gyrus and one for the CA1 (Figure 2a,b) and one region for perilesional cortex. Thresholds were set manually for each ROI (Figure 2c). For MPO cell counts, ROI was defined manually using captured RGB images and included the dorsal ipsilateral hippocampus. Prior to thresholding, colored images were split into RGB channels to reduce cresyl violet staining. Images were processed using the automated Sauvola local thresholding method via *ImageJ* software. Thresholding was manually checked prior to cell counting. Cell counts for both Iba1+ and MPO+ cells were divided by total area of ROI to give a final cells/area for each region and averaged across brain slices.

To determine our cell size and circularity parameters for cell counting, we selected a brain from each experimental group and took several measurements of the cell by completing the following steps:

a) The image was thresholded to create a binary image.
b) Using the selection wand, individual cells were selected representing cells of the smallest/largest as well as those with the highest/lowest circularity. Cells were added to the ROI manager.
c) Using the ROIs, all other cells were deleted except the selected cells. Selected cells were the only foreground pixels.

d) *Analyze Particles* selecting "Display results" was run on selected cells. This gave us area and circularity for each cell. From this information, cell area and circularity range was selected and used for further particle analysis. Note: Circularity was between 0–1, we made sure that at least one number after the decimal point was present in the "Set measurements…".

e) To confirm counts, manual counting of cells was compared to threshold counts based on parameters determined from individual cell analysis.

Method 2: Manual Counting with Random Fractionators

For each manually defined reference region, *ImageJ* software was used to randomly (see Appendix A) place six boxes of equal size within the reference region (Figure 2a,b). We used a randomly placed disector bounded by inclusion and exclusion lines (Figure 3d). Cells were manually counted if their somata fell within the box or crossed the inclusion lines and were not counted if they crossed the exclusion lines [15,16,27]. For Iba1+ cell counts, each brain slice had three reference regions, including the dentate gyrus and CA1 regions of the hippocampus and one region in the perilesional cortex. For MPO+ cell counts, the dorsal hippocampus was the only bounding reference region. Due to overt regional differences in Iba1+ cell density in the hippocampus, hippocampal Iba1+ reference regions included the dentate gyrus (DG) and CA1 regions. Two distinct regions were chosen as a homogenous tissue response cannot be assumed. These regional differences were not observed for MPO+ cells and therefore only one reference region was created for the dorsal hippocampus. For

analysis, cell counts for both Iba1+ and MPO+ cells were divided by total area of the disector and averaged across boxes and brain slices to give a final cells/area for each region.

Random Fractionation with ImageJ

Random fractionation of the reference region reduces the need for counting all cells within the reference region and provides an accurate estimate of the total number of cells within the reference region. It also reduces reference region selection bias. An *ImageJ* macro was developed to create randomly placed boxes representing fractionation of the tissue (Figure 2D). Cells were counted using *ImageJ Cell Counting* plug-in. Our developed macro allows for modification of box width and height, line color and thickness, number of iterations for random placement and number of boxes to be placed (Appendix A).

Comparison of Methods

Manual counting with random disectors was compared with the threshold and automated count method. Both methods showed robust increases in neutrophils (Figure 3A) and microglia (Figure 3B) following injury (data shown only for manual counting). To compare methods, linear regression of counts for each individual brain slice was completed. Neutrophil counts for both methods were highly correlated in the dorsal hippocampus (Figure 3C, $r = 0.942$). Microglia counts were also highly correlated (Figure 3 D–F) in perilesional cortex ($r = 0.654$), CA1 ($r = 0.4122$) and dentate gyrus ($r = 0.9161$). Threshold with automatic cell counting resulted in higher cell counts for neutrophils (slope =

1.468) and lower counts for microglia in the CA1 (slope = 0.788) and perilesional cortex (slope = 0.7929).

Morphology Quantification and Analysis

Image Acquisition and Processing for Morphology

Images of Iba1 stained tissue sections were acquired using the Keyence 9000 (Keyence Corporation, Osaka, Japan) using the 60x oil-immersion objective and full-focus capturing software. Images were analyzed using *ImageJ* software. All morphology analysis was performed by individuals blinded to treatment group on binary images isolated using the following procedure (Figure 4):

1) Roughly selected around the cell. No other cell components were within the selection.
2) Added the selection to the ROI manager and duplicated the image to isolate the cell of interest (Figure 4A, step 1).

   Smoothed the image once, thresholded image to create binary image (Figure 4A, step 2). When image was thresholded not all of the ramifications were connected to the main cell. We evaluated the effect of connecting the ramifications (Figure 4A, top image) with images that were not connected (Figure 4B, bottom image) and morphological parameters were highly correlated between the two isolation methods (Figure 4B). Not connecting ramifications reduced time without losing comparative value.
3) Created a binary outline image from the binary image (Figure 4A, step 3).

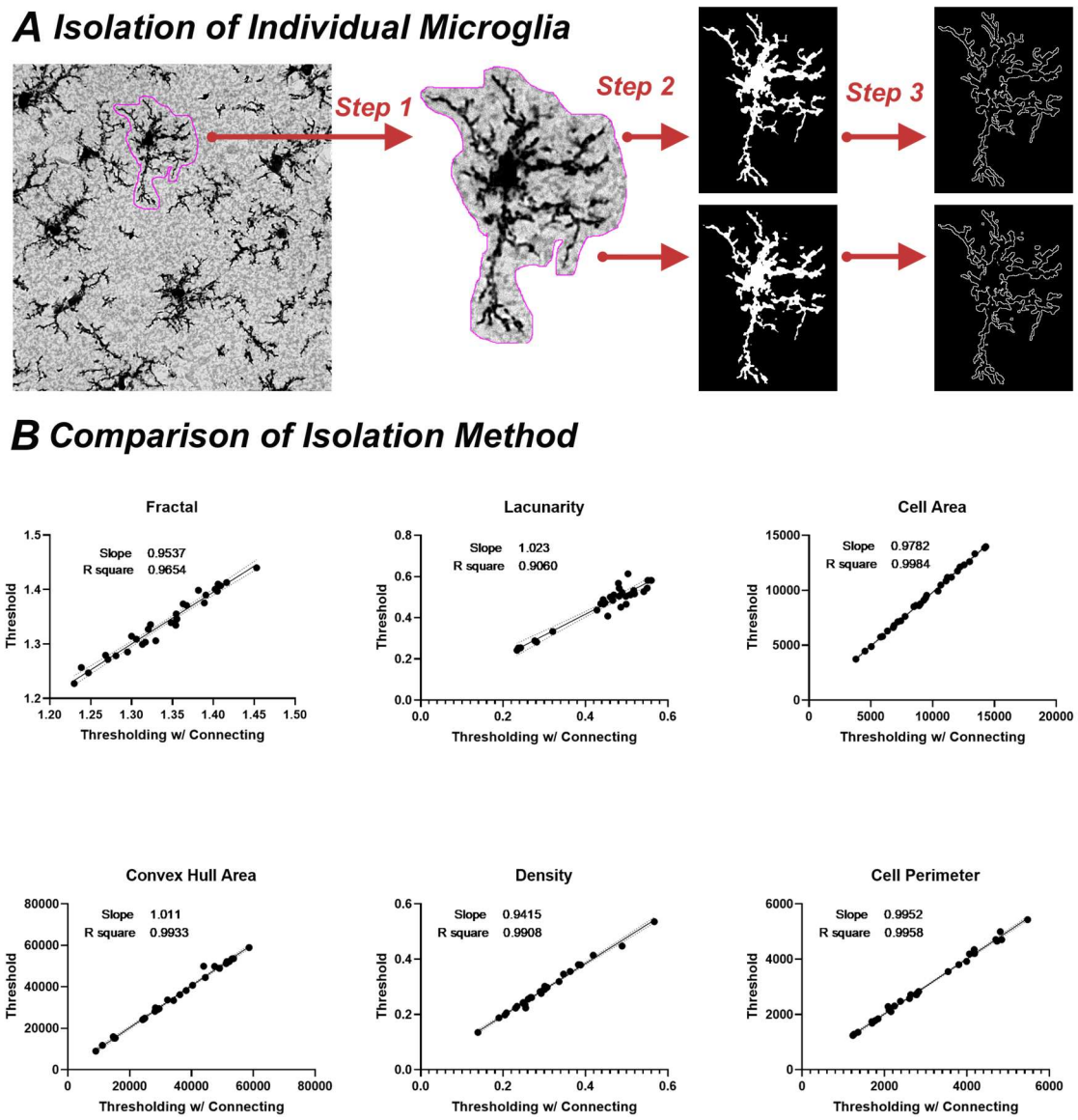

Figure 4. Isolation of microglia for morphological analysis. A) Isolation of microglia from Iba1+ IHC 25 micrometer mouse brain sections. B) Comparing connected-thresholded images with threshold only isolation methods. Comparisons show high correlation between two methods.

Quantification of Morphology

Following microglia cell isolation, *FracLac* for *ImageJ* was used to quantify morphology [9]. While additional parameters and information can be obtained from the analysis, we report twelve morphological features (Figure 5A). Microglia isolation and *FracLac* is able to distinguish between different microglia morphology as exhibited by the heat map of normalized data (Figure 5B). When using *FracLac*, we chose to analyze microglia using 12 randomized grids with power series scaling method at 45% of maximum image size. Hull and circle metrics were also calculated during analysis. To increase processing, all individual cells were saved as individual images and were batch-processed using the *FracLac* Batch Process option. These parameters were chosen based in their ability to distinguish morphological differences between three artificially created microglia representing the range of microglia morphology.

Conclusion

Immune cells have a robust response to injury and are frequently evaluated as an endpoint for pharmaceutical interventions in pre-clinical research. Open source methods for evaluation provide opportunities for all lab types to quantify tissue response following injury and treatment. Along with cell count quantification, morphology enhances our understanding of microglia response to injury and treatment. Quantification of morphology not only allows for linear and dichotomous (M1 or M2) labeling of activation but provides the opportunity for more advanced statistical evaluation [9,24]. Additional research is

needed to evaluate the relationship between morphology and identified markers for microglia phenotypes.

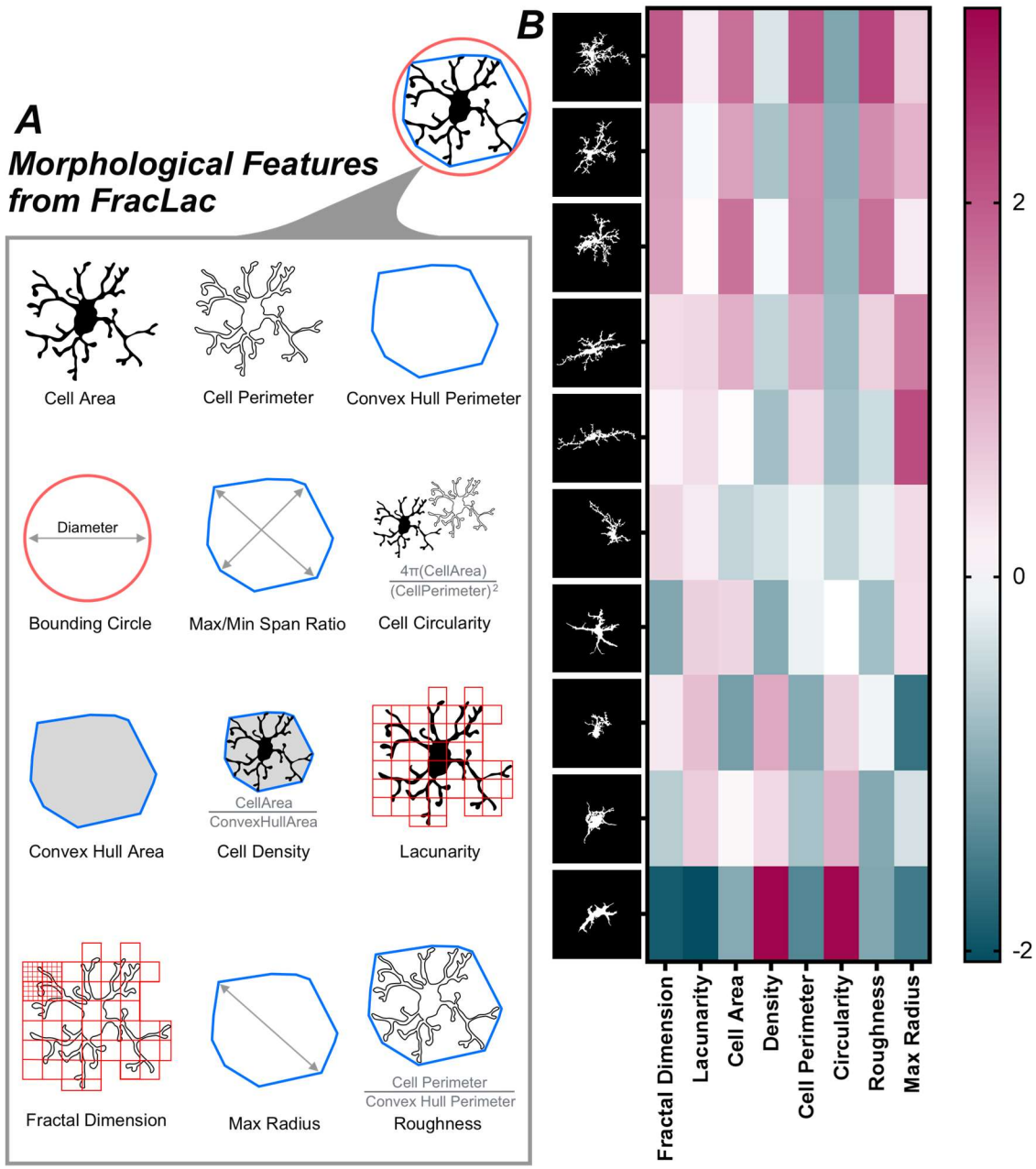

Figure 5. *FracLac* used for morphological quantification of isolated cells. A) Twelve morphological features were calculated. B) Morphological features vary according to morphology type, visualized by the heat map of normalized data.

References

1. Faul, M. & Coronado, V. Epidemiology of traumatic brain injury. in *Handbook of Clinical Neurology* vol. 127 3–13 (Elsevier, 2015).

2. Henry, R. J. *et al.* Microglial depletion with CSF1R inhibitor during chronic phase of experimental traumatic brain injury reduces neurodegeneration and neurological deficits. *J. Neurosci.* 2402–19 (2020) doi:10.1523/JNEUROSCI.2402-19.2020.

3. Willis, E. F. *et al.* Repopulating Microglia Promote Brain Repair in an IL-6-Dependent Manner. *Cell* **180**, 833-846.e16 (2020).

4. Davalos, D. *et al.* ATP mediates rapid microglial response to local brain injury in vivo. *Nature Neuroscience* **8**, 752–758 (2005).

5. Donat, C. K., Scott, G., Gentleman, S. M. & Sastre, M. Microglial Activation in Traumatic Brain Injury. *Frontiers in Aging Neuroscience* **9**, (2017).

6. Cherry, J. D. *et al.* Microglial neuroinflammation contributes to tau accumulation in chronic traumatic encephalopathy. *Acta Neuropathologica Communications* **4**, (2016).

7. Johnson, V. E. *et al.* Inflammation and white matter degeneration persist for years after a single traumatic brain injury. *Brain* **136**, 28–42 (2013).

8. Nimmerjahn, A., Kirchhoff, F. & Helmchen, F. Resting Microglial Cells Are Highly Dynamic Surveillants of Brain Parenchyma in Vivo. **308**, 6 (2005).

9. Fernández-Arjona, M. del M., Grondona, J. M., Granados-Durán, P., Fernández-Llebrez, P. & López-Ávalos, M. D. Microglia Morphological Categorization in a Rat Model of Neuroinflammation by Hierarchical Cluster and Principal Components Analysis. *Frontiers in Cellular Neuroscience* **11**, (2017).

10. Carlos, T. M., Clark, R. S. B., Franicola-Higgins, D., Schiding, J. K. & Kochanek, P. M. Expression of endothelial adhesion molecules and recruitment of neutrophils after traumatic brain injury in rats. *J Leukoc Biol* **61**, 279–285 (1997).

11. Kenne, E., Erlandsson, A., Lindbom, L., Hillered, L. & Clausen, F. Neutrophil depletion reduces edema formation and tissue loss following traumatic brain injury in mice. *Journal of Neuroinflammation* **9**, (2012).

12. Jin, X., Ishii, H., Bai, Z., Itokazu, T. & Yamashita, T. Temporal Changes in Cell Marker Expression and Cellular Infiltration in a Controlled Cortical Impact Model in Adult Male C57BL/6 Mice. *PLoS ONE* **7**, e41892 (2012).

13. Bai, R. *et al.* Flow Cytometric Characterization of T Cell Subsets and Microglia After Repetitive Mild Traumatic Brain Injury in Rats. *Neurochem Res* **42**, 2892–2901 (2017).

14. Chen, S. *et al.* Activation of melanocortin receptor 4 with RO27-3225 attenuates neuroinflammation through AMPK/JNK/p38 MAPK pathway after intracerebral hemorrhage in mice. *Journal of Neuroinflammation* **15**, (2018).

15. Mouton, Peter R. *Principles and Practices of Unbiased Stereology: An Introduction for Bioscientists*. (Johns Hopkins University Press, 2002).

16. Brown, D. L. Bias in image analysis and its solution: unbiased stereology. *J Toxicol Pathol* **30**, 183–191 (2017).

17. Cao, T., Thomas, T. C., Ziebell, J. M., Pauly, J. R. & Lifshitz, J. Morphological and genetic activation of microglia after diffuse traumatic brain injury in the rat. *Neuroscience* **225**, 65–75 (2012).

18. Genove, G., Mollick, T. & Johansson, K. Photoreceptor degeneration, structural remodeling and glial activation: a morphological study on a genetic mouse model for pericyte deficiency. *Neuroscience* **279**, 269–284 (2014).

19. Tokizane, K. *et al.* Phospholipid localization implies microglial morphology and function via Cdc42 in vitro. *Glia* **65**, 740–755 (2017).

20. Matyash, M., Zabiegalov, O., Wendt, S., Matyash, V. & Kettenmann, H. The adenosine generating enzymes CD39/CD73 control microglial processes ramification in the mouse brain. *PLoS One* **12**, e0175012 (2017).

21. Chaaya, N. *et al.* Contextual Fear Conditioning Alter Microglia Number and Morphology in the Rat Dorsal Hippocampus. *Front. Cell. Neurosci.* **13**, 214 (2019).

22. Karperien, A., Ahammer, H. & Jelinek, H. F. Quantitating the subtleties of microglial morphology with fractal analysis. *Frontiers in Cellular Neuroscience* **7**, (2013).

23. Kozlowski, C. & Weimer, R. M. An Automated Method to Quantify Microglia Morphology and Application to Monitor Activation State Longitudinally In Vivo. *PLoS ONE* **7**, e31814 (2012).

24. Verdonk, F. *et al.* Phenotypic clustering: a novel method for microglial morphology analysis. *Journal of Neuroinflammation* **13**, (2016).

25. Bajwa, N. M. *et al.* Mild Concussion, but Not Moderate Traumatic Brain Injury, Is Associated with Long-Term Depression-Like Phenotype in Mice. *PLOS ONE* **11**, e0146886 (2016).

26. Siebold, L., Obenaus, A. & Goyal, R. Criteria to define mild, moderate, and severe traumatic brain injury in the mouse controlled cortical impact model. *Experimental Neurology* **310**, 48–57 (2018).

27. Golub, V. M. *et al.* Neurostereology protocol for unbiased quantification of neuronal injury and neurodegeneration. *Front. Aging Neurosci.* **7**, (2015).

CHAPTER THREE

COSYNTROPIN ATTENUATES NEUROINFLAMMATION IN A MOUSE MODEL OF TRAUMATIC BRAIN INJURY

Lorraine Siebold, Amy C. Krueger, Jonathan Abdala, Johnny D. Figueroa, Brenda Bartnik-Olson, Barbara Holshouser, Christopher G. Wilson, Stephen Ashwal

The Lawrence D. Longo, MD Center for Perinatal Biology
Department of Basic Sciences
Division of Physiology
Loma Linda University School of Medicine
Loma Linda, California 92350

Adapted from Siebold, L. et al. Cosyntopin Attenuates Neuroinflammation in a Mouse Model of Traumatic Brain Injury. Frontiers in Molecules Neuroscience 13, 109 (2020).

Abstract

Traumatic brain injury (TBI) is a leading cause of mortality/morbidity and is associated with chronic neuroinflammation. Melanocortin receptor agonists including adrenocorticotropic hormone (ACTH) ameliorate inflammation and provide a novel therapeutic approach. We examined the effect of long-acting cosyntropin (CoSyn), a synthetic ACTH analog, on the early inflammatory response and functional outcome following experimental TBI. The controlled cortical impact model was used to induce TBI in mice. Mice were assigned to injury and treatment protocols resulting in four experimental groups including sham + saline, sham + CoSyn, TBI + saline and TBI + CoSyn. Treatment was administered subcutaneously 3 hrs post injury and daily injections were given for up to seven days post injury. Early inflammatory response was evaluated at three days post injury through evaluation of cytokine expression (IL1β and TNFα) and immune cell response. Quantification of immune cell response included cell counts of microglia/macrophages (Iba1+ cells) and neutrophils (MPO+ cells) in cortex and hippocampus. Behavioral testing (n=10-14 animals/group) included open field and novel object recognition during the first week following injury and Morris water maze at 10-15 days post injury. Immune cell quantification showed decreased accumulation of Iba1+ cells in the perilesional cortex and CA1 region of the hippocampus for CoSyn-treated TBI animals compared to saline-treated. Reduced numbers of MPO+ cells were also found in the perilesional cortex and hippocampus in CoSyn treated TBI mice

compared to their saline treated counterparts. Furthermore, CoSyn treatment reduced IL1β expression in the cortex of TBI mice. Behavioral testing showed a treatment effect of CoSyn for novel object recognition with CoSyn increasing the discrimination ratio in both TBI and Sham groups, indicating increased memory performance. CoSyn also decreased latency to find platform during the early training period of the Morris water maze when comparing CoSyn to saline-treated TBI mice suggesting moderate improvements in spatial memory following CoSyn treatment. Reduced microglia/macrophage accumulation and neutrophil infiltration in conjunction with moderate improvements in spatial learning in our CoSyn treated TBI mice suggests a beneficial anti-inflammatory effect of CoSyn following TBI.

Key Words: Traumatic brain injury, ACTH, microglia, behavior, neuroinflammation, neutrophils, Cosyntropin

Introduction

Traumatic brain injury (TBI) is a major health concern in the United States resulting in a substantial number of hospitalizations and deaths [1]. TBI causes subsequent morbidity and long-term effects that are influenced by age, sex, injury severity, and inflammatory status [2,3]. Several studies have shown persistent neuroinflammation following TBI, lasting as long as 17 years [4–6]. However, it is unclear which components of the inflammatory response are indicators of repair and which continue to drive pathology and brain vulnerability [6]. Clinically, neuroinflammation following TBI is associated with increased intracranial pressure, increased mortality, poor functional outcomes [7], reduced processing speed [4], and increased risk of epilepsy and neurodegenerative disorders [6,8,9]. Together, these findings suggest that pharmaceutical agents that modulate inflammation are attractive targets to address acute and chronic symptoms of brain injury.

Under physiologically normal conditions, the brain parenchyma is isolated from the periphery by the blood brain barrier (BBB). However, this immune privilege is severely undermined following TBI resulting in a robust immune response influenced by infiltrating peripheral immune cells [10]. As the tissue-resident macrophage, microglia are key players in the inflammatory process [11]. Along with microglia, peripheral monocyte and neutrophil invasion into the brain parenchyma also contributes to the inflammatory process [10]. Peripheral monocyte and neutrophil infiltration are associated with increased

edema, exaggerated inflammatory responses, and poorer functional outcomes following brain injury [12,13]. Quantification of total microglia/macrophages and neutrophils show peak levels within the first week after injury with robust increases within the first few days [10,14]. Due to their dynamic response to injury, tissue resident and peripheral immune cells are essential to the early secondary injury cascade and a target for anti-inflammatory compounds.

Melanocortins are a family of peptides with diverse functions including energy homeostasis, immunomodulation, steroidogenesis, pigmentation and synaptic plasticity [15]. Melanocortins (MCs) are endogenously derived from pro-opiomelanocortin precursors [15]. MCs include compounds such as adrenocorticotropic hormone (ACTH) and alpha-melanocyte stimulating hormone (α-MSH), both of which are agonists for melanocortin receptors [15,16]. There are five MC receptor subtypes with tissue-specific expression, including melanocytes (MC1R), peripheral immune cells (MC1,3,5R), endothelial cells (MC1R), the adrenal cortex (MC2R) and the central nervous system (MC3-4R). In the central nervous system, MC receptor distribution is ubiquitous, showing expression in cortex, hippocampus, arcuate nucleus of the hypothalamus, limbic system and thalamus [17]. Furthermore, MC receptors are expressed in neural and glial cells, contributing to their multifaceted functions [17–19]. Of particular interest, MCs have been shown to have glucocorticoid-independent immune modulatory and neuroprotective effects following brain insult [20–22]. Independent of MC2R activation, which results in glucocorticoid production, MC1, MC3 and MC4

receptor signaling have all demonstrated neuroprotective effects [18,20,23,24]. In these studies, MC3R and MC4R-agonist treatment reduced lesion size, inflammation, and cell death resulting in overall improvements in behavior following experimental TBI [24,25]. In a model of cerebral ischemia reperfusion, MC1R and MC3R signaling diminish inflammation and suppressed leukocyte recruitment following insult [23]. While the mechanisms are still unclear and are subtype and injury dependent, in vitro studies show that MC4R agonists reduce NFκB translocation and therefore downstream pro-inflammatory cascades, suppress pro-inflammatory microglia and protect oligodendrocytes from inflammation-related damage [26]. MC1/3R agonists also regulate the neuroinflammatory response by reducing expression of adhesion molecules and chemoattractants resulting in subsequent reduction in peripheral immune cell infiltration [23,27,28]. There is limited research investigating neuroprotective effects of melanocortin agonists following TBI and, to our knowledge, no research has been conducted investigating adrenocorticotrophic hormone (ACTH) or ACTH analogues as a post-TBI therapeutic [25].

In this study, we investigated the effects of a long-acting synthetic ACTH analog (CoSyn, ACTH 1-24) on neuroinflammation and immune cell response following experimental TBI in mice and their subsequent functional outcomes. We hypothesized that CoSyn would reduce the early neuroinflammatory response and improve cognitive functioning following TBI.

Methods

Experimental Design

Our study included two research strategies in order to evaluate the effect of CoSyn on the 1) early neuroinflammatory response and 2) behavioral outcomes following TBI (Figure 1A,B). To assess the effect of daily CoSyn administration on the early neuroinflammatory response, we quantified protein expression at day post injury (DPI) 3 using enzyme-linked immunosorbent assays (ELISA). We also quantified microglia/macrophages and neutrophils in the ipsilateral cortex and hippocampus using immunohistochemistry at DPI 3 (Figure 1A). Day post injury 3 was chosen based on previous literature demonstrating robust increases in microglia/macrophages and neutrophils at this time-point [10,14]. Our second research strategy included evaluation of behavioral outcomes during and following an extended treatment protocol (Figure 1B). Taking into account both the potential for side-effects as a result of extended use (> 2 weeks) and the clinical treatment protocols that suggest multiple treatment days (>5 days), we tested a 7-day protocol using a subcutaneous injection of long-acting cosyntropin [29–32]. We assessed behavior both during and following our treatment period. To assess anxiety-like behavior and memory within our treatment period, we used low anxiogenic behavioral protocols to assess anxiety-like behavior using the open field (OF) test and novel object recognition (NOR) to assess non-spatial memory (Figure 1B). Hippocampal-dependent memory was assessed through.

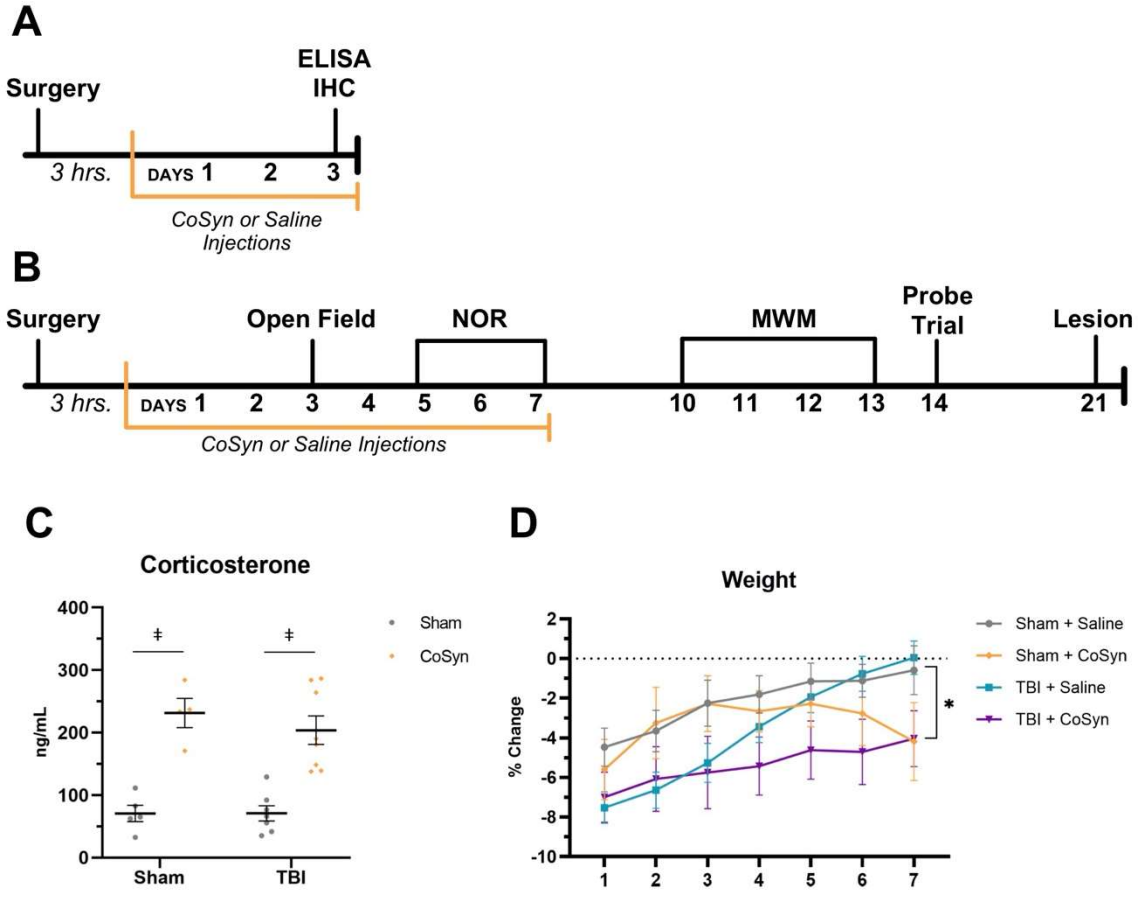

Figure 1. CoSyn increases serum corticosterone levels and decreases weight gain. **(A)** Experimental design for early inflammatory response. **(B)** Experimental design for behavioral outcomes**. (C)** Serum corticosterone levels were increased at DPI 3 in both sham- and TBI-treated animals. Sham-saline (n=4), sham-CoSyn (n=4), TBI-saline (n=7), TBI-CoSyn (n=8). **(D)** All experimental groups exhibited post-surgery weight loss. **(D)** Mice treated with CoSyn did not show post-surgical increased weight loss but did demonstrate sustained levels of weight loss at DPI 7 compared to saline-treated mice. Sham-saline (n=10), sham-CoSyn (n=11), TBI-saline (n=14), TBI-CoSyn (n=14). Significance was determined using two-way ANOVA with Tukey post hoc testing **(C,E)** and repeated-measures ANOVA **(D)**. Graphs represent means and error bars show SEM, *Main effect of treatment, $p<0.05$, # $p<0.001$.

the Morris water maze (MWM, Figure 1B). Mice that underwent behavioral testing were used for DPI 21 lesion and hippocampal loss quantification

Animals

One-hundred and twenty-eight (128) 3-month old male C57Bl6 (Jackson Lab) mice were used for this study. Mice were housed in LLU's Animal Care Facilty on a 12-hour light-dark cycle with lights turned on/off at 7:00 am/pm. Food and water were supplied *ad libitum* and food pellets were placed on the cage floor following surgery to allow access to food. Mice were randomly assigned to four experimental groups: sham + saline, sham + CoSyn, TBI + saline, or TBI + CoSyn. All procedures were approved by the Institutional Animal Care and Use Committee at Loma Linda University, Loma Linda, California. To avoid unnecessary use of experimental animals, we performed interim statistical analyses after pre-specified N values were collected.

Controlled Cortical Impact Model

We used the controlled cortical impact model as previously described [33]. Animals were anesthetized with isoflurane (1–3%), shaved, and the surgical area cleaned with surgical soap, 70% isopropyl alcohol and betadine. A lidocaine injection was given prior to incision to expose the skull. After skin was retracted, we made a 5.0 mm diameter craniectomy—centered between bregma and lambda and 2.5 mm lateral to the sagittal suture—to expose underlying dura and cortex. The injury was induced with a 3.0 mm flat-tipped, metal impactor. The impactor was centered within the craniectomy site and impact occurred with a

velocity of 5.3 m/s, depth of 1.5 mm, and dwell time of 100 ms. Immediately following injury, the injury site was cleaned of blood and a sterile polystyrene skull-cap was placed over the craniectomy site and sealed with VetBond (3M, St. Paul MN). The incision was sutured and mice received an injection of saline for hydration and buprenorphine for pain prevention. Mice were placed in a heated recovery chamber and monitored for 1 hr prior to returning to their home cage. Daily weights were taken for the first 7 days to monitor recovery. These injury parameters resulted in a severe injury composed of cortical and hippocampal loss and sustained behavioral deficits [34]. The same investigator performed all TBI and sham surgeries.

CoSyn or Vehicle Treatment

For our treatment we used a subcutaneous injection of long-acting cosyntropin, a synthetic analogue of ACTH (amino acids 1-24) that maintains steroidogenic effects (Figure 1C). Based on previous literature, a dosage of 1.8 U/mouse/day was selected [35–37]. A 3-hour post-injury treatment was selected to modulate the early inflammatory response using a clinically relevant time-point [3839]. For treatment and vehicle experimental groups, we administered CoSyn or saline treatments 3-hours following cortical impact (TBI groups) or craniectomy (sham groups) with all initial treatments taking place prior to 19:00 on the day of surgery. Following the surgical day, mice were treated for 3 (Research Strategy 1) or 7 (Research Strategy 2) consecutive days with morning (07:00) injections. Mice were administered 50 µL of saline or CoSyn (50 µL = 1.8 units/dose)

subcutaneously. CoSyn was supplied by West Therapeutic Development, LLC (Grayslake, IL, USA).

Tissue Collection, Cytokine and Corticosterone

For cytokine analysis, we anesthetized mice at DPI 3 and performed a cardiac puncture for blood collection. Blood was transferred to an EDTA blood collection tube for plasma isolation. Mice were then perfused with PBS and brains were quickly extracted. The hippocampus and ipsilateral cortex, containing the lesion and perilesional cortex were isolated in ice-cold PBS followed by flash-freezing in liquid nitrogen. Samples were homogenized in a protein isolation buffer with protease inhibitors (Halt Protease Inhibitor Cocktail; Sigma-Aldrich, St. Louis, MO, USA) as previously described [40]. Homogenized tissue was spun down at 14k g for 20 minutes at 4° C and supernatant collected. Total protein content of supernatant was quantified using the Pierce BCA protein assay (Pierce Biotechnology, Rockford, IL, USA). IL1β and TNFα were quantified using high-sensitivity ELISA kits per manufacturer's instructions—Mouse IL-1β/IL-1F2 Quantikine HS ELISA (Assay range 0.8–50 pg/mL, Intra-assay precision CV%<5.1) and Mouse TNFα Quantikine HS ELISA kits (Assay range 0.8–50 pg/mL, Intra-assay precision CV%<2.8, R&D Systems, Minneapolis, MN, USA). All tissue homogenates fell within the stated ranges of the high-sensitivity ELISAs. However, CoSyn-induced decreases in TNFα resulted in values below the lowest point on the standard curve (<0.8 pg/mL) and values were extrapolated from standard curve. Corticosterone (CORT) levels were quantified

using a Corticosterone ELISA kit with use of steroid displacement reagent supplied with the kit (Enzo, Life Sciences, USA, sensitivity = 27 pg/ml=20,000 pg/mL). Prior to quantification, serum was incubated with steroid displacement reagent to displace CORT from bound proteins and diluted to (1:100) using supplied assay buffer. All data points are averages of duplicate runs and tissue homogenates are reported as picogram (pg) of analyte per milligram (mg) of total protein.

Immunohistochemistry

For immunostaining analysis, mice were perfused at DPI 3 with PBS followed by 4% PFA. Brains were extracted and placed in 4% PFA overnight followed by PBS washes and 30% sucrose for 48 hours. Twenty-five micrometer sections separated by 400 micrometers were cut between Bregma –2.5 and –1.0 to capture the entire lesion. Four consecutive brain sections within the lesion were used for cell count analysis. For microglia/macrophage (Iba1) and neutrophil (MPO) cell counts, staining consisted of blocking endogenous peroxide activity with quenching buffer (10% methanol, 1% hydrogen peroxide in PBS) followed by blocking with Avidin/Biotin blocking Kit (AbCam, USA) and normal serum (5% Donkey and 5% Goat serum) with 1% Triton-X in PBS. Sections were incubated overnight with a polyclonal rabbit anti-Iba1 primary antibody (1:750, Rabbit anti-Iba1, Catalog no. 019-19741, Wako, USA) or monoclonal primary anti-MPO (1:800, Rabbit anti-Iba1, Catalog no. ab208670, Abcam, USA) and followed by secondary biotinylated antibody incubation (1:200, goat anti-rabbit

IgG, Vector). The Vectastain Elite ABC HRP kit and DAB peroxidase substrate kit with nickel (Vector, Burlingame, CA) were used to visualize staining according to manufacturer instructions. Slides stained with anti-MPO were counter-stained with cresyl-violet for reference region selection. Following staining, slides were dehydrated in ethanol and coverslipped with Permount Mounting Medium (Fisher Chemical).

Image Acquisition, Processing and Unbiased Stereological Analysis

Images of Iba1 and MPO stained tissue sections were acquired using the Keyence X700 (Keyence Corporation, Osaka, Japan). Images were analyzed using *ImageJ* software (https://imagej.net/Welcome). All cell counts were performed in a blinded fashion using an unbiased-counting methodology [41] developed in our laboratory and based on the unbiased stereology methods described in Mouton's *Principles and Practices of Unbiased Stereology* [42]. For each manually defined reference region, *ImageJ* software was used to randomly place six boxes of equal size within the reference region. We used an unbiased disector bounded by inclusion and exclusion lines. Cells were manually counted if their soma fell within the box or crossed the inclusion lines and were not counted if they crossed the exclusion lines [41–43]. For Iba1+ cell counts, each brain slice had five reference regions, including the dentate gyrus, CA1, and three separate regions representing the perilesional cortex. Each cortical reference region spanned 1000 pixels (equivalent to 264 μm) in width and progressively got further from the lesion. For MPO+ cell counts, the dorsal hippocampus and perilesional cortex

were defined as the two bounding reference regions incorporating these areas. Due to overt regional differences in Iba1+ cell density in the hippocampus, hippocampal Iba1+ reference regions included the dentate gyrus (DG) and CA1 regions. These regional differences were not observed for MPO+ cells, and therefore only one reference region was created for the dorsal hippocampus. For analysis, cell counts for both Iba1+ and MPO+ cells were divided by the total area of the randomly placed box and averaged across boxes and brain slices to give a final cells/area for each region."

Lesion Size and Hippocampal Loss

For calculation of the lesion size, every 16th section of the brain from DPI 21 mice representing a separation of approximately 400 µm and spanning the entire extent of the injured cortex were stained with cresyl violet. For cresyl violet staining, mice were perfused at DPI 21 with PBS followed by 4% PFA. Brains were extracted and placed in 4% PFA overnight followed by PBS washes and 30% sucrose for 48 hours. Twenty-five micrometer sections separated by 400 micrometers were cut between Bregma –3.5 and 1.0 to capture the entire lesion. All brain sections within Bregma –3.5 to 1.0 mm containing overt cortical lesions were used for lesion analysis. The lesion area, hippocampus and ventricle area were calculated using the point-counting method using *ImageJ* software (https://imagej.net/Welcome)[44]. Regions of interest for lesion, hippocampus and ventricles were manually drawn by technicians blinded to the experimental groups. Points acquired from the regions of interest were multiplied by the area

represented by each point to get final areas for each tissue section. If the cortical loss extended into the ventricle, the total area (lesion and ventricle) was calculated and the ventricle area from the contralateral side was subtracted from the total area. Total volume was calculated using area under the curve for each individual brain based on lesion area and separation of 400 µm per brain section.

Behavioral Testing

All behavior testing was conducted between 16:00 and 21:00 to reduce stress-induced effects caused by 07:00 injections during the first week following injury. All mice were individually handled daily beginning four days prior to behavioral testing to acclimate mice to the investigator. All behavioral testing was conducted in cohorts that were balanced across treatment groups and was replicated with three different cohorts. Testing of behavioral set-up showed lighting levels between 31–45 lux and sound levels between 57–62 dB.

Open Field (OF) Test

Locomotor activity and anxiety-like behavior was monitored through analysis in an open field apparatus, as previously described (Tucker, Velosky, and McCabe 2018). At DPI 3, mice were placed in a 30-cm square arena with no spatial cues (Figure 1B). Mice were gently placed in the middle of the apparatus and allowed to roam freely for 15 minutes. Movements were recorded and analyzed using video tracking with ANY-maze software (ANY-maze, Stoelting, Inc.; Wood Dale, IL, USA).

Novel Object Recognition (NOR)

We performed the NOR test to assess non-spatial memory performance on DPI 7 (Figure 1B) (Antunes and Biala 2012; Baratz et al. 2015). Mice were habituated for two days prior to object exposure using the same area used for the open field. No spatial cues were present. On the third day of the NOR protocol, mice were placed in the square arena along with two identical objects and were allowed to explore for 10 minutes and then returned to their home cage. Three hours post object exposure, mice were returned to the arena and exposed to one novel and one previous object. Objects used for previous and novel objects were balanced across experimental conditions to account for object preference. Arena and objects were thoroughly cleaned with 70% ethanol between all trials. Mice remained in the arena for 5-minutes before being returned to their home cage. Movements and time spent exploring were recorded, tracked and analyzed using video tracking with ANY-maze software (ANY-maze, Stoelting, Inc.; Wood Dale, IL, USA). Object discrimination ratio was calculated by dividing the total time exploring the new object by the total time exploring both objects with values greater than 0.5 indicating a preference for the novel object and therefore indicates better memory performance.

Morris Water Maze (MWM)

As previously described, the MWM was used to assess hippocampal-dependent spatial learning and memory function (Tucker, Velosky, and McCabe 2018). The MWM apparatus was composed of a round pool filled with opaque

water using non-toxic, white tempera paint with water temperatures maintained between 26–28 degrees Celsius. Black geometric shapes on a white background were placed around the pool for external spatial cues. Four days of training were conducted with five trials for each training day. On the first day of training, a flag was placed on the platform and mice were placed on the platform for 60 seconds. With the flag remaining, mice were placed on the opposite side of the pool and allowed to return to the platform. The flag was removed and the mice were allowed to remain on the platform for 30 seconds before the next 60-second trial occurred. For all consecutive training days, mice received five 60-second trials separated by 30-second inter-trial intervals. If the mice did not find the platform after the 60-second period, they were gently guided to the platform and given a latency score of 60-seconds for that trial. Twenty-four hours following the last training day, mice underwent a probe trial. For the probe trial, mice were placed in the pool without a platform and were allowed to swim for 60 seconds before removal. Following all MWM days, mice were returned to a warmed chamber to recover before being returned to their home cage. All videos were quantified and analyzed using video tracking with ANY-maze software (ANY-maze, Stoelting, Inc.; Wood Dale, IL, USA).

Statistical Analysis and Exclusion Criteria

All bar graph values in figures and text are expressed as mean and standard error of the mean. Two-way ANOVA was used to evaluate difference in means between the four experimental groups for ELISA, cell counts and

behavior data. Repeated-measures ANOVA was used for training day analysis of the MWM and weight changes. Tukey's multiple comparisons test was completed for post hoc analysis. T-test analysis was used for comparison of lesion size, hippocampal ratios and MPO+ counts in lesion. Four mice were excluded from the MWM (n = 2 for both TBI groups) due to inability to swim resulting in absence of searching for escape. Outliers were excluded from data sets using the Tukey method. Using the Tukey method, the excluded values did not exceed more than one data point per experimental group in this study. All statistical analyses were performed and graphs created with GraphPad Prism software, version 8.1.2 (GraphPad Software, Inc., San Diego, CA), p values < 0.05 were considered statistically significant.

Results

CoSyn Increases Serum Corticosterone and Reduces Post-Injury Weight Gain

To validate drug efficacy, serum corticosterone levels were evaluated at DPI 3. CoSyn resulted in robust increases in corticosterone in serum [Figure 1C, $F(3,40)=35.2$, $p<0.0001$] with no significant injury [$F(1,40=0.918$, $p=0.344$] or interaction effect [$F(3,40)=0.313$, $p=0.816$]. Elevations in corticosterone were also present in fecal matter evaluated at DPI 2, 4, and 6 (data not shown). No difference was seen in overall post-surgical percent weight-loss between treatment [$F(1,44)=0.071$, $p=0.791$] or injury groups [Figure 1D, $F(1,44)=3.80$, $p=0.058$]. However, both CoSyn-treated groups showed sustained weight loss at DPI 7 compared to saline-treated groups [Figure 1D, $F(1,41)=8.34$, $p=0.0062$] with

no injury effect [F(1,41)=0.178, p=0.676]. TBI mice exhibited signs of distress during the first 24 hours following injury including reduced movement, grooming and nesting with no overt differences between saline and CoSyn treated mice.

CoSyn Does Not Alter Hippocampal Loss or Cortical Lesion Volume Following TBI

To determine the effect of CoSyn on lesion size and hippocampal loss, we calculated ipsilateral cortical loss and hippocampal ratios between ipsilateral and contralateral brain regions (Figure 2A). At DPI 21, no difference was seen in cortical lesion volume between saline-treated and CoSyn-treated TBI brains [Figure 2B, t(16)=0.3171, p=0.7553]. The CoSyn-treated TBI group exhibited no difference between ipsilateral and contralateral hippocampal volume indicating no treatment-effect of CoSyn on hippocampal loss following TBI [Figure 2C, t(16)=0.9765, p=0.3434]. Our lesion volumes were consistent with previous research [45].

CoSyn Reduces Microglia/Macrophages following injury

Ionized calcium binding adaptor molecule 1 (Iba1) was used to evaluate the microglial/macrophage response via quantification of Iba1-positive cells within the perilesional cortex and ipsilateral hippocampus (Figure 3A,B). As illustrated in figure 3, injury induced an increase in Iba1+ cells in both the cortical regions surrounding the lesion and hippocampus (Figure 3C,D). For the perilesional cortex, we found a main effect of cortical region [Figure 3C, F(2,49.37)=64.29,

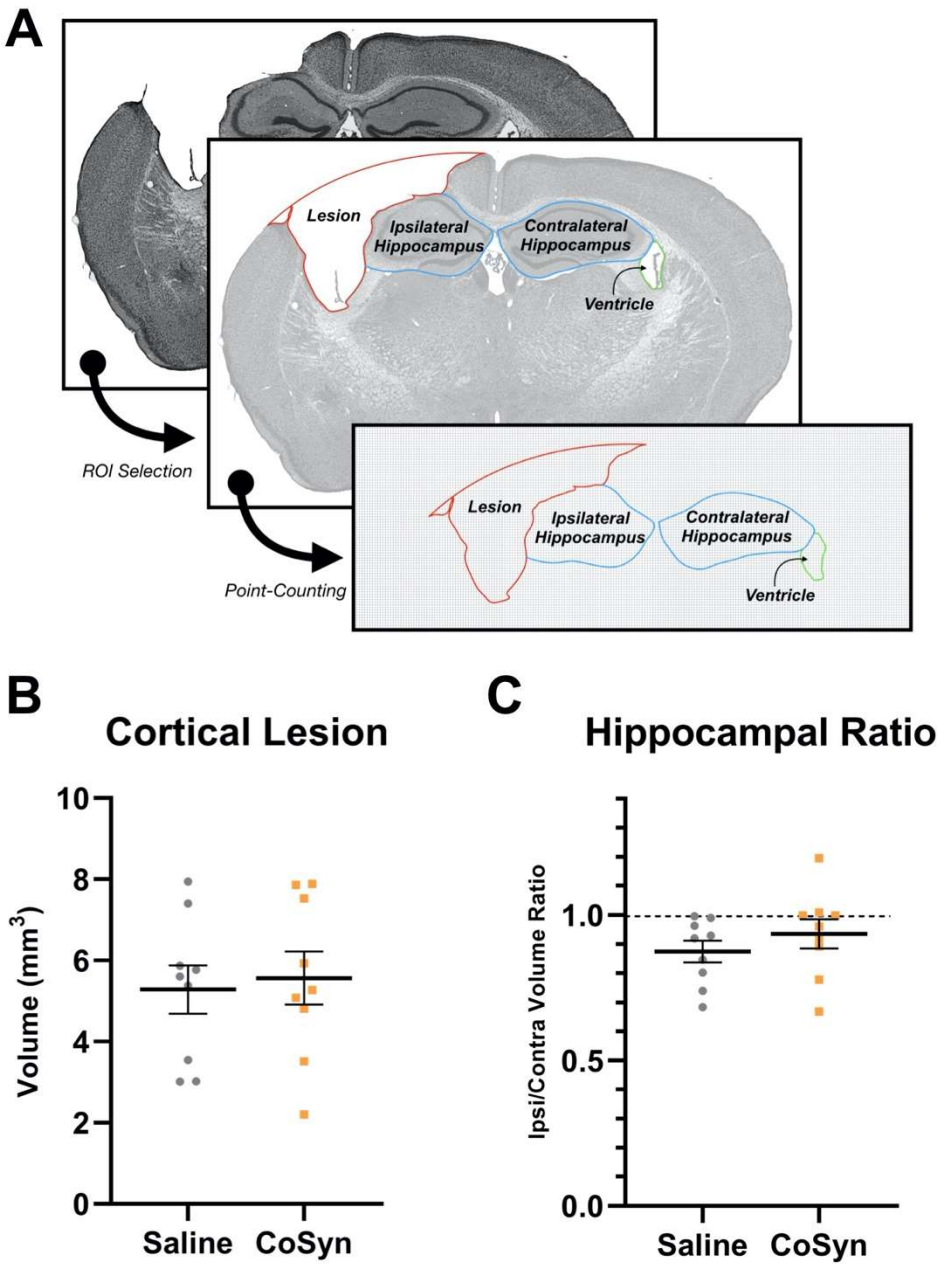

Figure 2. CoSyn does not alter hippocampal loss or cortical lesion size following TBI at DPI 21. (A) Cresyl violet stained tissue was used to quantify lesion, hippocampal and ventricular size. (B) No difference was seen in cortical lesion volume between saline (n=9) and CoSyn-treated (n=9) mice following TBI. (C) CoSyn-treatment did not alter ipsilatera/contralateral hippocampal volume ratio compared to saline-treatment. Significance was determined using unpaired T-test. Graphs represent means and error bars show SEM.

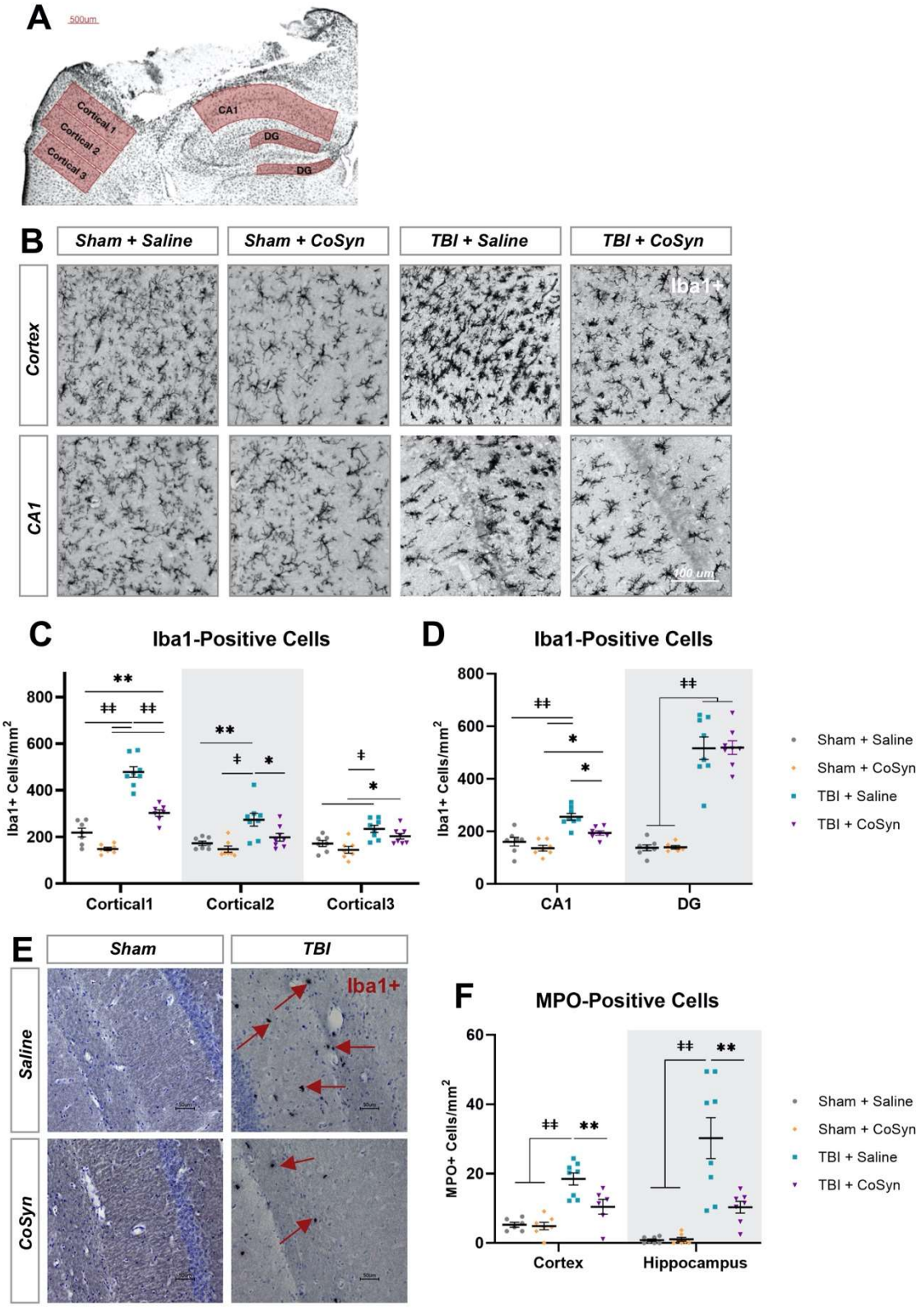
A
500um
Cortical 1
Cortical 2
Cortical 3
CA1
DG
DG
B
Sham + Saline
Sham + CoSyn
TBI + Saline
TBI + CoSyn
Cortex
CA1
Iba1+
100 um
C
Iba1-Positive Cells
Iba1+ Cells/mm2
Cortical1
Cortical2
Cortical3
D
Iba1-Positive Cells
Iba1+ Cells/mm2
CA1
DG
Sham + Saline
Sham + CoSyn
TBI + Saline
TBI + CoSyn
E
Sham
TBI
Saline
CoSyn
Iba1+
F
MPO-Positive Cells
MPO+ Cells/mm2
Cortex
Hippocampus
Sham + Saline
Sham + CoSyn
TBI + Saline
TBI + CoSyn

Figure 3. CoSyn reduced Iba1+ and MPO+ cells in perilesional cortex and hippocampus. (A) Iba1+ cells were quantified at DPI 3 selected from perilesional and hippocampal regions. (B) Representative images of perilesional Iba1+ cells. (C,D) Iba1+ cells in the perilesional (C) as well as the CA1 and DG regions of the hippocampus (D) increased following injury. Injury-induced increases were reduced following treatment in the perilesional regions and CA1 region of the hippocampus. (E) Representative images of MPO+ positive cells in the hippocampus. (F) MPO+ cells increase after injury and are reduced with CoSyn treatment. Sham-saline (n=7), sham-CoSyn (n=6), TBI-saline (n=9), TBI-CoSyn (n=9). Significance was determined using two-way ANOVA with Tukey post hoc testing. Graphs represent means and error bars show SEM, *$p<0.05$, **$p<0.01$, ǂ $p<0.001$, ǂǂ $p<0.0001$.

p<0.0001] and experimental group [F(3,26)=39.22, p<0.0001] with significant interaction [F(6,51)=17.74, p<0.0001]. These differences were also seen in the hippocampus with region [Figure 3D, F(1,50)=81.92, p<0.0001] and experimental group main effects [F(3,50)=71.52, p<0.0001] and a significant interaction [F(3,50)=31.91, p<0.0001]. Post hoc analysis showed CoSyn-treatment decreased injury-induced increases of Iba1+ cells in the perilesional cortical regions (Figure 3C, p<0.001) as well as the CA1 region of the hippocampus (Figure 3D, p=0.0103). CoSyn did not alter the number of Iba1+ cells in the DG at DPI 3 (Figure 3D, p=>0.999). Of interest, CoSyn-treatment in the TBI group resulted in Iba1+ cell counts equivalent to shams in cortical regions further from the lesion site while the saline-treated TBI group maintained elevated levels of Iba1+ cells in comparison to both shams in all cortical regions and the CoSyn-treated TBI group in the two regions closest to the lesion indicating a more widespread microglia/macrophage response (Figure 3C).

CoSyn Reduces Neutrophil Infiltration in Cortex and Hippocampus Following TBI

Following injury, MPO+ cells (Figure 3E) increased in both the perilesional cortex [Figure 3F, F(1,23)=36.09, p<0.0001] and hippocampus [Figure 3F, F(1,25)=32.12, p<0.0001]. Main effect of treatment as well as interaction between injury and treatment were observed in both cortex [Injury effect F(1,23)=6.036, p=0.022, Interaction F(1,23)=7.261, p=0.0129] and hippocampus [Injury effect F(1,25)=8.712, p=0.0068, Interaction F(1,23)=8.342, p=0.0079]. Post

hoc analysis demonstrated CoSyn treatment reduced neutrophil infiltration in both the cortex (p=0.0071) and hippocampus (p=0.0018) following injury (Figure 3F). There was no difference in MPO+ cells in the lesion site when comparing saline and CoSyn treated TBI mice [data not shown].

CoSyn Reduces IL1β in Cortex

To test the anti-inflammatory properties of CoSyn, we evaluated expression levels of IL1β and TNFα in ipsilateral cortical and hippocampal tissue. We found that CoSyn reduced IL1β in the cortex with a main effect of treatment [Figure 4A, $F(1,41)=10.57$, $p=0.0023$] $p<0.05$) without altering IL1β levels in the hippocampus. Post hoc analysis showed reduced IL1β expression in CoSyn treated versus Saline treated TBI mice (Figure 4A, p=0.0074). We did not see differences in TNFα expression at DPI 3 between injury or treatment groups in cortical tissue (Figure 4B). Interestingly, we found that injury reduced TNFα in the hippocampus compared to sham mice with no differences seen between treatment groups [Figure 4B, $F(1,37)=16.66$, Injury effect, $p=0.0002$]. IL1β serum levels showed no injury-induced increases [Figure 4C, Injury effect $F(1,42)=0.2434$, $p=0.6243$] but did show a treatment effect [$F(1,42)=6.352$, $p=0.0156$] with CoSyn contributing to decreased IL1β. Similar to hippocampal tissue, serum TNFα decreased following injury [Figure 4C, $F(1,29)=5.751$, $p=0.0231$). Unlike cortical and hippocampal tissue, CoSyn administration resulted in a robust decrease in TNFα in serum at DPI 3 [Treatment effect $F(1,29)=78.08$, $p<0.0001$].

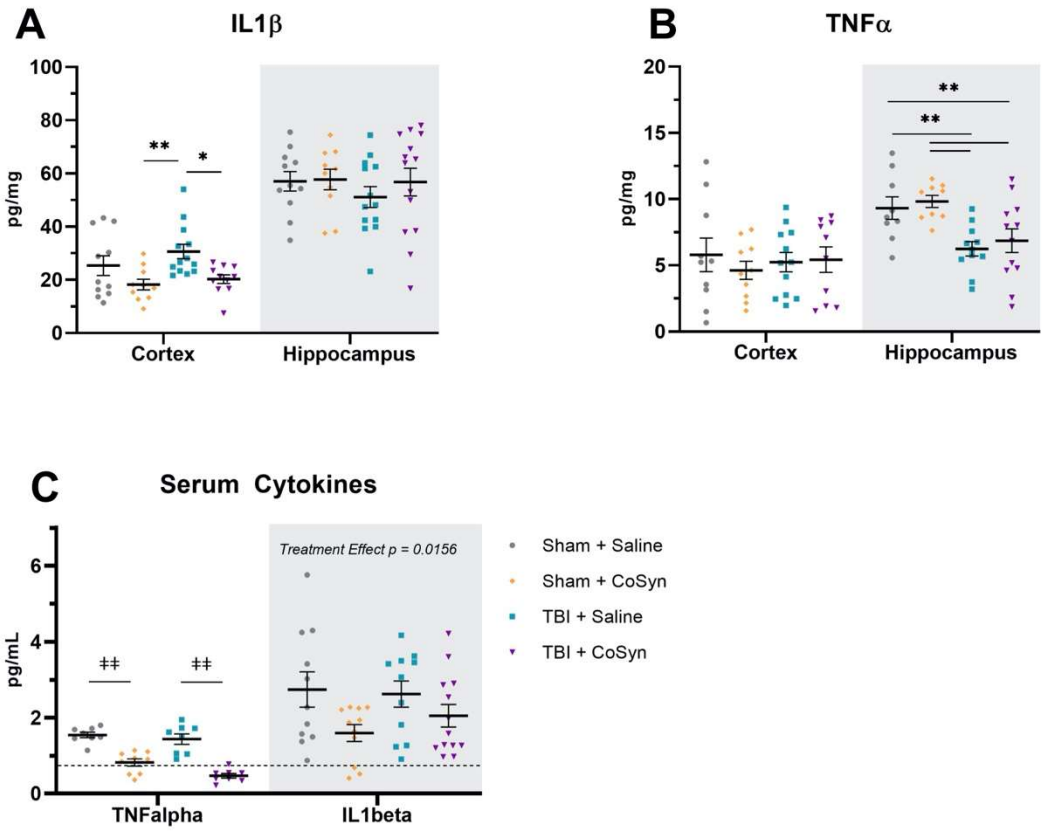

Figure 4. CoSyn reduces IL1β expression in cortex and serum and TNFα in serum. (A) Cortical IL1β levels at DPI 3 were reduced in TBI groups with CoSyn-treatment with no alteration in IL1β levels in the hippocampus between groups. (B) TNFα expression levels were the same between groups in the cortical tissue with lower levels exhibited in the hippocampal tissue of the TBI group compared to sham. Sham-saline (n=10), sham-CoSyn (n=11), TBI-saline (n=13), TBI-CoSyn (n=14). (C) TNFα and IL1β levels in serum at DPI 3, both cytokines showed decreased levels following CoSyn administration. Dashed line indicates lowest detectable concentration for high-sensitivity ELISA. Significance was determined using two-way ANOVA with Tukey post hoc testing. Graphs represent means and error bars show SEM, *p<0.05, **p<0.01.

TBI Increased Anxiety-like Behavior with no Alteration in Overall Movement

Open field testing was completed at DPI 3 to evaluate anxiety-like behavior and spontaneous motor activity. Following injury, mice exhibited reduced time spent in the center compared to shams indicating increased anxiety-like behavior [Figure 5A, $F(1,41)=6.819$, Injury effect, $p=0.0298$]. No differences were seen between saline and CoSyn treated mice [$F(1,41)=0.04$, Treatment effect, $p=0.842$]. Furthermore, no injury [$F(1,41)=2.235$, $p=0.143$] or treatment [$F(1,41)=0.027$, $p=0.871$] effects were seen between groups when comparing average speeds (Figure 5B).

CoSyn Improves Non-spatial Memory

Non-spatial dependent memory was evaluated through the use of novel object recognition (NOR) testing at DPI 7. Mice did not display alterations in memory as a result of injury status [Figure 5C, $F(1,44)=0.099$, $p=0.755$] but did show increased preference for the novel object following CoSyn-treatment [Figure 5C, $F(1,44)=6.872$, Treatment effect, $p=0.0120$]. Increased discrimination ratio suggests improved memory performance with CoSyn administration (Figure 5C).

CoSyn Provides Modest Improvements in Early Spatial Learning Following TBI

To determine the effect of CoSyn on memory and learning following TBI, we conducted the Morris water maze at 10–15 days post-injury. All treatment groups learned the MWM task as indicated by reduced latency to find the hidden

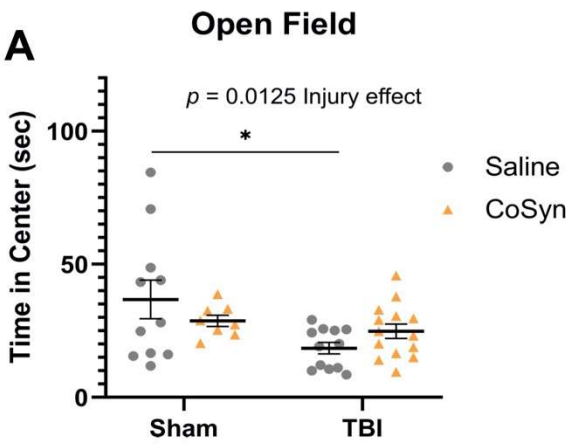
A
Open Field
p = 0.0125 Injury effect
*
Time in Center (sec)
100
50
0
Sham
TBI
Saline
CoSyn

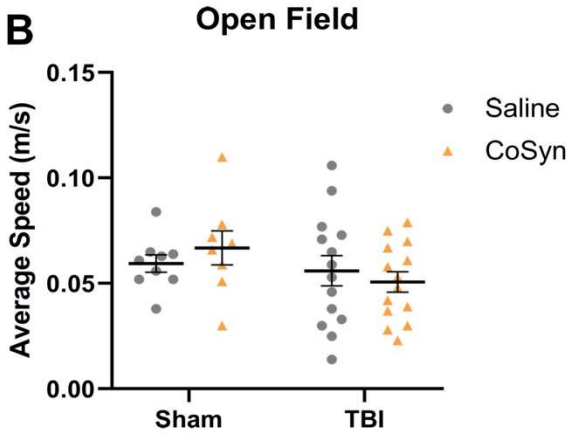
B
Open Field
Average Speed (m/s)
0.15
0.10
0.05
0.00
Sham
TBI
Saline
CoSyn

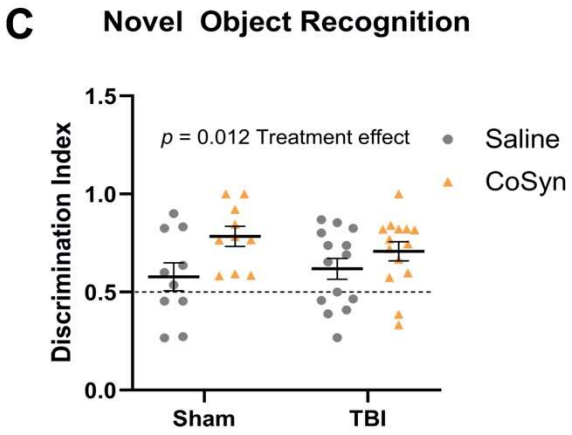
C
Novel Object Recognition
p = 0.012 Treatment effect
Discrimination Index
1.5
1.0
0.5
0.0
Sham
TBI
Saline
CoSyn

Figure 5. Injury-induced anxiety-like behavior and increased memory with treatment. (A) TBI mice exhibit reduced time in center compare to sham animals. No effect of treatment in either group was seen. (B) No difference between average speed at DPI 3 between any treatment or injury group. (C) CoSyn increased time-spent exploring novel object during NOR testing as indicated by increased discrimination index. Sham-saline (n=10), sham-CoSyn (n=11), TBI-saline (n=14), TBI-CoSyn (n=14). Significance was determined using two-way ANOVA with Tukey post hoc testing. Graphs represent means and error bars show SEM, *$p<0.05$.

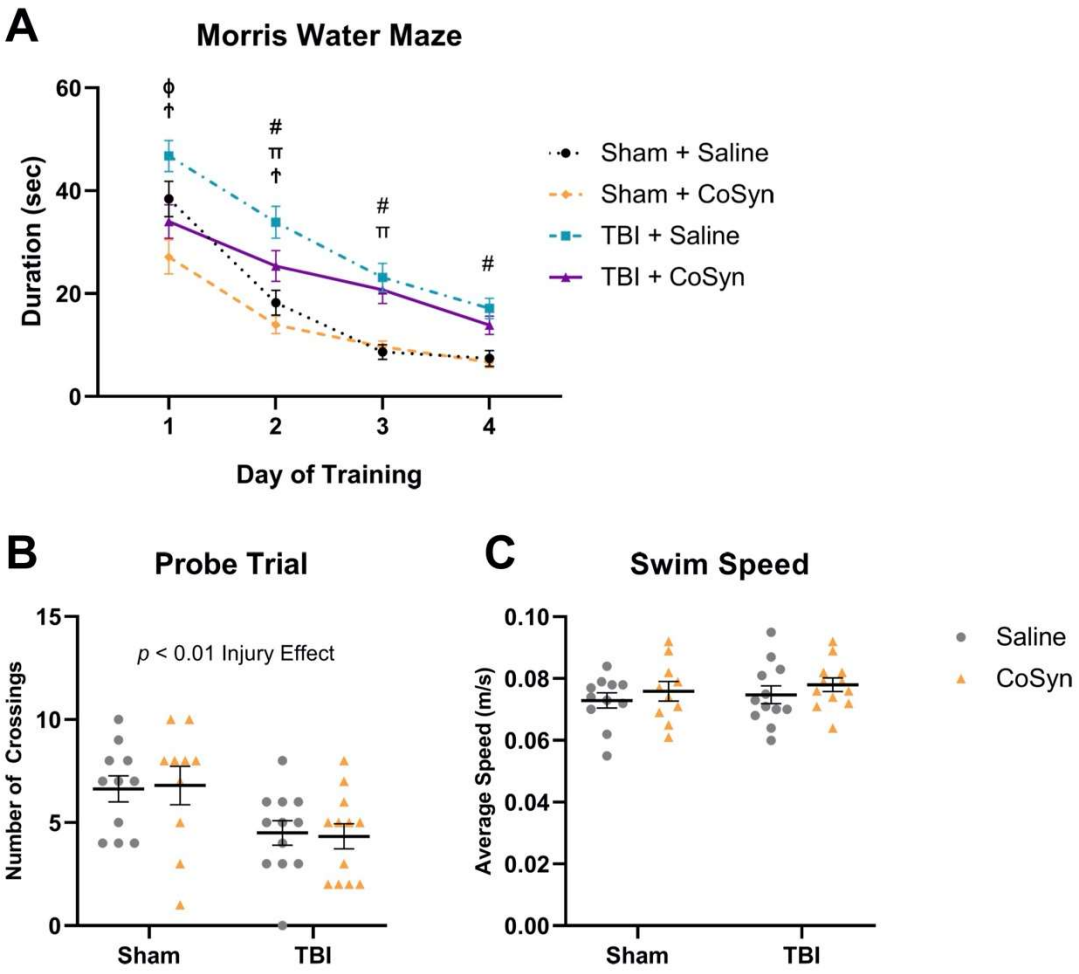

Figure 6. CoSyn induces modest improvements in early Morris water maze (MWM) performance post-TBI. (A) Mean duration to find platform across training days. All groups improved over the course of consecutive learning days. TBI mice treated with saline spent more time finding the platform compared to TBI mice treated with CoSyn and both sham groups on training days 1 and 2. Training day comparisons: Sham groups (ϕ), TBI groups (†), Saline groups (#), CoSyn groups (π). (B) A probe test was performed following the final training day. Both TBI groups had fewer platform crossings compared to sham groups. There was no significant difference between treated and untreated groups. (C) No differences were detected in swim speed between experimental groups during the probe trial. Sham-saline (n=10), sham-CoSyn (n=11), TBI-saline (n=12), TBI-CoSyn (n=12). Significance was determined using two-way ANOVA (B,C) and repeated-measures ANOVA (A) with Tukey post hoc testing. Graphs represent means and error bars show SEM, *p<0.05, **p<0.01, # p<0.0001.

platform over four consecutive days (Figure 6a). We saw both main effects for training day [$F(3,829)=75.7$, $p<0.0001$] and experimental group [$F(3,829)=31.19$, $p<0.0001$]. Post hoc analysis revealed that for both treatment groups, TBI resulted in overall spatial learning deficits as demonstrated by increased latency to find the platform during the final training days compared to sham groups (Figure 6a). On the first trial day, the Sham + CoSyn group found the platform significantly faster than the Sham + Saline group (Figure 6a, $p=0.0204$) with no difference in overall swim speed (data not shown). This pattern was replicated in the TBI groups with CoSyn-treated mice having reduced latency to find platform compared to the saline-treated TBI mice (Figure 6a, $p=0.0028$). Sham groups showed no differences in latency to find platform on days 2-4 of training (Figure 6a). CoSyn-treated TBI mice continued to show reduced latency time compared to saline-treated TBI mice on day two of training that did not persist through days 3–4 (Figure 6a, $p=0.0490$). Together, these data suggest a modest improvement in spatial reference memory acquisition for TBI animals when treated with CoSyn. To assess spatial memory retention, we performed the probe test 24 hours following the last training day and quantified the number of times the mice crossed the location which originally contained the platform during the training phase. We saw reduced number of crossings in injured versus sham groups [Figure 6B, $F(1,41)=11.15$, Injury effect, $p=0.0018$] with no treatment effect [Figure 6B. $F(1,41)<0.0001$, $p=0.998$]. No differences were detected in average swimming speed during the probe trial (Figure 6C).

Discussion

In this study, we investigated the effect of CoSyn administration in modulating inflammatory and behavioral outcomes following an experimental model of traumatic brain injury in mice. This is the first study to evaluate the therapeutic potential of CoSyn for the treatment of TBI. Our data showed that a one-week regimen of CoSyn following injury resulted in increased preservation of gross hippocampal size and improved spatial learning. At 3-days post injury, a 3 hr post-injury CoSyn treatment with daily administration attenuated accumulation of microglia/macrophages in perilesional cortex and the CA1 region of the hippocampus and led to decreased IL1β expression in cortical tissue but did not alter cytokine expression (IL1β and TNFα) in hippocampus. Our one-week treatment regimen did not alter chronic cortical loss as measured by cortical lesion size three-weeks post injury. Improved spatial learning in conjunction with reduced microglia/macrophage accumulation and neutrophil infiltration in our CoSyn treated TBI mice suggests an immune-cell mediated therapeutic effect of CoSyn following TBI.

Current acute management following TBI includes intracranial pressure monitoring, hypertonic saline, surgical intervention and seizure monitoring [46]. While chronic inflammation is well documented in TBI patients [4-6], limited pharmaceutical interventions directly target the inflammatory response. Long-acting cosyntropin could be such a compound and is an attractive pharmaceutical for its multifaceted immuno-modulatory capacity. Cosyntropin,

also referred to as tetracosactide, is a synthetic analog composed of the first 24 amino acids of the full length ACTH. ACTH was originally FDA approved in 1952 and, currently, two forms of ACTH have Food and Drug Administration approval for use in diagnostic testing of adrenal functioning including cosyntropin and H.P. Acthar Gel Repository Injection (Questcor Pharmaceuticals), the 39 amino acid natural form of the peptide [47]. Both the natural and synthetic variants stimulate all subtypes of the melanocortin receptors resulting in stimulation of the adrenal cortex to secrete glucocorticoids [20]. The most common indications for the use ACTH include adrenocortical testing and the treatment of multiple sclerosis and infantile spasms [47]. Due to a half-life of approximately 20 minutes in humans, several compounds have been developed to increase length of activity for the natural or synthetic variants of ACTH through the use of gels or zinc suspensions [48]. Both the Synacthen Depot (Novartis Pharmaceuticals) and the long-acting cosyntropin supplied by West Therapeutics use a zinc suspension to extend activity. H.P. Acthar Gel (Mallinckrodt Pharmaceuticals) has FDA approval in the US and Synacthen has approval for use in several European countries [32,47].

The most effective dosage and length of treatment for the synthetic and natural variants of ACTH remains uncertain. ACTH has been used clinically in the treatment of multiple sclerosis (MS) and infantile spasms with prolonged treatment periods extending several days to weeks [29,30,32]. A proposed clinical algorithm for MS relapse management suggests a 5–15 day regimen of ACTH

following non-response to methylprednisolone treatment [29]. Extended use of ACTH in the clinic results in side effects that include Cushing's syndrome, hypertension, ulcers and mood disturbances [32]. Taking into account both potential for side-effects as a result of extended use and the clinical treatment protocols that suggest multiple treatment days, we tested a 7-day protocol using a subcutaneous injection of long-acting cosyntropin and found reduction in early inflammatory response and improvements in cognitive functioning following TBI. Further research is needed to determine the best effective dosage and length of treatment to maximize drug efficacy and minimize side effects following TBI.

Furthermore, our study shows a CoSyn-induced increase in corticosterone following subcutaneous injection. Corticosterone is an agonist for glucocorticoid (GC) and mineralocorticoid receptors with differing binding affinities and dose-dependent effects on CNS function [49,50]. Several synthetic GC receptor agonists are widely used in the clinical setting with greater potency compared to endogenous GC agonists, including dexamethasone and methylprednisolone [49]. Unlike synthetic GC agonists, the circulating GC level induced by CoSyn is a result of MC2R activation and limited by the endogenous production capabilities of the adrenal glands. GCs have well-documented anti-inflammatory and neuroprotective effects. Some beneficial effects include decreased iNOS-mediated neurotoxicity *in vitro* [51], attenuation of LPS-induced TNFα expression [52] and suppression of IL1β and TNFα in the hippocampus (Dinkel, 2003, see review Sorrell et al., 2007). Due to its anti-inflammatory and potential neuroprotective

effects, methylprednisolone was used in a large, randomized, multi-center TBI clinical trial evaluating the effect of early administration on death and disability [38]. Results from this study indicate that high-dose methylprednisolone increases mortality following significant head injury and therefore suggests that synthetic glucocorticoids should not be used for the treatment of TBI [38,53]. Due to increased potency of synthetic GC agonists, the use of high-dose may have contributed to increased mortality. GC actions in the CNS are dosage, timing, and regionally-specific, with both pro- and anti-inflammatory effects contributing to neuronal vulnerability and survival [54]. In pre-clinical studies, the supraphysiological activation of GC receptors via synthetic analogs has also been shown to increase mortality along with contributing to increased hippocampal cell death following TBI [55].

Additionally, GCs have been shown to impair metabolism through inhibition of glucose uptake [54], reduce injury-induced BDNF [56] and contribute to CA1 hippocampal neuronal vulnerability following TBI [57]. In the kainic acid model of CNS injury, high glucocorticoid levels were also associated with increased macrophages and microglia density after three days of glucocorticoid exposure [58]. Conversely, glucocorticoids have also been shown to attenuate microglia/macrophage activation [59], reduce edema and brain infarct [60] and contribute to injury-induced increases in NGF following TBI [61]. Furthermore, as part of the HPA axis, GCs inhibit CRF and ACTH resulting in reduced expression of both hormones and chronic usage results in HPA axis suppression

[50]. As a melanocortin receptor agonist, ACTH also contributes to anti-inflammatory effects and metabolic regulation. In contrast to GCs, ACTH 1–24 increases glucose uptake in neurons through stimulation of transport protein synthesis, and MC4R-agonists increase BDNF *in vitro,* suggesting melanocortin receptor signaling may counteract deleterious effects of GC signaling [62,63]. The delicate balance between CRF, ACTH, and GCs in the maintenance of homeostasis and response to stress is vital for normal functioning and is disrupted following TBI [64]. Additional research is needed to evaluate the effect of synthetic ACTH as a post-TBI therapeutic specifically addressing if its effects are dependent on its GC-inducing capacity or extend beyond this mechanism of action, potentially counteracting the side effects of supraphysiological or prolonged GC activation.

Injury-induced weight loss is typical following experimental TBI and, in healthy mice, is followed by subsequent weight gain. Our research demonstrated these trends for both sham and TBI saline-treated mice. However, CoSyn-treated mice did not exhibit compensatory weight gain over the evaluated 7-days post-injury compared to their saline-treated counterparts resulting in a treatment effect of CoSyn administration. Along with grooming, nesting, posture, and movement, weight changes are an indicator of animal health [65]. As expected, both saline and CoSyn-treated mice displayed acute injury-induced signs of distress including hunched posture, sluggish movements and reduced nesting behavior. Along with our current selected dosage, our lab also investigated a

higher dose of CoSyn (3.4 U/mouse/day) which resulted in prolonged signs of distress including reduced grooming, sustained weight-loss and hunched posture (data not shown). While the CoSyn-treated mice did exhibit reduced weight gain, overt changes in grooming, nesting or posture between saline and CoSyn were not seen in the current study (1.2 U/mouse/day). Consistent with our recovery observations, CoSyn administration did not alter average speed in the open field test. However, lack of weight gain is concerning and additional dosage research is needed. Furthermore, the influence of ACTH and GCs on food intake, weight gain, and fat metabolism confounds the use of weight as an indicator of overall health. Prolonged exposure to increased GC levels can result in weight gain [66,67]. However, the GC-induced weight gain may require a dosage regimen extending further than 7-days, as used in our study, as previous work has shown that one week of increased GC levels did not result in increased body weight [66]. Furthermore, several studies have demonstrated that central administration of ACTH results in reduced food intake [68–70] and weight loss compared to vehicle when given *ad libitum* access to food [68]. Reduced weight gain following post-trauma weight loss could be indicative of poor outcome, and dosage studies taking into account food consumption and metabolic rates would be beneficial.

Traumatic brain injury results in a complex and dynamic cytokine profile. Interleukin-1-beta (IL1β) is an early inflammatory cytokine that is restored back to sham-levels within one week following injury and has been shown to be

involved in the secondary injury cascade [71–73]. IL1β neutralization studies demonstrated the causal role of increased IL1β levels in driving neuronal loss [74], circulating macrophage recruitment [75], injury-induced oligodendrocyte damage [76], and microglial activation and proliferation following TBI [74]. Collectively, these data suggest reduced IL1β is beneficial following experimental TBI. Our data did not show any alterations in IL1β expression in the hippocampus 3-days post-injury but did show significant reduction in IL1β expression following CoSyn treatment in cortical tissue and a treatment effect of CoSyn in serum. We also did not see any IL1β expression differences between sham and TBI-mice in the hippocampus although we saw differences in Iba1+ cell counts between TBI and Sham mice in the CA1 region at this time-point. Sham surgeries result in an acute inflammatory response that diminishes rapidly compared to brain-injured mice [73]. It is possible that we are seeing peak levels of IL1β expression at DPI 3 without time-dependent alterations in inflammatory resolution. Reduction in IL1β expression in cortical tissue at DPI 3 is consistent with previous research indicating melanocortin agonists reduce IL1β expression and NFkB signaling following CNS injury or an inflammatory insult [24,25,77]. No treatment or injury effect was observed with TNFα in cortical tissue. However, it is possible that we missed the window for TNFα expression increases as it has been shown to peak at 12 hours post injury and return to baseline by 18 hours following injury, with no differences between sham and TBI at DPI 1 and 3 in injured cortical or hippocampal tissue [78–80]. In contrast, TNFα has been reported to be increased in

patients' cerebrospinal fluid following moderate and severe TBI for one week post injury [81]. Interestingly, we found a main effect of injury in both hippocampal tissue and serum, showing decreased levels of TNFα in the injured compared to the sham group. During pro-inflammatory insults, TNFα modulates hippocampal circuitry and impairs learning [82]. However, genetic inhibition of TNFα alone does not alter lesion volume or functional outcome following TBI [45]. Dual inhibition of TNFα and Fas are required to confer neuroprotection and improved spatial memory performance after TBI [45]. Thus, reduced TNFα could be a beneficial endogenous and immunosuppressive response to TBI [83,84].

A limitation of our study is that we only evaluated cytokine expression at one time-point. Due to the complex and time-dependent nature of cytokine expression following TBI, additional research is needed to determine the effect of CoSyn on inflammatory resolution of cytokine expression in cortical and hippocampal tissue including earlier and later cytokine expression time-points and longitudinal changes in the cytokine storm.

Microglia activation has both beneficial and deleterious outcomes resulting from their dynamic response to injury. As demonstrated by microglia-depletion studies, microglia are neuroprotective resulting in decreased inflammation following brain injury [85]. However, microglia can also exaggerate the inflammatory response through TLR4 activation and NFκB signaling [86,87]. Sustained microglial activation also has been observed in patients who have experienced single TBIs and repeated-hit injuries that are associated with

reduced cognitive functioning [4–6]. Our observations indicate that CoSyn treatment following TBI results in reduced microglia/macrophage activation and recruitment in the perilesional cortex and CA1 region of the hippocampus. In the cortex, the microglia/macrophage response was limited in distribution indicating a more contained inflammatory response. As a result of IL1β involvement in microglia activation and proliferation as well as monocyte recruitment, our observed decreased microglia/macrophage density in the perilesional cortex and CA1 may be a result of CoSyn-mediated reduction in IL1β expression [74,75]. As the tissue-resident macrophage, microglia are key players in the inflammatory process following brain injury resulting in regenerative, phagocytic, and pro-/anti-inflammatory phenotypes [11]. Microglia not only phagocytose dying neurons but also play an important role in synaptic plasticity, a process necessary for healthy cognition [88]. Studies of microglia activation have demonstrated that melanocortin agonists suppress microglia/macrophage activation and promote a regenerative/anti-inflammatory phenotype, corresponding to increased Arg1 and decreased IL4Rα and TLR4 gene expression as well as prevention of HMGB1 translation from the nucleus to cytoplasm [18,26]. Along with suppression of microglia/macrophage proliferation and recruitment, an enhancement of regenerative microglia phenotypes may underlie the neuroprotective effects of CoSyn. Along with alterations in microglia/macrophage density, our data also demonstrate reduced neutrophil infiltration following CoSyn treatment during the early

neuroinflammatory response. Neutrophils infiltrate the brain following injury contributing to the TBI pathology [12,89]. Neutrophil infiltration exaggerates tissue loss and increases edema providing evidence for reduced neutrophil infiltration as beneficial following TBI [12].

Learning and memory deficits are one of the most frequently reported symptoms in TBI patients—along with fatigue and headaches—and are among the most enduring and disruptive consequences [90]. We have observed injury-induced spatial memory impairments with moderate CoSyn-mediated improvement of spatial learning as demonstrated by reduced latency time to the hidden platform in the Morris water maze. Normal learning and memory requires a delicate interplay of glia and neurons to form proper circuitry and dynamic synaptic connections [91]. Following injury, hippocampal circuitry and synaptic connections are altered resulting in spatial learning deficits [92,93]. Within the hippocampus, MC4Rs have been implicated in modulating synaptic plasticity, inflammation and cognition and may explain the effect of CoSyn on injury-induced cognitive deficits [94–96]. Melanocortin receptor 4 is found in the hippocampus, located in CA1–3 and in the dentate gyrus, a brain region vulnerable following TBI and involved in spatial memory [97,98]. Following ischemia, an MC4R-specific agonist improved injury-induced deficits in spatial learning [99]. A necessary mechanism of spatial learning is synaptic plasticity and dendritic stability in the hippocampus, which are compromised following TBI [100]. In an Alzheimer's disease model, α-MSH resulted in increased synaptic plasticity

as well as rescued synaptic plasticity deficits [98]. Not only do MC4R-specific agonists improve memory but ACTH-treatment in epileptic KCNA1-null mice demonstrated protection against learning and memory deficits induced by epilepsy [101]. ACTH administration also has been shown to reduce corticotropin-releasing factor (CRF) in the hippocampus via MC4R-signaling [96,102]. On the dendritic spines of the CA1 pyramidal cells, binding of CRF to CRF1 receptors lead to loss of dendritic spines which could impair synaptic plasticity and subsequent spatial learning [96]. Additional research is needed to determine if alterations in synaptic plasticity is contributing to the alterations in memory performance following CoSyn-treatment in our TBI mice.

A majority of research on the benefits of melanocortins following neuroinflammatory insult and acquired brain injuries investigates MC4R-signaling via synthetic variants of α-MSH. However, unlike α-MSH, ACTH is the only endogenous MC that activates MC2R in the adrenal cortex, stimulating corticosteroid (CS) production [20]. ACTH has been shown to be superior to CS in the treatment of multiple sclerosis and infantile spasms with hypsarrhythmia suggesting that stimulation of endogenously produced CS does not fully explain the immune modulatory effect of ACTH [103]. Corticosteroid use for the treatment of TBI has been evaluated in clinical studies with conflicting outcomes [2,38,46]. Dual activation of corticosteroid-dependent and independent responses through a synthetic ACTH analog may result in a more controlled and thorough resolution of the complex inflammatory response following TBI and may improve on

current clinical trials only evaluating corticosteroid use. In this study, we have not addressed the potential role of corticosteroid production on our observed outcomes and additional research is needed to identify the specific mechanisms of cosyntropin following TBI. Due to their varied expression in tissue and cell type, melanocortins have diverse functions documented in several reviews [15,99,104]. Of relevance to acquired brain injury, these functions include modulation of energy homeostasis [105], steroidogenesis [106,107], CNS immune modulation [25,108,109], neurogenesis and neuronal survival [19,99,110], synaptic plasticity [96,98] and peripheral immune cell trafficking [18,111]. While not within the scope of this study, the specific melanocortin receptors mediating neuroinflammatory modulation and neuroprotection following TBI is ripe for future investigation. Our study continues to support the increasing evidence for the use of melanocortin receptor agonists in the treatment of acquired brain injuries. Furthermore, melanocortin receptor agonists may have therapeutic potential not only in treatment of traumatic brain injury but may extend to other CNS disorders including Alzheimer's disease and chronic traumatic encephalopathy.

References

1. Flanagan, S. R. Invited Commentary on 'Centers for Disease Control and Prevention Report to Congress: Traumatic Brain Injury in the United States: Epidemiology and Rehabilitation'. *Arch Phys Med Rehabil* **96**, 1753–5 (2015).

2. Simon, D. W. *et al.* The far-reaching scope of neuroinflammation after traumatic brain injury. *Nature Reviews Neurology* **13**, 171–191 (2017).

3. Scherbel, U. *et al.* Differential acute and chronic responses of tumor necrosis factor-deficient mice to experimental brain injury. *Proc Natl Acad Sci U S A* **96**, 8721–6 (1999).

4. Ramlackhansingh, A. F. *et al.* Inflammation after trauma: Microglial activation and traumatic brain injury. *Annals of Neurology* **70**, 374–383 (2011).

5. Johnson, V. E. *et al.* Inflammation and white matter degeneration persist for years after a single traumatic brain injury. *Brain* **136**, 28–42 (2013).

6. Cherry, J. D. *et al.* Microglial neuroinflammation contributes to tau accumulation in chronic traumatic encephalopathy. *Acta Neuropathologica Communications* **4**, (2016).

7. Lindolfo da Silva Meirelles, Daniel Simon & Andrea Regner. Neurotrauma: The Crosstalk between Neurotrophins and Inflammation in the Acutely Injured Brain. *International Journal of Molecular Sciences* **18**, 1082 (2017).

8. Appleton, R. E. Post-traumatic epilepsy in children requiring inpatient rehabilitation following head injury. *Journal of Neurology, Neurosurgery & Psychiatry* **72**, 669–672 (2002).

9. Faden, A. I. & Loane, D. J. Chronic Neurodegeneration After Traumatic Brain Injury: Alzheimer Disease, Chronic Traumatic Encephalopathy, or Persistent Neuroinflammation? *Neurotherapeutics* **12**, 143–150 (2015).

10. Jin, X., Ishii, H., Bai, Z., Itokazu, T. & Yamashita, T. Temporal Changes in Cell Marker Expression and Cellular Infiltration in a Controlled Cortical Impact Model in Adult Male C57BL/6 Mice. *PLoS ONE* **7**, e41892 (2012).

11. Xu, H. *et al.* The Polarization States of Microglia in TBI: A New Paradigm for Pharmacological Intervention. *Neural Plasticity* **2017**, 1–11 (2017).

12. Kenne, E., Erlandsson, A., Lindbom, L., Hillered, L. & Clausen, F. Neutrophil depletion reduces edema formation and tissue loss following traumatic brain injury in mice. *Journal of Neuroinflammation* **9**, (2012).

13. Ma, Y. *et al.* Macrophage depletion reduced brain injury following middle cerebral artery occlusion in mice. *J Neuroinflammation* **13**, 38 (2016).

14. Younger, D., Murugan, M., Rama Rao, K. V., Wu, L.-J. & Chandra, N. Microglia Receptors in Animal Models of Traumatic Brain Injury. *Mol Neurobiol* **56**, 5202–5228 (2019).

15. Gallo-Payet, N. 60 YEARS OF POMC: Adrenal and extra-adrenal functions of ACTH. *Journal of Molecular Endocrinology* **56**, T135–T156 (2016).

16. Bertolini, A., Tacchi, R. & Vergoni, A. Brain effects of melanocortins☆. *Pharmacological Research* **59**, 13–47 (2009).

17. Kishi, T. *et al.* Expression of melanocortin 4 receptor mRNA in the central nervous system of the rat. *The Journal of Comparative Neurology* **457**, 213–235 (2003).

18. Chen, S. *et al.* Activation of melanocortin receptor 4 with RO27-3225 attenuates neuroinflammation through AMPK/JNK/p38 MAPK pathway after intracerebral hemorrhage in mice. *Journal of Neuroinflammation* **15**, (2018).

19. Lisak, R. P., Nedelkoska, L., Bealmear, B. & Benjamins, J. A. Melanocortin receptor agonist ACTH 1–39 protects rat forebrain neurons from apoptotic, excitotoxic and inflammation-related damage. *Experimental Neurology* **273**, 161–167 (2015).

20. Catania, A. Targeting Melanocortin Receptors as a Novel Strategy to Control Inflammation. *Pharmacological Reviews* **56**, 1–29 (2004).

21. Catania, A. Neuroprotective actions of melanocortins: a therapeutic opportunity. *Trends in Neurosciences* **31**, 353–360 (2008).

22. Montero-Melendez, T. ACTH: The forgotten therapy. *Seminars in Immunology* **27**, 216–226 (2015).

23. Holloway, P. M. *et al.* Both MC_1 and MC_3 Receptors Provide Protection From Cerebral Ischemia-Reperfusion–Induced Neutrophil Recruitment. *Arterioscler Thromb Vasc Biol.* **35**, 1936–1944 (2015).

24. Schaible, E.-V. *et al.* Single Administration of Tripeptide α-MSH(11–13) Attenuates Brain Damage by Reduced Inflammation and Apoptosis after Experimental Traumatic Brain Injury in Mice. *PLoS ONE* **8**, e71056 (2013).

25. Bitto, A. *et al.* Protective effects of melanocortins on short-term changes in a rat model of traumatic brain injury*. *Critical Care Medicine* **40**, 945–951 (2012).

26. Carniglia, L. *et al.* [Nle4, D-Phe7]-α-MSH Inhibits Toll-Like Receptor (TLR)2- and TLR4-Induced Microglial Activation and Promotes a M2-Like Phenotype. *PLOS ONE* **11**, e0158564 (2016).

27. Scholzen, T. E. *et al.* α-Melanocyte Stimulating Hormone Prevents Lipopolysaccharide-Induced Vasculitis by Down-Regulating Endothelial Cell Adhesion Molecule Expression. *Endocrinology* **144**, 360–370 (2003).

28. Harazin, A. *et al.* Protection of cultured brain endothelial cells from cytokine-induced damage by α-melanocyte stimulating hormone. *PeerJ* **6**, e4774 (2018).

29. Berkovich, R. Treatment of Acute Relapses in Multiple Sclerosis. *Neurotherapeutics* **10**, 97–105 (2013).

30. Nasiri, J., Sarajan, A., Salari, M. & Sedghi, M. Therapeutic Effects of Adrenocorticotropic Hormone ACTH in Children with Severely Intractable Seizure. **11**, 8 (2017).

31. Antunes, M. & Biala, G. The novel object recognition memory: neurobiology, test procedure, and its modifications. *Cognitive Processing* **13**, 93–110 (2012).

32. Food and Drug Administration. H.P. Acthar Gel (repository corticotropin) Injection. (2010).

33. Bajwa, N. M. *et al.* Mild Concussion, but Not Moderate Traumatic Brain Injury, Is Associated with Long-Term Depression-Like Phenotype in Mice. *PLOS ONE* **11**, e0146886 (2016).

34. Siebold, L., Obenaus, A. & Goyal, R. Criteria to define mild, moderate, and severe traumatic brain injury in the mouse controlled cortical impact model. *Experimental Neurology* **310**, 48–57 (2018).

35. Decker, D. *et al.* Immunomodulatory effects of H.P. Acthar Gel on B cell development in the NZB/W F1 mouse model of systemic lupus erythematosus. *Lupus* **23**, 802–812 (2014).

36. Cusick, M. F., Libbey, J. E., Oh, L., Jordan, S. & Fujinami, R. S. Acthar gel treatment suppresses acute exacerbations in a murine model of relapsing-remitting multiple sclerosis. *Autoimmunity* **48**, 222–230 (2015).

37. Arrat, H., Lukas, T. J. & Siddique, T. ACTH (Acthar Gel) Reduces Toxic SOD1 Protein Linked to Amyotrophic Lateral Sclerosis in Transgenic Mice: A Novel Observation. *PLOS ONE* **10**, e0125638 (2015).

38. Roberts, I, Yates, D & Sandercock, P. Effect of intravenous corticosteroids on death within 14 days in 10008 adults with clinically significant head injury (MRC CRASH trial): randomized placebo-controlled trial.

39. Mohamadpour, M., Whitney, K. & Bergold, P. J. The Importance of Therapeutic Time Window in the Treatment of Traumatic Brain Injury. *Frontiers in Neuroscience* **13**, (2019).

40. Fox, C. *et al.* Minocycline Confers Early but Transient Protection in the Immature Brain following Focal Cerebral Ischemia—Reperfusion. *J Cereb Blood Flow Metab* **25**, 1138–1149 (2005).

41. Brown, D. L. Bias in image analysis and its solution: unbiased stereology. *J Toxicol Pathol* **30**, 183–191 (2017).

42. Mouton, Peter R. *Principles and Practices of Unbiased Stereology: An Introduction for Bioscientists*. (Johns Hopkins University Press, 2002).

43. Golub, V. M. *et al.* Neurostereology protocol for unbiased quantification of neuronal injury and neurodegeneration. *Front. Aging Neurosci.* **7**, (2015).

44. Marcos, R., Monteiro, R. A. F. & Rocha, E. The use of design-based stereology to evaluate volumes and numbers in the liver: a review with practical guidelines: Design-based stereology in hepatology. *Journal of Anatomy* **220**, 303–317 (2012).

45. Bermpohl, D., You, Z., Lo, E. H., Kim, H.-H. & Whalen, M. J. TNF Alpha and Fas Mediate Tissue Damage and Functional Outcome after Traumatic Brain Injury in Mice. *J Cereb Blood Flow Metab* **27**, 1806–1818 (2007).

46. Vella, M. A., Crandall, M. L. & Patel, M. B. Acute Management of Traumatic Brain Injury. *Surgical Clinics of North America* **97**, 1015–1030 (2017).

47. Gettig, J., Cummings, J. P. & Matuszewski, K. H.P. Acthar Gel and Cosyntropin Review. 8 (2009).

48. Veldhuis, J. D. *et al.* Corticotropin Secretory Dynamics in Humans under Low Glucocorticoid Feedback. 10.

49. Aharon, M. A., Prittie, J. E. & Buriko, K. A review of associated controversies surrounding glucocorticoid use in veterinary emergency and critical care: Glucocorticoid use in emergency and critical care. *Journal of Veterinary Emergency and Critical Care* **27**, 267–277 (2017).

50. Paragliola, R. M., Papi, G., Pontecorvi, A. & Corsello, S. M. Treatment with Synthetic Glucocorticoids and the Hypothalamus-Pituitary-Adrenal Axis. *IJMS* **18**, 2201 (2017).

51. Golde, S., Coles, A., Lindquist, J. A. & Compston, A. Decreased iNOS synthesis mediates dexamethasone-induced protection of neurons from inflammatory injury in vitro. *Eur J Neurosci* **18**, 2527–2537 (2003).

52. Nadeau, S. & Rivest, S. Endotoxemia Prevents the Cerebral Inflammatory Wave Induced by Intraparenchymal Lipopolysaccharide Injection: Role of Glucocorticoids and CD14. *J Immunol* **169**, 3370–3381 (2002).

53. Edwards, P., Arango, M., Balica, L., Cottingham, R. & El-Sayed, H. Final results of MRC CRASH, a randomised placebo-controlled trial of intravenous corticosteroid in adults with head injury—outcomes at 6 months. *The Lancet* **365**, 1957–1959 (2005).

54. Sorrells, S. F. & Sapolsky, R. M. An inflammatory review of glucocorticoid actions in the CNS. *Brain, Behavior, and Immunity* **21**, 259–272 (2007).

55. Chen, X., Zhang, K.-L., Yang, S.-Y., Dong, J.-F. & Zhang, J.-N. Glucocorticoids Aggravate Retrograde Memory Deficiency Associated with Traumatic Brain Injury in Rats. *Journal of Neurotrauma* **26**, 253–260 (2009).

56. Grundy, P. L., Patel, N., Harbuz, M. S., Lightman, S. L. & Sharples, P. M. Glucocorticoids modulate BDNF mRNA expression in the rat hippocampus after traumatic brain injury: *NeuroReport* **11**, 3381–3384 (2000).

57. McCullers, D. L., Sullivan, P. G., Scheff, S. W. & Herman, J. P. Mifepristone protects CA1 hippocampal neurons following traumatic brain injury in rat. *Neuroscience* **109**, 219–230 (2002).

58. Dinkel, K., MacPherson, A. & Sapolsky, R. M. Novel glucocorticoid effects on acute inflammation in the CNS: Glucocorticoids and CNS inflammation. *Journal of Neurochemistry* **84**, 705–716 (2003).

59. Zhang, Z., Zhang, Z., Artelt, M., Burnet, M. & Schluesener, H. J. Dexamethasone attenuates early expression of three molecules associated with microglia/macrophages activation following rat traumatic brain injury. *Acta Neuropathol* **113**, 675–682 (2007).

60. Campolo, M. *et al.* Combination therapy with melatonin and dexamethasone in a mouse model of traumatic brain injury. *The Journal of endocrinology* **217**, 291–301 (2013).

61. Grundy, P. L., Patel, N., Harbuz, M. S., Lightman, S. L. & Sharples, P. M. Glucocorticoids modulate the NGF mRNA response in the rat hippocampus after traumatic brain injury. *Brain Research* **892**, 386–390 (2001).

62. Daval, J.-L., Anglard, P., Gerard, M.-J., Vincendon, G. & Louis, J.-C. Regulation of deoxyglucose uptake by adrenocorticotropic hormone in cultured neurons. *J. Cell. Physiol.* **124**, 75–80 (1985).

63. Saba, J. *et al.* Melanocortin 4 receptor activation protects striatal neurons and glial cells from 3-nitropropionic acid toxicity. *Molecular and Cellular Neuroscience* **94**, 41–51 (2019).

64. Tapp, Z. M., Godbout, J. P. & Kokiko-Cochran, O. N. A Tilted Axis: Maladaptive Inflammation and HPA Axis Dysfunction Contribute to Consequences of TBI. *Front. Neurol.* **10**, 345 (2019).

65. Burkholder, T., Foltz, C., Karlsson, E., Linton, C. G. & Smith, J. M. Health Evaluation of Experimental Laboratory Mice. *Current Protocols in Mouse Biology* **2**, 145–165 (2012).

66. Do, T. T. H. *et al.* Glucocorticoid-induced insulin resistance is related to macrophage visceral adipose tissue infiltration. *The Journal of Steroid Biochemistry and Molecular Biology* **185**, 150–162 (2019).

67. Scerif, M. *et al.* CB1 receptor mediates the effects of glucocorticoids on AMPK activity in the hypothalamus. *Journal of Endocrinology* **219**, 79–88 (2013).

68. Al-Barazanji, K. A., Miller, J. E., Rice, S. Q. J., Arch, J. R. S. & Chambers, J. K. C-Terminal Fragments of ACTH Stimulate Feeding in Fasted Rats. *Horm Metab Res* **33**, 480–485 (2001).

69. Shipp, S. L., Yi, J., Dridi, S., Gilbert, E. R. & Cline, M. A. The central anorexigenic mechanism of adrenocorticotropic hormone involves the caudal hypothalamus in chicks. *Neuropeptides* **53**, 29–35 (2015).

70. Schulz, C., Paulus, K., Lobmann, R., Dallman, M. & Lehnert, H. Endogenous ACTH, not only α-melanocyte-stimulating hormone, reduces food intake mediated by hypothalamic mechanisms. *American Journal of Physiology-Endocrinology and Metabolism* **298**, E237–E244 (2010).

71. Dalgard, C. L. *et al.* The cytokine temporal profile in rat cortex after controlled cortical impact. *Front Mol Neurosci* **5**, 6 (2012).

72. Taib, T. *et al.* Neuroinflammation, myelin and behavior: Temporal patterns following mild traumatic brain injury in mice. *PLOS ONE* **12**, e0184811 (2017).

73. Lagraoui, M. *et al.* Controlled Cortical Impact and Craniotomy Induce Strikingly Similar Profiles of Inflammatory Gene Expression, but with Distinct Kinetics. *Frontiers in Neurology* **3**, (2012).

74. Ozen, I. *et al.* Interleukin-1 Beta Neutralization Attenuates Traumatic Brain Injury-Induced Microglia Activation and Neuronal Changes in the Globus Pallidus. *IJMS* **21**, 387 (2020).

75. Basu, A. *et al.* The Type 1 Interleukin-1 Receptor Is Essential for the Efficient Activation of Microglia and the Induction of Multiple Proinflammatory Mediators in Response to Brain Injury. *J. Neurosci.* **22**, 6071–6082 (2002).

76. Flygt, J. *et al.* Neutralization of Interleukin-1β following Diffuse Traumatic Brain Injury in the Mouse Attenuates the Loss of Mature Oligodendrocytes. *Journal of Neurotrauma* **35**, 2837–2849 (2018).

77. Ichiyama, T. *et al.* Systemically administered a-melanocyte-stimulating peptides inhibit NF-kB activation in experimental brain inflammation. 7 (1999).

78. Baratz, R. *et al.* Transiently lowering tumor necrosis factor-α synthesis ameliorates neuronal cell loss and cognitive impairments induced by minimal traumatic brain injury in mice. *J Neuroinflammation* **12**, 45 (2015).

79. Dong, T., Zhi, L., Bhayana, B. & Wu, M. X. Cortisol-induced immune suppression by a blockade of lymphocyte egress in traumatic brain injury. *Journal of Neuroinflammation* **13**, (2016).

80. Robinson, S. *et al.* Microstructural and microglial changes after repetitive mild traumatic brain injury in mice: Microstructure in Repetitive Mild Brain Injury. *Journal of Neuroscience Research* **95**, 1025–1035 (2017).

81. Feng, G. *et al.* Altered levels of α-melanocyte stimulating hormone in cerebrospinal fluid and plasma of patients with traumatic brain injury. *Brain Research* **1696**, 22–30 (2018).

82. Habbas, S. *et al.* Neuroinflammatory TNFα Impairs Memory via Astrocyte Signaling. *Cell* **163**, 1730–1741 (2015).

83. Mazzeo, A. T. *et al.* Severe Human Traumatic Brain Injury, but Not Cyclosporin A Treatment, Depresses Activated T Lymphocytes Early after Injury. *Journal of Neurotrauma* **23**, 962–975 (2006).

84. Hazeldine, J., Lord, J. M. & Belli, A. Traumatic Brain Injury and Peripheral Immune Suppression: Primer and Prospectus. *Front. Neurol.* **6**, (2015).

85. Jin, W.-N. *et al.* Depletion of microglia exacerbates postischemic inflammation and brain injury. *Journal of Cerebral Blood Flow & Metabolism* **37**, 2224–2236 (2017).

86. Ahmad, A. *et al.* Absence of TLR4 reduces neurovascular unit and secondary inflammatory process after traumatic brain injury in mice. *PLoS One* **8**, e57208 (2013).

87. Yao, X. *et al.* TLR4 signal ablation attenuated neurological deficits by regulating microglial M1/M2 phenotype after traumatic brain injury in mice. *Journal of neuroimmunology* **310**, 38–45 (2017).

88. Blank, T. & Prinz, M. Microglia as modulators of cognition and neuropsychiatric disorders. *Glia* **61**, 62–70 (2013).

89. Carlos, T. M., Clark, R. S. B., Franicola-Higgins, D., Schiding, J. K. & Kochanek, P. M. Expression of endothelial adhesion molecules and recruitment of neutrophils after traumatic brain injury in rats. *J Leukoc Biol* **61**, 279–285 (1997).

90. Paniak, C. *et al.* Patient complaints within 1 month of mild traumatic brain injury: A controlled study. *Archives of Clinical Neuropsychology* 16 (2002).

91. Sajja, V. S. S. S., Hlavac, N. & VandeVord, P. J. Role of Glia in Memory Deficits Following Traumatic Brain Injury: Biomarkers of Glia Dysfunction. *Front. Integr. Neurosci.* **10**, (2016).

92. Merlo, L. *et al.* Alteration in Synaptic Junction Proteins following Traumatic Brain Injury. *Journal of Neurotrauma* **31**, 1375–1385 (2014).

93. Logue, O. C., Cramer, N. P., Xu, X., Perl, D. P. & Galdzicki, Z. Alterations of functional properties of hippocampal networks following repetitive closed-head injury. *Experimental Neurology* **277**, 227–243 (2016).

94. Yang, J. *et al.* Neonatal BCG vaccination of mice improves neurogenesis and behavior in early life. *Brain Res Bull* **120**, 25–33 (2016).

95. Machado, I., Schiöth, H. B., Lasaga, M. & Scimonelli, T. IL-1β reduces GluA1 phosphorylation and its surface expression during memory reconsolidation and α-melanocyte-stimulating hormone can modulate these effects. *Neuropharmacology* **128**, 314–323 (2018).

96. Shen, Y., Fu, W.-Y., Cheng, E. Y. L., Fu, A. K. Y. & Ip, N. Y. Melanocortin-4 Receptor Regulates Hippocampal Synaptic Plasticity through a Protein Kinase A-Dependent Mechanism. *Journal of Neuroscience* **33**, 464–472 (2013).

97. Joksimovic, J. *et al.* Exercise Attenuates Anabolic Steroids-Induced Anxiety via Hippocampal NPY and MC4 Receptor in Rats. *Front. Neurosci.* **13**, 172 (2019).

98. Shen, Y. *et al.* Stimulation of the Hippocampal POMC/MC4R Circuit Alleviates Synaptic Plasticity Impairment in an Alzheimer's Disease Model. *Cell Reports* **17**, 1819–1831 (2016).

99. Spaccapelo, L. *et al.* Melanocortin MC4 receptor agonists counteract late inflammatory and apoptotic responses and improve neuronal functionality after cerebral ischemia. *European Journal of Pharmacology* **670**, 479–486 (2011).

100. Gao, X., Deng, P., Xu, Z. C. & Chen, J. Moderate Traumatic Brain Injury Causes Acute Dendritic and Synaptic Degeneration in the Hippocampal Dentate Gyrus. *PLoS ONE* **6**, e24566 (2011).

101. Scantlebury, M. H., Chun, K.-C., Ma, S.-C., Rho, J. M. & Kim, D. Y. Adrenocorticotropic hormone protects learning and memory function in epileptic Kcna1 -null mice. *Neuroscience Letters* **645**, 14–18 (2017).

102. Brunson, K. L., Khan, N., Eghbal-Ahmadi, M. & Baram, T. Z. Corticotropin (ACTH) Acts Directly on Amygdala Neurons to Down-Regulate Corticotropin-Releasing Hormone Gene Expression. 17 (2010).

103. Ross, A. P., Ben-Zacharia, A., Harris, C. & Smrtka, J. Multiple Sclerosis, Relapses, and the Mechanism of Action of Adrenocorticotropic Hormone. *Frontiers in Neurology* **4**, (2013).

104. Montero-Melendez, T., Gobbetti, T., Cooray, S. N., Jonassen, T. E. N. & Perretti, M. Biased Agonism as a Novel Strategy To Harness the Proresolving Properties of Melanocortin Receptors without Eliciting Melanogenic Effects. *The Journal of Immunology* **194**, 3381–3388 (2015).

105. Krashes, M. J., Lowell, B. B. & Garfield, A. S. Melanocortin-4 receptor–regulated energy homeostasis. *Nature Neuroscience* **19**, 206–219 (2016).

106. Chen, M., Aprahamian, C. J., Kesterson, R. A., Harmon, C. M. & Yang, Y. Molecular Identification of the Human Melanocortin-2 Receptor Responsible for Ligand Binding and Signaling †. *Biochemistry* **46**, 11389–11397 (2007).

107. Goverde, H. J. M. & Smals, A. G. H. The anomalous effect of some ACTH-fragments missing the amino acid sequence 1-10 on the corticosteroidogenesis in purified isolated rat adrenal cells. *FEBS Letters* **173**, 23–26 (1984).

108. Montero-Melendez, T. *et al.* The Melanocortin Agonist AP214 Exerts Anti-Inflammatory and Proresolving Properties. *The American Journal of Pathology* **179**, 259–269 (2011).

109. Huang, Q. & Tatro, J. B. a-melanocyte stimulating hormone suppresses intracerebral tumor necrosis factor-a and interleukin-1b gene expression following transient cerebral ischemia in mice. *Neuroscience Letters* 5 (2002).

110. Giuliani, D. *et al.* Treatment of cerebral ischemia with melanocortins acting at MC4 receptors induces marked neurogenesis and long-lasting functional recovery. *Acta Neuropathol* **122**, 443–453 (2011).

111. Getting, S. J., Christian, H. C., Flower, R. J. & Perretti, M. Activation of melanocortin type 3 receptor as a molecular mechanism for adrenocorticotropic hormone efficacy in gouty arthritis. *Arthritis & Rheumatism* **46**, 2765–2775 (2002).

CHAPTER FOUR

COSYNTROPIN MODULATES MICROGLIA MORPHOLOGY AND CYTOKINE EXPRESSION FOLLOWING EXPERIMENTAL TRAUMATIC BRAIN INJURY IN MICE

Lorraine Siebold, Jonathan Abdala, Johnny D. Figueroa, Brenda Bartnik-Olson, Barbara Holshouser, Stephen Ashwal, Christopher G. Wilson

The Lawrence D. Longo, MD Center for Perinatal Biology
Department of Basic Sciences
Division of Physiology
Loma Linda University School of Medicine
Loma Linda, California 92350

Introduction

Traumatic brain injury (TBI) is a significant public health concern and a leading cause of death and disability in the United States. Estimates place adult lifetime prevalence of TBI at almost 40% with over two million TBI-related emergency department visits and 50,000 deaths reported by the Centers for Disease Control and Prevention in 2014 [1,2]. TBI is a result of an external mechanical force to the brain that alters brain function and can lead to devastating long-term consequences [3]. Following the initial mechanical force, referred to as the primary injury, a secondary injury cascade contributes to injury pathology. The secondary response includes glutamate-induced excitotoxicity [4,5], programmed neuronal death [6], mitochondrial dysfunctions [7,8], cerebrovascular abnormalities [9,10], and a robust inflammatory response [3]. The neuroinflammatory response is initiated minutes after injury and is associated with increased intracranial pressure and mortality [11] as well as a risk factor for the development of epilepsy and neurodegenerative disorders [12–14]. Furthermore, chronic neuroinflammation has been reported decades after the primary injury and is associated with cognitive deficits [15].

Neuroinflammation is a result of increased cytokine expression, including both pro and anti-inflammatory cytokines, in response to detection of damage-associated molecular patterns (DAMPS) and gene expression changes through NF-kB signaling [3,16]. Elevations in TNFα, IL1β, IL-10 and IL-6 have all been reported within the first few days following injury in both pre-clinical and

clinical studies [17–22]. Along with cytokine expression, microglia activation and peripheral immune cell infiltration into the brain parenchyma contribute to the inflammatory response. As the tissue resident macrophage, microglia contribute to injury progression as well as assist in recovery through cleaning of the injured area and tissue remodeling indicative of their diverse phenotypes [23,24]. Following injury, microglia undergo rapid and robust morphological changes taking on a more amoeboid shape with a reduction, thickening and shortening of their ramifications [25–27] Microglia-depletion and repopulation studies have suggested modulation of microglia phenotype, rather than quantity alone, is necessary for the neuroprotective effect of microglia following TBI [28]. Due to the chronic, unresolved and robust nature of neuroinflammation following TBI, anti-inflammatory compounds have been evaluated for us in the clinic. However, to date, no pharmaceutical interventions modulating post-TBI neuroinflammation have been successful in improving clinical outcomes [29].

Melanocortins (MCs) are a family of peptides endogenously derived from pro-opiomelanocortin precursors [30]. MCs include compounds such as adrenocorticotropic hormone (ACTH) and α-melanocyte stimulating hormone (α-MSH), both of which are agonists for melanocortin receptor 4 (MC4R) with ACTH being the only endogenous agonist for melanocortin receptor 2 (MC2R) [30,31]. MC2Rs are located in the adrenal glands and binding of ACTH results in an increase in circulating glucocorticoids [32]. MC4R is expressed in the hypothalamus, hippocampus and cortex in the central nervous system owing to

its involvement in a diverse set of behavioral responses, including yawning, grooming, food consumption and memory [31]. Along with its role in behavior, MC4R agonists have also been shown to be immune modulators and neuroprotective following both brain ischemia and TBI [33–35]. MC4R agonists have also been shown to inhibit NF-kB activation in LPS-induced inflammation and reduce neuronal cell death *in vitro* [36,37]. Furthermore, administration of α-MSH—an MCR agonist without glucocorticoid-inducing effects—reduced injury-induced changes in microglia morphology following TBI, decreased microglia/macrophage density following intracerebral hemorrhage, and modulated microglia phenotype through increased Arg1 expression *in vivo* [33,38,39]. Taken together, these data suggest that MC4R agonists may be beneficial following TBI through inhibition of cytokine expression and modulation of microglia phenotype.

Cosyntropin is a synthetic ACTH analog and agonist for all five subtypes of melanocortin receptors, with high affinity for receptors MC2R and MC4R [32,40]. In this study, we investigated the effects of a long-acting synthetic ACTH analog (CoSyn, ACTH 1-24) on neuroinflammation and immune cell response following experimental TBI. We hypothesized that CoSyn would reduce the early neuroinflammatory response following TBI.

Methods

Animals

Ninety-seven 3-month old male C57Bl6 (Jackson Lab) mice were used for this study. Mice were housed in LLU's Animal Care Facilty on a 12-hour light-dark cycle with lights turned on/off at 7:00 am/pm. Food and water were supplied *ad libitum* and food pellets were placed on the cage floor following surgery to allow access to food. Mice were randomly assigned to four experimental groups: sham + saline, sham + CoSyn, TBI + saline, or TBI + CoSyn. All procedures were approved by the Institutional Animal Care and Use Committee at Loma Linda University, Loma Linda, California. To avoid unnecessary use of experimental animals, we performed interim statistical analyses after pre-specified N values were collected.

Controlled Cortical Impact Model

We used the controlled cortical impact model as previously described [41]. Animals were anesthetized with isoflurane (1–3%), shaved, and the surgical area cleaned with surgical soap, 70% isopropyl alcohol and βdine. A lidocaine injection was given prior to incision to expose the skull. After skin was retracted, we made a 5.0 mm diameter craniectomy—centered between bregma and lambda and 2.5 mm lateral to the sagittal suture—to expose underlying dura and cortex. The injury was induced with a 3.0 mm flat-tipped, metal impactor. The impactor was centered within the craniectomy site and impact occurred with a velocity of 5.3 m/s, depth of 1.5 mm, and dwell time of 100 ms. Immediately

following injury, the injury site was cleaned of blood and a sterile polystyrene skull-cap was placed over the craniectomy site and sealed with VetBond (3M, St. Paul MN). The incision was sutured and mice received an injection of saline for hydration and buprenorphine for pain prevention. Mice were placed in a heated recovery chamber and monitored for 1 hr prior to returning to their home cage. Daily weights were taken for the first 7 days to monitor recovery. These injury parameters resulted in a severe injury composed of cortical and hippocampal loss and sustained behavioral deficits [42]. The same investigator performed all TBI and sham surgeries.

CoSyn or Vehicle Treatment

For our treatment we used a subcutaneous injection of long-acting cosyntropin, a synthetic analogue of ACTH (amino acids 1-24). Based on previous literature, a dosage of 1.8 U/mouse/day was selected [43–45]. A 3-hour post-injury treatment was selected to modulate the early inflammatory response using a clinically relevant time-point [46,47]. For treatment and vehicle experimental groups, we administered CoSyn or saline treatments 3-hours following cortical impact (TBI groups) or craniectomy (sham groups) with all initial treatments taking place prior to 19:00 on the day of surgery. Following the surgical day, mice were treated for up to 7 consecutive days with morning (07:00) injections. Mice were administered 50 µL of saline or CoSyn (50 µL = 1.8 units/dose) subcutaneously. CoSyn was supplied by West Therapeutic Development, LLC (Grayslake, IL, USA).

Tissue Collection and Cytokine Quantification

For cytokine analysis, we anesthetized mice at day post injury (DPI) one, three and seven (Figure1A). Mice were then perfused with PBS and brains were quickly extracted. The hippocampus and ipsilateral cortex, containing the lesion and perilesional cortex were isolated in ice-cold PBS followed by flash-freezing in liquid nitrogen (N = 3-5/group). Samples were homogenized in a protein isolation buffer with protease inhibitors (Halt Protease Inhibitor Cocktail; Sigma-Aldrich, St. Louis, MO, USA) as previously described [48]. Homogenized tissue was spun down at 14k g for 20 minutes at 4° C and supernatant collected. Total protein content of supernatant was quantified using the Pierce BCA protein assay (Pierce Biotechnology, Rockford, IL, USA). Cytokines were quantified with the use of the 16-plex, Multiplex ELISA kit for mouse cytokines (Boster Biological Technology, Pleasanton, CA). The multiplex ELISA quantified protein levels for the following cytokines: IL-1α, IL-1β, IL-2, IL-3, IL-4, IL-5, IL-6, IL-10, IL-12p70, IL-17, MCP-1, IFNy, TNFα, MIP-1α, GMCSF, and RANTES. Buffer-only tests were run to confirm no false-positive values were present due to buffer interactions. All tissue homogenates fell within the stated ranges of the multiplex ELISA. All data points are averages of triplicate runs and tissue homogenates are reported as picogram (pg) of analyte per milligram (mg) of total protein.

Immunohistochemistry

For immunostaining analysis, mice were perfused at DPI 3 with PBS followed by 4% PFA. Brains were extracted and placed in 4% PFA overnight

followed by PBS washes and 30% sucrose for 48 hours. Twenty-five micrometer sections between at approximately Bregma -2.0 were captured. For microglia/macrophage (Iba1), staining consisted of blocking endogenous peroxide activity with quenching buffer (10% methanol, 1% hydrogen peroxide in PBS) followed by blocking with Avidin/Biotin blocking Kit (AbCam, USA) and normal serum (5% Donkey and 5% Goat serum) with 1% Triton-X in PBS. Sections were incubated overnight with a polyclonal rabbit anti-Iba1 primary antibody (1:750, Rabbit anti-Iba1, Catalog no. 019-19741, Wako, USA) and followed by secondary biotinylated antibody incubation (1:200, goat anti-rabbit IgG, Vector). The Vectastain Elite ABC HRP kit and DAB peroxidase substrate kit with nickel (Vector, Burlingame, CA) were used to visualize staining according to manufacturer instructions. Following staining, slides were dehydrated in ethanol and coverslipped with Permount Mounting Medium (Fisher Chemical).

Image Acquisition and Processing for Morphology

Images of Iba1 stained tissue sections were acquired using the Keyence 9000 (Keyence Corporation, Osaka, Japan) using the 60x oil-immersion objective and full-focus capturing software. Images were analyzed using *ImageJ* software **.** All morphology analysis was performed in a blinded fashion on binary images isolated using the following procedure (Figure1B):

1) Roughly selected around the cell. No other cell components were within the selection. Added the selection to the ROI manager and duplicated the image to isolate the cell of interest (Figure1B, Step 1).
2) Smoothed the image once, thresholded image to create binary image (Figure1B, Step 2).
3) Created a binary outline image from the binary image (Figure 1B, Step 2).

Following microglia cell isolation, *FracLac* for *ImageJ* was used to quantify morphology (Figure 1B, Step 3)[49]. While additional parameters and information can be obtained from the analysis, we report twelve morphological features (Figure 1C). Injury induces robust changes in microglia/macrophage morphology (Figure 1D). When using *FracLac*, we chose to analyze microglia using 12 randomized grids with power series scaling method at 45% of maximum image size. Hull and circle metrics were also calculated during analysis. To increase processing, all individual cells were saved as individual images and were batch-processed using the *FracLac* Batch Process option. These parameters were chosen based in their ability to distinguish morphological differences between three artificially created microglia representing the range of microglia morphology.

Statistical Analysis

All bar graph values in figures and text are expressed as mean and standard error of the mean. Two-way ANOVA was used to evaluate difference in means between the four experimental groups for ELISA analytes and

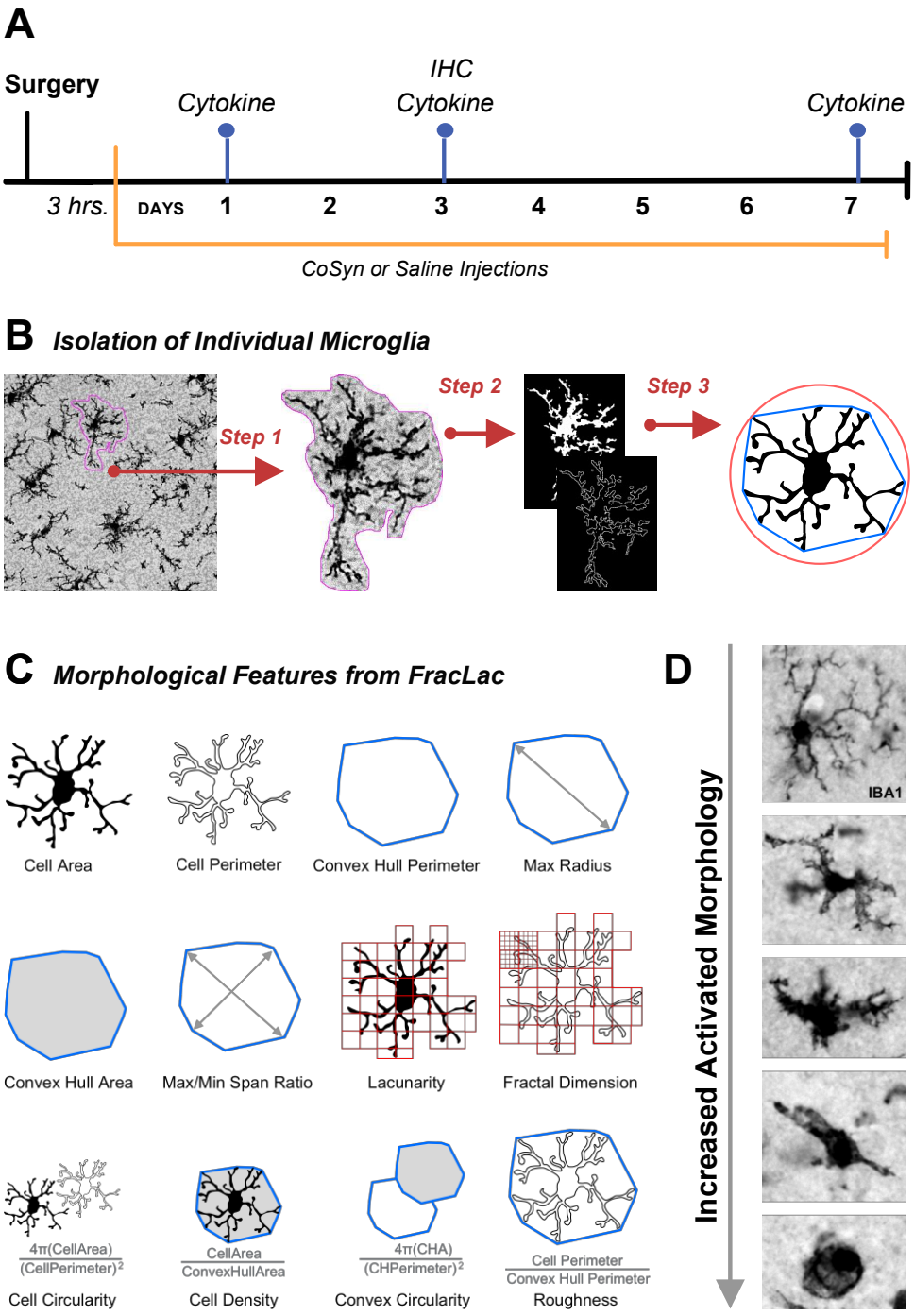

Figure 1. Representation of experimental design (A), microglia/macrophage isolation method (B) and morphological quantification (C-D).

morphology. Morphological parameters of circularity and density did not meet the assumption of homogeneity of variance and Levene's median test was performed. Tukey's multiple comparisons test was completed for post hoc analysis. No values were excluded. All statistical analyses were performed and graphs created with GraphPad Prism software, version 8.1.2 (GraphPad Software, Inc., San Diego, CA), p values < 0.05 were considered statistically significant.

Results

CoSyn Attenuates Injury-Induced Microglia/Macrophage Changes

To test the influence of CoSyn on microglia activation, we quantified morphological features of Iba1-positive cell at DPI three (Figure 2). Several morphological parameters exhibited both injury and treatment effects (Table 1). CoSyn attenuated injury-induced increases in both circularity (p=0.005) and density (p=0.00, Figure 2A). Nested graph shows variability in density within individual mouse brains with more variability in the TBI + Saline group than the CoSyn-treated brains (Figure 2B), comparison of variability through calculation of absolute distance from the median shows both main effect and injury-induced differences in density with post hoc comparison revealing a significant difference between the TBI groups (Figure 2C, p=0.0011, main effect of injury [F(1,305)=21.47, p<0.0001, main effect of treatment [F(1,305)=6.459, p=0.0115]).

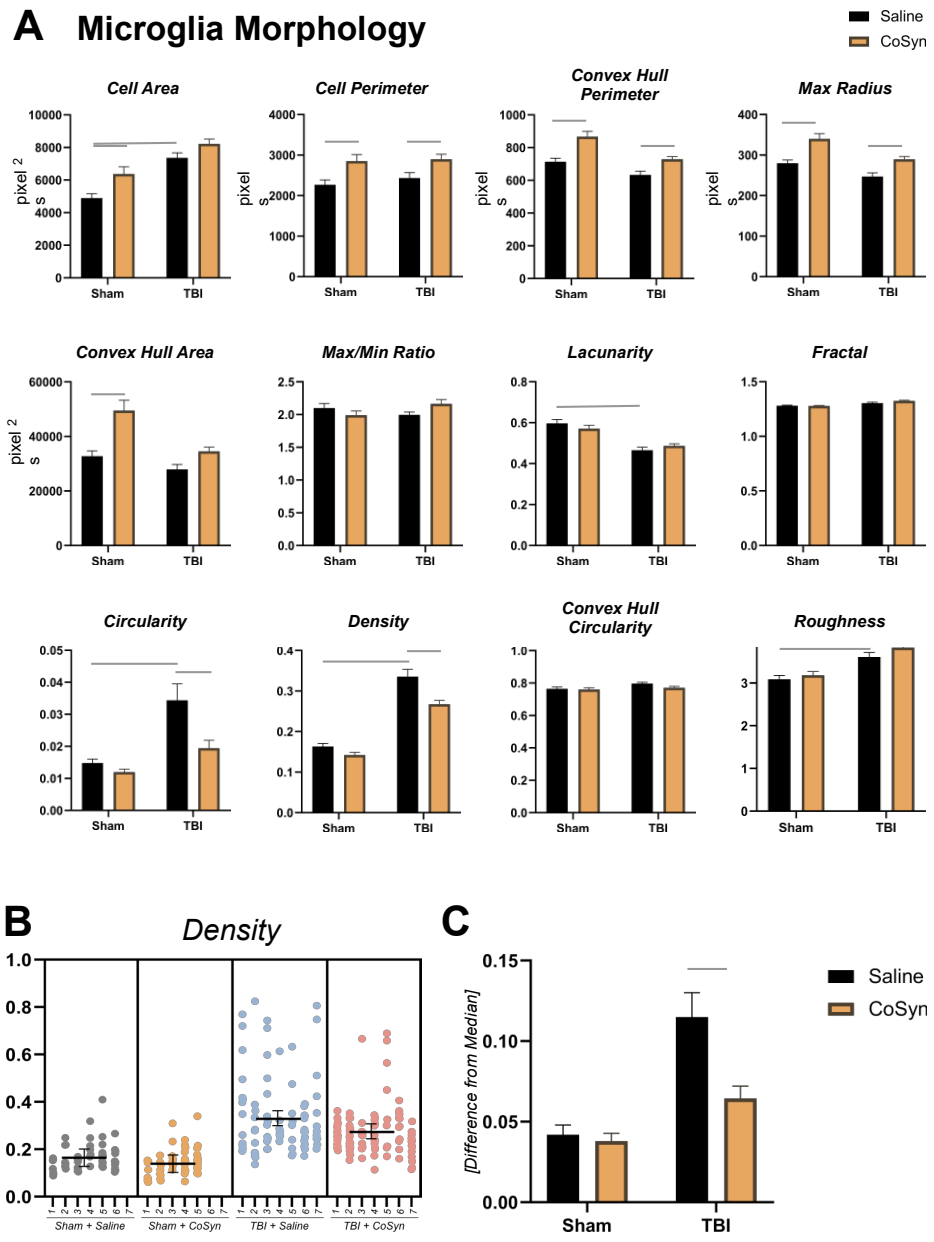

Figure 2. CoSyn alters microglia/macrophage morphology in CA1. (A) TBI and CoSyn modulates microglia/macrophage morphology as quantified through *FracLac* analysis. (B) Nested graphs of density and max radius demonstrate injury and treatment induced variance. (C) Density values transformed to absolute value from median show increased variability in the Saline-treated TBI group. Density did not exhibit homogenous variance while max radius did meet this assumption for the use of ANOVA tests. Significance was determined using two-way ANOVA with Tukey post hoc testing. Levene's median test was completed for Circularity and Density. Graphs represent means and error bars show SEM, grey lines indicate $p<0.05$.

Table 1: Main effects of morphology parameters

Parameter	*Injury Main Effect*		*Treatment Main Effect*	
	P value	*Statistics*	*P value*	*Statistics*
Cell Area	<0.0001	F (1, 305) = 39.47	0.0008	F (1, 305) = 11.48
Cell Perimeter			P=0.0002	F (1,305) = 14.01
CH Perimeter	P<0.0001	F (1,305) = 21.81	P<0.0001	F (1,305) = 28.16
Max Radius	P<0.0001	F (1,305) = 19.54	P<0.0001	F (1,305) = 30.01
CH Area	P<0.0001	F (1,305) = 18.77	P<0.0001	F (1,305) = 25.86
Lacunarity	P<0.0001	F (1,305) = 53.68		
Fractal	P<0.0001	F (1,305) = 24.03		
Circularity	P=0.0004	F (1,305) = 12.97	P=0.0207	F (1,305) = 5.409
Density	P<0.0001	F (1,305) = 21.47	P=0.0115	F (1,305) = 6.459
CH Circularity	P=0.0319	F (1,305) = 4.646		
Roughness	P<0.0001	F (1,305) = 31.95		

CoSyn Alters Cytokine Profile following Injury

Due to the complex and time-dependent nature of cytokine expression following TBI, we evaluated the effect of CoSyn on inflammatory resolution of cytokine expression in cortical and hippocampal tissue at one, three and seven days following injury. Our heatmap figures of cytokine expression demonstrates a robust early inflammatory response followed by initiation of resolution within the first week after injury (Figure 3). We show alterations in several cytokines with the most robust alterations in IL-6, IL-12, MCP-1 and MIP-1α (Table 2-3). CoSyn reduced injury-induced increases in IL-6 in both the lesional cortex (Figure 3A) and hippocampus (Figure 3B) at DPI one. CoSyn also attenuated injury-induced increases in MIP-1α at DPI one in the cortex (Figure 3A) and hippocampus with suppression of MIP-1α to sham levels in the CoSyn-treated TBI group at DPI three and seven (Figure 3B). Interestingly, CoSyn treatment increased injury-induced increases in MCP-1 expression in both the hippocampus and cortex at DPI one and increased IL-12 expression only in the lesional cortex at DPI seven (Figure 3A-B).

Discussion

In this study, we investigated the effect of CoSyn administration in modulating microglia activation and the neuroinflammatory response through cytokine expression of cortical and hippocampal tissue. Our data showed that a one-week regimen of CoSyn following injury resulted in alterations in cytokine expression in cortical lesion and hippocampal tissue. Cytokine modulation

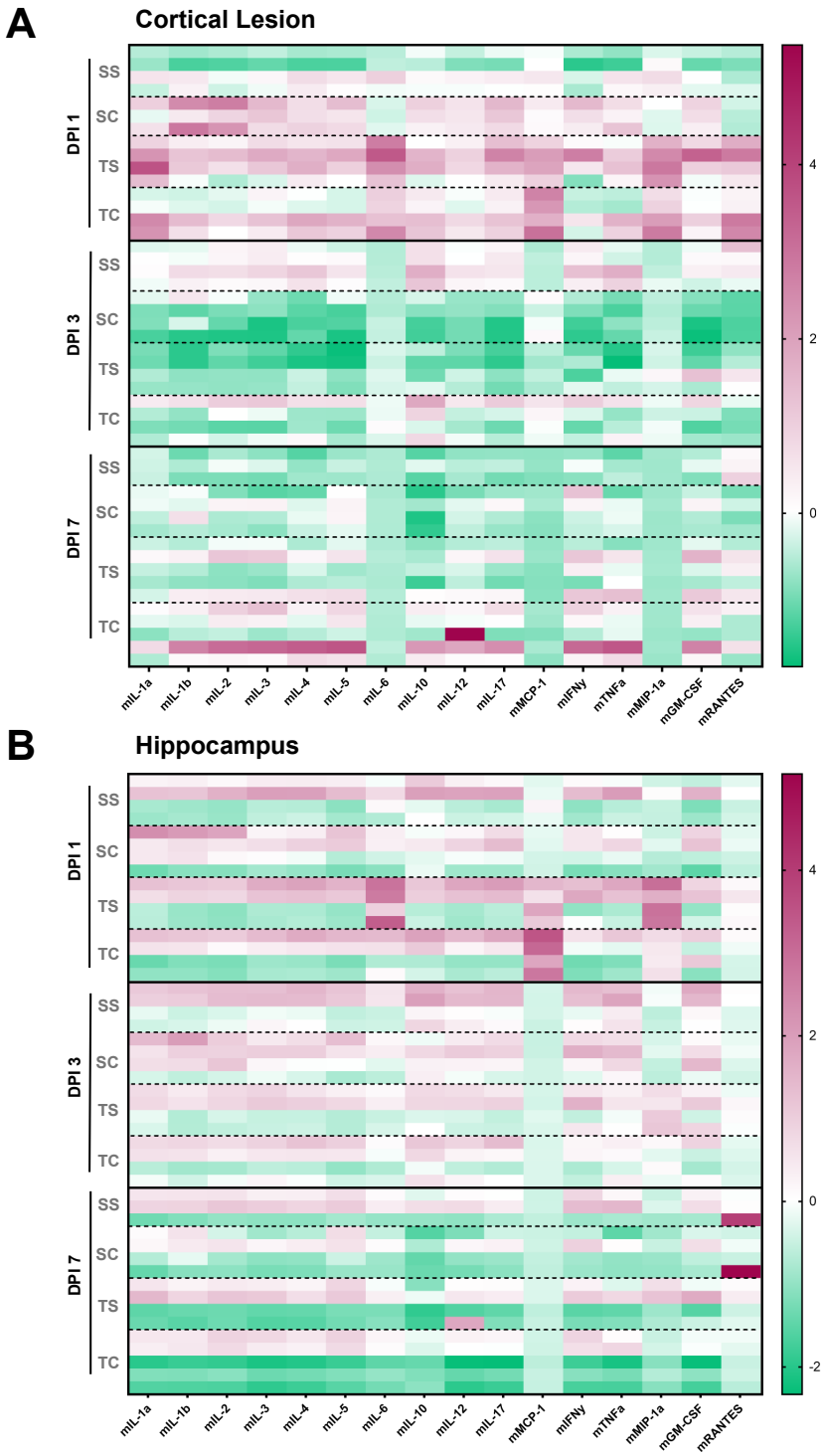

Figure 3. CoSyn alters cytokine expression in lesional cortical tissue and hippocampus. (A) Heatmap of quantification of cytokines in cortical lesion. (B) Heatmap of quantification of cytokines in cortical lesion.

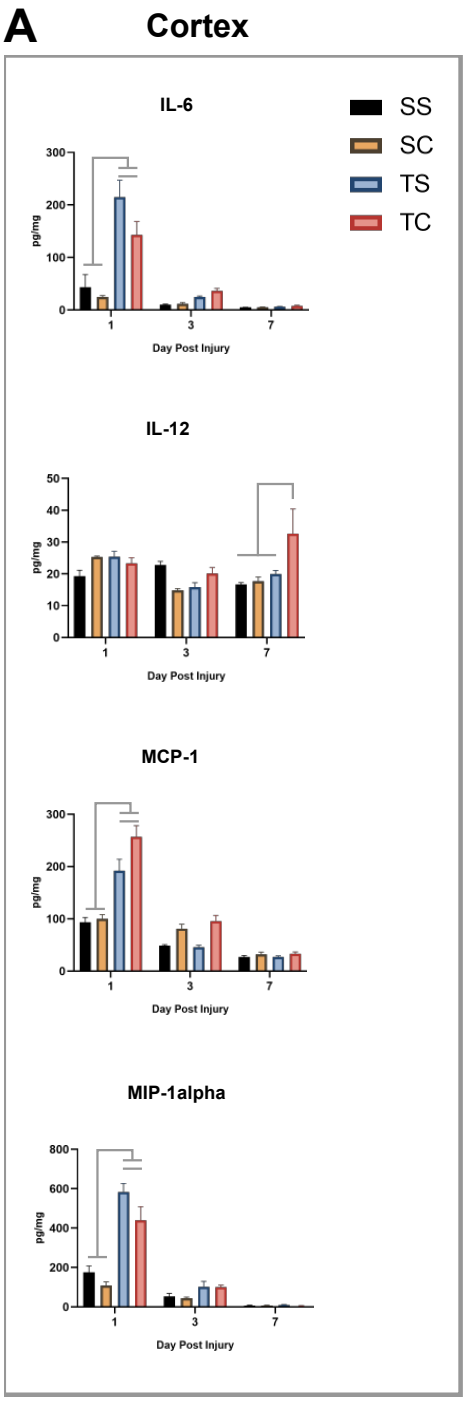
A
Cortex
IL-6
SS
SC
TS
TC
pg/mg
Day Post Injury
IL-12
MCP-1
MIP-1alpha

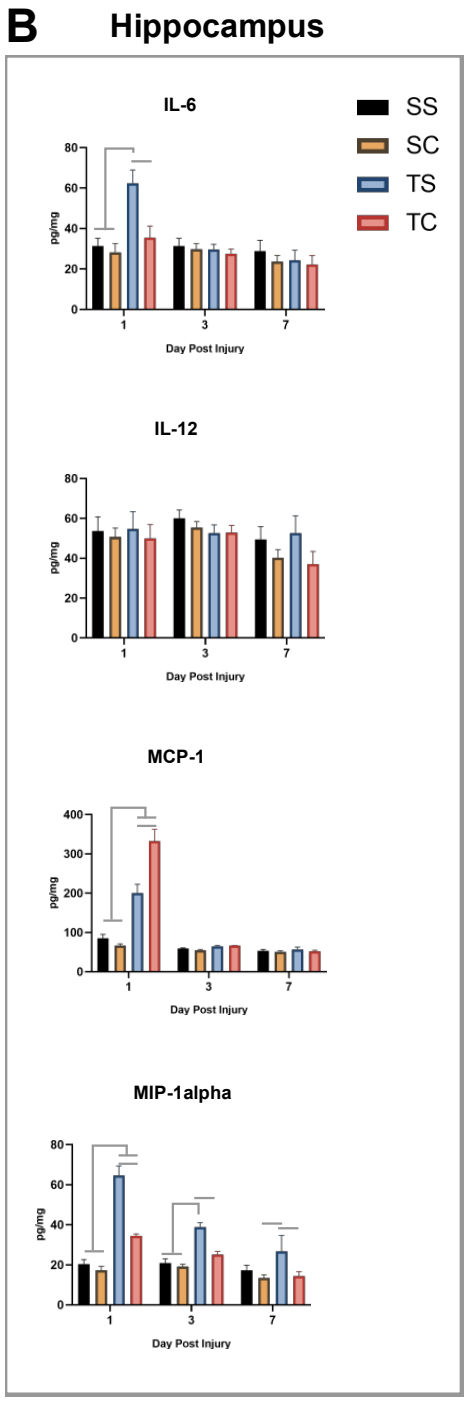
B
Hippocampus
IL-6
SS
SC
TS
TC
pg/mg
Day Post Injury
IL-12
MCP-1
MIP-1alpha

Figure 4. CoSyn modulates cytokine expression in lesional cortical tissue and hippocampus. (A) In cortex, injury induces increase in IL-6, MCP-1 and MIP-1α at DPI one. CoSyn reduced early IL-6 and MIP-1α while increasing MCP-1. CoSyn increases IL-12 at DPI seven. (B) In hippocampus, injury induces increase in IL-6, MCP-1 and MIP-1α at DPI one, with sustained increases in MIP-1α. CoSyn reduced injury-induced increases in IL-6 and MIP-1α while increasing MCP-1. Significance was determined using two-way ANOVA with Tukey post hoc testing. Graphs represent means and error bars show SEM, grey lines indicate $p<0.05$.

Table 2: Cytokine expression in lesional cortex

	Day Post Injury	Comparison	Adjusted P Value
IL-6	DPI 1	Sham-Saline vs. TBI-Saline	<0.0001
	DPI 1	Sham-Saline vs. TBI-CoSyn	<0.0001
	DPI 1	Sham-CoSyn vs. TBI-Saline	<0.0001
	DPI 1	Sham-CoSyn vs. TBI-CoSyn	<0.001
	DPI 1	TBI-Saline vs. TBI-CoSyn	<0.01
IL-12	DPI 7	Sham-Saline vs. TBI-CoSyn	<0.01
	DPI 7	Sham-CoSyn vs. TBI-CoSyn	<0.01
	DPI 7	TBI-Saline vs. TBI-CoSyn	<0.05
MCP-1	DPI 1	Sham-Saline vs. TBI-Saline	<0.0001
	DPI 1	Sham-Saline vs. TBI-CoSyn	<0.0001
	DPI 1	Sham-CoSyn vs. TBI-Saline	<0.0001
	DPI 1	Sham-CoSyn vs. TBI-CoSyn	<0.0001
	DPI 1	TBI-Saline vs. TBI-CoSyn	<0.01
MIP1α	DPI 1	Sham-Saline vs. TBI-Saline	<0.0001
	DPI 1	Sham-Saline vs. TBI-CoSyn	<0.0001
	DPI 1	Sham-CoSyn vs. TBI-Saline	<0.0001
	DPI 1	Sham-CoSyn vs. TBI-CoSyn	<0.0001
	DPI 1	TBI-Saline vs. TBI-CoSyn	<0.01

Table 3: Cytokine expression in hippocampus

	Day Post Injury	Comparison	Adjusted P Value
IL-6	DPI 1	Sham-Saline vs. TBI-Saline	<0.0001
	DPI 1	Sham-CoSyn vs. TBI-Saline	<0.0001
	DPI 1	TBI-Saline vs. TBI-CoSyn	<0.001
MCP-1	DPI 1	Sham-Saline vs. TBI-Saline	<0.0001
	DPI 1	Sham-Saline vs. TBI-CoSyn	<0.0001
	DPI 1	Sham-CoSyn vs. TBI-Saline	<0.0001
	DPI 1	Sham-CoSyn vs. TBI-CoSyn	<0.0001
	DPI 1	TBI-Saline vs. TBI-CoSyn	<0.0001
MIP1 α	DPI 1	Sham-Saline vs. TBI-Saline	<0.0001
	DPI 1	Sham-Saline vs. TBI-CoSyn	<0.05
	DPI 1	Sham-CoSyn vs. TBI-Saline	<0.0001
	DPI 1	Sham-CoSyn vs. TBI-CoSyn	<0.01
	DPI 1	TBI-Saline vs. TBI-CoSyn	<0.0001
	DPI 3	Sham-Saline vs. TBI-Saline	<0.01
	DPI 3	Sham-CoSyn vs. TBI-Saline	<0.001
	DPI 3	TBI-Saline vs. TBI-CoSyn	<0.05
	DPI 7	Sham-CoSyn vs. TBI-Saline	<0.05
	DPI 7	TBI-Saline vs. TBI-CoSyn	<0.05

included acute suppression of IL-6 and prolonged suppression of MIP-1α expression with early increases in MCP-1 and late increases in IL-12. CoSyn also attenuated microglia/macrophage injury-induced morphological features at DPI three suggesting a reduced activation state. Altered microglia morphological features in conjunction with changes in cytokine expression suggest an immune modulatory effect of CoSyn following TBI.

Cosyntropin, also referred to as tetracosactide, is a synthetic analog composed of the first 24 amino acids of the full length ACTH. ACTH was originally FDA approved in 1952 and, currently, two forms of ACTH have Food and Drug Administration approval for use in diagnostic testing of adrenal functioning [50]. Both the natural (H.P. Acthar Gel Repository Injection from Mallinckrodt Pharmaceuticals) and synthetic (cosyntropin) variants stimulate all five subtypes of the melanocortin (MC) receptors [40]. ACTH is the only endogenous melanocortin agonist that stimulates MC2R resulting in glucocorticoid secretion from the adrenal glands. Due to a half-life of approximately 20 minutes in humans, several compounds have been developed to increase length of activity for the natural or synthetic variants of ACTH through the use of gels or zinc suspensions [51]. Both Synacthen Depot (Novartis Pharmaceuticals) and long-acting cosyntropin (West Therapeutics) use a zinc suspension to extend activity. When considering both potential for side-effects as a result of extended use and the clinical treatment protocols that suggest multiple treatment days, we tested a 7-day protocol using a subcutaneous injection of

long-acting cosyntropin. Our study was limited in that we did not address dosage, route, and length of treatment regimens or chronic effects including alterations in cardiovascular health.

A majority of research on the benefits of melanocortins following neuroinflammatory insult and acquired brain injuries investigates MC4R-signaling via synthetic variants of α-MSH. However, unlike α-MSH, ACTH is the only endogenous MC that activates MC2R in the adrenal cortex, stimulating glucocorticoid (GC) production [40]. Dual activation of corticosteroid-dependent and independent responses through a synthetic ACTH analog may result in a more controlled and thorough resolution of the complex inflammatory response following TBI and may improve on current clinical trials only evaluating CS use.

Due to its well-documented anti-inflammatory effects, high-dose methylprednisolone, a synthetic GC receptor agonist, was tested in the clinic through a large, randomized, multi-center TBI clinical trial evaluating the effect of early administration on death and disability [46]. Results from this study indicate that high-dose methylprednisolone increases mortality following significant head injury and therefore suggests that synthetic glucocorticoids should not be used for the treatment of TBI [29,46]. GC actions in the CNS are dosage, timing, and regionally-specific, with both pro- and anti-inflammatory effects contributing to neuronal vulnerability and survival [52]. While GCs have been shown to decrease iNOS-mediated neurotoxicity, reduce TNFα and IL1 β expression, attenuate microglia/macrophage activation and increase NGF

following injury, GCs also demonstrate deleterious effects as exhibited through increasing hippocampal cell death following TBI, impairing metabolism and reducing injury-induced BDNF [52–59]. To further complicate the dual-nature of GCs, GCs are also part of the HPA axis resulting in inhibition of CRF and ACTH and chronic usage results in HPA axis suppression [60]. As a melanocortin receptor agonist, ACTH also contributes to anti-inflammatory effects and metabolic regulation. In contrast to GCs, ACTH 1–24 increases glucose uptake in neurons through stimulation of transport protein synthesis, and MC4R-agonists increase BDNF *in vitro,* suggesting melanocortin receptor signaling may counteract deleterious effects of GC signaling [61,62]. The delicate balance between CRF, ACTH, and GCs in the maintenance of homeostasis and response to stress is vital for normal functioning and is disrupted following TBI [63]. Additional research is needed to evaluate the effect of synthetic ACTH as a post-TBI therapeutic specifically addressing if its effects are dependent on its GC-inducing capacity or extend beyond this mechanism of action, potentially counteracting the side effects of supraphysiological or prolonged GC activation. In this study, we have not addressed the potential role of corticosteroid production on our observed outcomes and additional research is needed to identify the specific mechanisms of CoSyn following TBI.

Traumatic brain injury results in a complex and dynamic cytokine profile. Previous work from our lab has demonstrated an anti-inflammatory effect of CoSyn through reduced IL1β in the cortical lesion at DPI three as well as

decreased microglia/macrophage accumulation in the perilesional and hippocampal regions. The role of microglia following injury is complex and time dependent. Previous research using both drug-induced and genetic depletion of microglia/macrophages have demonstrated beneficial, deleterious and inconsequential effects of microglia/macrophages following TBI [28,64,65]. These studies demonstrate the importance of microglia/macrophage phenotype modulation as a therapeutic target and the need for enhanced phenotype quantification. Several markers have been used to define phenotype following TBI (see review [24]). In support of the use of MCs as a post-TBI therapeutic, the use of α-MSH results in decreased microglia/macrophage density following intracerebral hemorrhage and modulation of microglia phenotype as evidenced by increased microglia Arg1 expression [38,39]. Along with phenotype markers, morphological changes of immune cells can indicate changes in function [25]. Based on hierarchical cluster and principal component analysis, several microglia morphological categories have been proposed relying on parameters such as density, perimeter and convex hull span ratio [27]. Quiescent microglia have long, thin ramifications resulting in low density with higher perimeter values. Activated microglia exhibit reduced number of ramifications with increased soma size resulting in increased circularity and density as well as decreased maximum radius compared to quiescent microglia. The quantification of morphology in our study suggests a reduced activation state following treatment with CoSyn. The reduction in TBI-induced morphological changes have also

been seen following α-MSH administration, a melanocortin receptor without glucocorticoid stimulating capabilities [33]. While our study did demonstrate a morphology consistent with reduced microglia/macrophage activation, the particular functional response as elucidated by known phenotype markers or functional assays is a limitation of our study. Furthermore, in contrast with a pro-resolving IL-6 microglia phenotype following TBI described by Willis and colleagues, our study showed decreased IL-6 levels in our CoSyn-treated TBI group compared to their saline-treated counterparts [28]. It is unclear what particular cells are contributing to the alterations in IL-6 expression as these values were quantified from whole tissue lysates. Colocalization studies with cell markers and identified cytokines would be beneficial to elucidate specific cellular contributions.

The acute increase in monocyte chemoattractant protein 1 (MCP-1) with CoSyn provides an intriguing result as MCP-1 is most well-known for its chemoattractant abilities. MCP-1, also referred to as C-C Chemokine Ligand 2 (CCL2), is a ligand for the C-C Motif Chemokine Receptor 2 (CCR2) along with CCL7 and CCL12. CCR2 is expressed on neurons as well as peripheral immune cells, including monocytes and T-cells, and MCP-1 is involved in recruitment of both these peripheral immune cell types[66,68]. In the CNS, MCP-1 is not expressed in neurons or microglia but is expressed in astrocytes with its receptor, CCR2, predominantly expressed in neurons [66,67].

Along with its well-known chemoattractant capabilities, this soluble immune factor also confers an immune modulatory effect by altering astrocyte cytokine expression and demonstrates alternative neuroactive properties. Semple and colleagues, using an MCP-1-/- and wildtype cultured mouse astrocytes, showed that MCP-1 attenuates LPS-induced expression of both IL-6 and MIP-1α [69]. Consistent with our DPI one cortical and hippocampal cytokine data, increased levels of MCP-1 corresponded with reduced levels of IL-6 and MIP-1α. Due to the current method of tissue homogenation, it is unclear what particular cells are contributing to these increases. Additional research using co-localization of cell type and cytokine expression along with knock-out or neutralization studies would be necessary to confirm the causal role of MCP-1 in the suppression of IL-6 and MIP-1α.

In contrast to the cytokine patterns seen in our study, IL-6 and IL-1β were both significantly reduced in an MCP-1-/- mouse model of stroke, suggesting that MCP-1 contributes to injury-induced IL-6 and IL1β expression. In the previous aforementioned study, MCP-1 contributed to increased infarct volume and late astrogliosis with no alteration in neutrophil infiltration suggesting that reduced levels of MCP-1 are beneficial following stroke [70]. While several studies have shown MCP-1 to be neuroprotective *in vitro* [71,72], the use of a CCR2 antagonist in a mouse model of TBI reduced TUNEL-positive cells and improved memory performance in a spatial learning task, suggesting that MCP-1 signaling contributes to neurodegeneration and memory impairments following TBI [67].

Furthermore, early increases in MCP-1 was associated with worse long-term functional outcomes in humans, but this association only occurred with acute increases in MCP-1 and instead was associated with good outcomes when MCP-1 elevated at a later time-point [73]. Taken together, MCP-1 may have time and cell-specific differential responses following TBI and it is unclear if the CoSyn-induced increase in MCP-1 is beneficial [69]. A more thorough understanding of the consequences of immune modulation at both the acute and chronic time-points may allow us to better tailor our therapeutic approaches for TBI patients.

Adding to the time-dependent effects of MCP-1, the CoSyn-induced increases in MCP-1 coincide with decreased IL-6 and MIP-1α. It has been suggested that MIP-1α is necessary for the initial recruitment of peripheral immune cells with MCP-1 contributing to the chemotactic gradient providing directional movement [74]. As a result, the reduced MIP-1α levels and overall ratio of MCP-1 to MIP-1α in conjunction with the surrounding inflammatory milieu could dictate the peripheral immune response more than the level of one cytokine. Unlike MCP-1, MIP-1α is colocalized with microglia and both MCP-1 and MIP-1α are expressed by human brain vascular endothelial cells [75]. However, unlike MIP-1α, MCP-1 is consecutively expressed in human brain microvessel endothelial cells an inflammatory stimulus resulting in increased expression in both cytokines [74]. Their dual expression in endothelial cells contributes to their chemoattractant abilities. Limited research is available regarding the role of MIP-1α following TBI, providing an interesting avenue for

future research and its role in peripheral immune cell infiltration and blood brain barrier integrity.

Along with changes in microglia/macrophage morphology, our results show increased injury-induced levels of MCP-1 at DPI one with CoSyn treatment. In contrast with our data showing morphology indicative of a less activated state, elevated MCP-1 was associated with morphological changes consistent with increased microglia activation [76]. In the retina, MCP-1 increased soma size and resulted in thickening and shortening of ramifications with a dose-dependent response [76]. However, this method of morphology was based on qualitative observations of images and no quantification was completed. While neither MCP-1 or CCR2 colocalize with microglia following TBI, CCR2 is expressed on monocyte/macrophage populations after brain insult [67]. In our study, a subset of the Iba1-positive cells showed gross alterations in injury-induced morphology. As Iba1 is not specific for microglia and can also label infiltrating peripheral monocytes that become macrophages within the brain parenchyma, this subset of cells could represent infiltrating CCR2-positive macrophages. It is unknown what morphological status the CCR2-positive cells would possess. To our knowledge, no studies have compared morphological characteristics of tissue-resident microglia to infiltrating macrophages following traumatic brain injury. Our current study does not quantify microglia activation through the use of known phenotype markers. Additional research is needed to

correlate our morphological findings with phenotype markers to evaluate role of CoSyn in modulating microglia phenotype.

The administration of CoSyn following TBI did not result in overall immune suppression but immune modulation. CoSyn resulted in an acute increase in levels of MCP-1 with subacute increases in IL-12. Interestingly, both of these cytokines are involved in T-cell biology. IL-12 is expressed by both astrocytes and microglia and is a T-cell activating cytokine [77,78]. Because CD8-positive T-cells have been shown to cause long-term neurological impairments, it is unclear if increased levels of IL-12 at DPI seven is beneficial or deleterious [79]. Furthermore, While IL-12 levels remained low throughout the first three days and showed no injury-induced effects, it is unclear if the seven-day dosage regimen resulted in prolonged inflammatory suppression that, while initially beneficial, lead to a deleterious compensatory response. The role of the adaptive immune response and T-cell activation following TBI is an understudied area of TBI research and may contribute to the chronic inflammatory response and vulnerability to repeated-hit injuries as seen in sports and military personnel.

Consistent with our data, in the retina of mice with diabetic retinopathy, MC1R and MC5R agonists reduced IL-6 and MIP-1α [80]. These changes were not seen when using an MC3-4R agonist. Additional studies have demonstrated that LPS-induced increases in IL-6 were reduced by administration of α-MSH in rat plasma and the attenuated IL-6 levels were not ameliorated by the administration of an MC3/MC4 agonist and MC5 partial agonist [81]. These data

suggest that the immune modulatory effects are not constrained to MC3/MC4R signaling and most likely are a combination of multiple melanocortin receptor subtype signaling, including MC1R and MC5R. As an agonist for all five subtypes of melanocortin receptors, CoSyn could act through peripheral and central MCRs, including MC2R resulting in increased glucocorticoid levels with well-documented anti-inflammatory actions. It is unclear what specific receptor types are contributing to the immune modulatory effects demonstrated in our study. To our knowledge, no study has evaluated the relative contribution that each of the melanocortin receptor subtypes play in the inflammatory response following TBI. Melanocortin receptor agonists may have therapeutic potential not only in treatment of traumatic brain injury but may extend to other CNS disorders including Alzheimer's disease and chronic traumatic encephalopathy.

References

1. Gardner, R. C., Dams-O'Connor, K., Morrissey, M. R. & Manley, G. T. Geriatric Traumatic Brain Injury: Epidemiology, Outcomes, Knowledge Gaps, and Future Directions. *Journal of Neurotrauma* **35**, 889–906 (2018).

2. *Surveillance Report of Traumatic Brain Injury-related Emergency Department Visits, Hospitalizations, and Deaths – United States, 2014*. (2019).

3. Postolache, T. T. *et al.* Inflammation in Traumatic Brain Injury. *JAD* **74**, 1–28 (2020).

4. Amorini, A. M. *et al.* Severity of experimental traumatic brain injury modulates changes in concentrations of cerebral free amino acids. *J. Cell. Mol. Med.* **21**, 530–542 (2017).

5. Hinzman, J. M., Thomas, T. C., Quintero, J. E., Gerhardt, G. A. & Lifshitz, J. Disruptions in the regulation of extracellular glutamate by neurons and glia in the rat striatum two days after diffuse brain injury. *J Neurotrauma* **29**, 1197–208 (2012).

6. Wang, C. *et al.* Depletion of Microglia Attenuates Dendritic Spine Loss and Neuronal Apoptosis in the Acute Stage of Moderate Traumatic Brain Injury in Mice. *Journal of Neurotrauma* **37**, 43–54 (2020).

7. Miller, D. M., Singh, I. N., Wang, J. A. & Hall, E. D. Nrf2-ARE activator carnosic acid decreases mitochondrial dysfunction, oxidative damage and neuronal cytoskeletal degradation following traumatic brain injury in mice. *Experimental neurology* **264**, 103–10 (2015).

8. Wu, Q. *et al.* Mitochondrial division inhibitor 1 (Mdivi-1) offers neuroprotection through diminishing cell death and improving functional outcome in a mouse model of traumatic brain injury. *Brain Res* **1630**, 134–43 (2016).

9. Jullienne, A. *et al.* Chronic cerebrovascular dysfunction after traumatic brain injury: Cerebrovascular Dysfunction After TBI. *Journal of Neuroscience Research* **94**, 609–622 (2016).

10. Salehi, A. *et al.* Up-regulation of Wnt/β-catenin expression is accompanied with vascular repair after traumatic brain injury. *J Cereb Blood Flow Metab* **38**, 274–289 (2018).

11. Lindolfo da Silva Meirelles, Daniel Simon & Andrea Regner. Neurotrauma: The Crosstalk between Neurotrophins and Inflammation in

the Acutely Injured Brain. *International Journal of Molecular Sciences* **18**, 1082 (2017).

12. Faden, A. I. & Loane, D. J. Chronic Neurodegeneration After Traumatic Brain Injury: Alzheimer Disease, Chronic Traumatic Encephalopathy, or Persistent Neuroinflammation? *Neurotherapeutics* **12**, 143–150 (2015).

13. Appleton, R. E. Post-traumatic epilepsy in children requiring inpatient rehabilitation following head injury. *Journal of Neurology, Neurosurgery & Psychiatry* **72**, 669–672 (2002).

14. Cherry, J. D. *et al.* Microglial neuroinflammation contributes to tau accumulation in chronic traumatic encephalopathy. *Acta Neuropathologica Communications* **4**, (2016).

15. Ramlackhansingh, A. F. *et al.* Inflammation after trauma: Microglial activation and traumatic brain injury. *Annals of Neurology* **70**, 374–383 (2011).

16. Liu, T., Zhang, L., Joo, D. & Sun, S.-C. NF-κB signaling in inflammation. *Sig Transduct Target Ther* **2**, 17023 (2017).

17. Abboud, A. *et al.* Inflammation Following Traumatic Brain Injury in Humans: Insights from Data-Driven and Mechanistic Models into Survival and Death. *Front. Pharmacol.* **7**, (2016).

18. Feng, G. *et al.* Altered levels of α-melanocyte stimulating hormone in cerebrospinal fluid and plasma of patients with traumatic brain injury. *Brain Research* **1696**, 22–30 (2018).

19. Frugier, T., Morganti-Kossmann, M. C., O'Reilly, D. & McLean, C. A. *In Situ* Detection of Inflammatory Mediators in *Post Mortem* Human Brain Tissue after Traumatic Injury. *Journal of Neurotrauma* **27**, 497–507 (2010).

20. Lagraoui, M. *et al.* Controlled Cortical Impact and Craniotomy Induce Strikingly Similar Profiles of Inflammatory Gene Expression, but with Distinct Kinetics. *Frontiers in Neurology* **3**, (2012).

21. Dong, T., Zhi, L., Bhayana, B. & Wu, M. X. Cortisol-induced immune suppression by a blockade of lymphocyte egress in traumatic brain injury. *Journal of Neuroinflammation* **13**, (2016).

22. Baratz, R. *et al.* Transiently lowering tumor necrosis factor-α synthesis ameliorates neuronal cell loss and cognitive impairments induced by minimal traumatic brain injury in mice. *J Neuroinflammation* **12**, 45 (2015).

23. Saijo, K. & Glass, C. K. Microglial cell origin and phenotypes in health and disease. *Nature Reviews Immunology* **11**, 775–787 (2011).

24. Donat, C. K., Scott, G., Gentleman, S. M. & Sastre, M. Microglial Activation in Traumatic Brain Injury. *Frontiers in Aging Neuroscience* **9**, (2017).

25. Nimmerjahn, A., Kirchhoff, F. & Helmchen, F. Resting Microglial Cells Are Highly Dynamic Surveillants of Brain Parenchyma in Vivo. **308**, 6 (2005).

26. Davalos, D. *et al.* ATP mediates rapid microglial response to local brain injury in vivo. *Nature Neuroscience* **8**, 752–758 (2005).

27. Fernández-Arjona, M. del M., Grondona, J. M., Granados-Durán, P., Fernández-Llebrez, P. & López-Ávalos, M. D. Microglia Morphological Categorization in a Rat Model of Neuroinflammation by Hierarchical Cluster and Principal Components Analysis. *Frontiers in Cellular Neuroscience* **11**, (2017).

28. Willis, E. F. *et al.* Repopulating Microglia Promote Brain Repair in an IL-6-Dependent Manner. *Cell* **180**, 833-846.e16 (2020).

29. Edwards, P., Arango, M., Balica, L., Cottingham, R. & El-Sayed, H. Final results of MRC CRASH, a randomised placebo-controlled trial of intravenous corticosteroid in adults with head injury—outcomes at 6 months. *The Lancet* **365**, 1957–1959 (2005).

30. Gallo-Payet, N. 60 YEARS OF POMC: Adrenal and extra-adrenal functions of ACTH. *Journal of Molecular Endocrinology* **56**, T135–T156 (2016).

31. Bertolini, A., Tacchi, R. & Vergoni, A. Brain effects of melanocortins☆. *Pharmacological Research* **59**, 13–47 (2009).

32. Buckley, D. I. & Ramachandran, J. Characterization of corticotropin receptors on adrenocortical cells. *Proceedings of the National Academy of Sciences* **78**, 7431–7435 (1981).

33. Schaible, E.-V. *et al.* Single Administration of Tripeptide α-MSH(11–13) Attenuates Brain Damage by Reduced Inflammation and Apoptosis after Experimental Traumatic Brain Injury in Mice. *PLoS ONE* **8**, e71056 (2013).

34. Bitto, A. *et al.* Protective effects of melanocortins on short-term changes in a rat model of traumatic brain injury*. *Critical Care Medicine* **40**, 945–951 (2012).

35. Spaccapelo, L. *et al.* Melanocortin MC4 receptor agonists counteract late inflammatory and apoptotic responses and improve neuronal functionality after cerebral ischemia. *European Journal of Pharmacology* **670**, 479–486 (2011).

36. Lisak, R. P., Nedelkoska, L., Bealmear, B. & Benjamins, J. A. Melanocortin receptor agonist ACTH 1–39 protects rat forebrain neurons from apoptotic, excitotoxic and inflammation-related damage. *Experimental Neurology* **273**, 161–167 (2015).

37. Ichiyama, T. *et al.* Systemically administered a-melanocyte-stimulating peptides inhibit NF-kB activation in experimental brain inflammation. 7 (1999).

38. Chen, S. *et al.* Activation of melanocortin receptor 4 with RO27-3225 attenuates neuroinflammation through AMPK/JNK/p38 MAPK pathway after intracerebral hemorrhage in mice. *Journal of Neuroinflammation* **15**, (2018).

39. Carniglia, L. *et al.* [Nle4, D-Phe7]-α-MSH Inhibits Toll-Like Receptor (TLR)2- and TLR4-Induced Microglial Activation and Promotes a M2-Like Phenotype. *PLOS ONE* **11**, e0158564 (2016).

40. Catania, A. Targeting Melanocortin Receptors as a Novel Strategy to Control Inflammation. *Pharmacological Reviews* **56**, 1–29 (2004).

41. Bajwa, N. M. *et al.* Mild Concussion, but Not Moderate Traumatic Brain Injury, Is Associated with Long-Term Depression-Like Phenotype in Mice. *PLOS ONE* **11**, e0146886 (2016).

42. Siebold, L., Obenaus, A. & Goyal, R. Criteria to define mild, moderate, and severe traumatic brain injury in the mouse controlled cortical impact model. *Experimental Neurology* **310**, 48–57 (2018).

43. Decker, D. *et al.* Immunomodulatory effects of H.P. Acthar Gel on B cell development in the NZB/W F1 mouse model of systemic lupus erythematosus. *Lupus* **23**, 802–812 (2014).

44. Cusick, M. F., Libbey, J. E., Oh, L., Jordan, S. & Fujinami, R. S. Acthar gel treatment suppresses acute exacerbations in a murine model of relapsing-remitting multiple sclerosis. *Autoimmunity* **48**, 222–230 (2015).

45. Arrat, H., Lukas, T. J. & Siddique, T. ACTH (Acthar Gel) Reduces Toxic SOD1 Protein Linked to Amyotrophic Lateral Sclerosis in Transgenic Mice: A Novel Observation. *PLOS ONE* **10**, e0125638 (2015).

46. Roberts, I, Yates, D & Sandercock, P. Effect of intravenous corticosteroids on death within 14 days in 10008 adults with clinically significant head injury (MRC CRASH trial): randomized placebo-controlled trial.

47. Mohamadpour, M., Whitney, K. & Bergold, P. J. The Importance of Therapeutic Time Window in the Treatment of Traumatic Brain Injury. *Frontiers in Neuroscience* **13**, (2019).

48. Fox, C. *et al.* Minocycline Confers Early but Transient Protection in the Immature Brain following Focal Cerebral Ischemia—Reperfusion. *J Cereb Blood Flow Metab* **25**, 1138–1149 (2005).

49. Fernandez-Suarez, D. *et al.* Monoacylglycerol lipase inhibitor JZL184 is neuroprotective and alters glial cell phenotype in the chronic MPTP mouse model. *Neurobiol Aging* **35**, 2603–2616 (2014).

50. Gettig, J., Cummings, J. P. & Matuszewski, K. H.P. Acthar Gel and Cosyntropin Review. 8 (2009).

51. Veldhuis, J. D. *et al.* Corticotropin Secretory Dynamics in Humans under Low Glucocorticoid Feedback. 10.

52. Sorrells, S. F. & Sapolsky, R. M. An inflammatory review of glucocorticoid actions in the CNS. *Brain, Behavior, and Immunity* **21**, 259–272 (2007).

53. Golde, S., Coles, A., Lindquist, J. A. & Compston, A. Decreased iNOS synthesis mediates dexamethasone-induced protection of neurons from inflammatory injury in vitro. *Eur J Neurosci* **18**, 2527–2537 (2003).

54. Nadeau, S. & Rivest, S. Endotoxemia Prevents the Cerebral Inflammatory Wave Induced by Intraparenchymal Lipopolysaccharide Injection: Role of Glucocorticoids and CD14. *J Immunol* **169**, 3370–3381 (2002).

55. Dinkel, K., MacPherson, A. & Sapolsky, R. M. Novel glucocorticoid effects on acute inflammation in the CNS: Glucocorticoids and CNS inflammation. *Journal of Neurochemistry* **84**, 705–716 (2003).

56. Zhang, Z., Zhang, Z., Artelt, M., Burnet, M. & Schluesener, H. J. Dexamethasone attenuates early expression of three molecules associated with microglia/macrophages activation following rat traumatic brain injury. *Acta Neuropathol* **113**, 675–682 (2007).

57. Chen, X., Zhang, K.-L., Yang, S.-Y., Dong, J.-F. & Zhang, J.-N. Glucocorticoids Aggravate Retrograde Memory Deficiency Associated with Traumatic Brain Injury in Rats. *Journal of Neurotrauma* **26**, 253–260 (2009).

58. Grundy, P. L., Patel, N., Harbuz, M. S., Lightman, S. L. & Sharples, P. M. Glucocorticoids modulate BDNF mRNA expression in the rat hippocampus after traumatic brain injury: *NeuroReport* **11**, 3381–3384 (2000).

59. McCullers, D. L., Sullivan, P. G., Scheff, S. W. & Herman, J. P. Mifepristone protects CA1 hippocampal neurons following traumatic brain injury in rat. *Neuroscience* **109**, 219–230 (2002).

60. Paragliola, R. M., Papi, G., Pontecorvi, A. & Corsello, S. M. Treatment with Synthetic Glucocorticoids and the Hypothalamus-Pituitary-Adrenal Axis. *IJMS* **18**, 2201 (2017).

61. Daval, J.-L., Anglard, P., Gerard, M.-J., Vincendon, G. & Louis, J.-C. Regulation of deoxyglucose uptake by adrenocorticotropic hormone in cultured neurons. *J. Cell. Physiol.* **124**, 75–80 (1985).

62. Saba, J. *et al.* Melanocortin 4 receptor activation protects striatal neurons and glial cells from 3-nitropropionic acid toxicity. *Molecular and Cellular Neuroscience* **94**, 41–51 (2019).

63. Tapp, Z. M., Godbout, J. P. & Kokiko-Cochran, O. N. A Tilted Axis: Maladaptive Inflammation and HPA Axis Dysfunction Contribute to Consequences of TBI. *Front. Neurol.* **10**, 345 (2019).

64. Aertker, B. M. *et al.* Pre-injury monocyte/macrophage depletion results in increased blood–brain barrier permeability after traumatic brain injury. *J Neurosci Res* 698–707 (2019) doi:10.1002/jnr.24395.

65. Henry, R. J. *et al.* Microglial depletion with CSF1R inhibitor during chronic phase of experimental traumatic brain injury reduces neurodegeneration and neurological deficits. *J. Neurosci.* 2402–19 (2020) doi:10.1523/JNEUROSCI.2402-19.2020.

66. Parillaud, V. R. *et al.* Analysis of monocyte infiltration in MPTP mice reveals that microglial CX3CR1 protects against neurotoxic over-induction of monocyte-attracting CCL2 by astrocytes. *J Neuroinflammation* **14**, 60 (2017).

67. Liu, S., Zhang, L., Wu, Q., Wu, Q. & Wang, T. Chemokine CCL2 Induces Apoptosis in Cortex Following Traumatic Brain Injury. *J Mol Neurosci* **51**, 1021–1029 (2013).

68. Cédile, O., Wlodarczyk, A. & Owens, T. CCL2 recruits T cells into the brain in a CCR2-independent manner. *APMIS* **125**, 945–956 (2017).

69. Semple, B. D., Frugier, T. & Morganti-Kossmann, M. C. CCL2 modulates cytokine production in cultured mouse astrocytes. *J Neuroinflammation* **7**, 67 (2010).

70. Hughes, P. M. *et al.* Monocyte Chemoattractant Protein-1 Deficiency is Protective in a Murine Stroke Model. *J Cereb Blood Flow Metab* **22**, 308–317 (2002).

71. Madrigal, J. L. M., Leza, J. C., Polak, P., Kalinin, S. & Feinstein, D. L. Astrocyte-Derived MCP-1 Mediates Neuroprotective Effects of Noradrenaline. *Journal of Neuroscience* **29**, 263–267 (2009).

72. Eugenin, E. A., D'Aversa, T. G., Lopez, L., Calderon, T. M. & Berman, J. W. MCP-1 (CCL2) protects human neurons and astrocytes from NMDA or HIV-tat-induced apoptosis: MCP-1 protection against NMDA and tat toxicity. *Journal of Neurochemistry* **85**, 1299–1311 (2003).

73. Landreneau, M. J. *et al.* CCL2 and CXCL10 are associated with poor outcome after intracerebral hemorrhage. *Ann Clin Transl Neurol* **5**, 962–970 (2018).

74. Chui, R. & Dorovini-Zis, K. Regulation of CCL2 and CCL3 expression in human brain endothelial cells by cytokines and lipopolysaccharide. *J Neuroinflammation* **7**, 1 (2010).

75. Redell, J. B. *et al.* Analysis of Functional Pathways Altered after Mild Traumatic Brain Injury. *Journal of Neurotrauma* **30**, 752–764 (2013).

76. Chiu, K., Yeung, S.-C., So, K.-F. & Chang, R. C.-C. Modulation of morphological changes of microglia and neuroprotection by monocyte chemoattractant protein-1 in experimental glaucoma. *Cell Mol Immunol* **7**, 61–68 (2010).

77. Stahel, P. F., Kossmann, T., Joller, H., Trentz, O. & Morganti-Kossmann, M. C. Increased interleukin-12 levels in human cerebrospinal fluid following severe head trauma. *Neuroscience Letters* **249**, 123–126 (1998).

78. Stalder, A. K. *et al.* Lipopolysaccharide-induced IL-12 expression in the central nervous system and cultured astrocytes and microglia. *J Immunol* 1344–1351 (1997).

79. Daglas, M. *et al.* Activated CD8+ T Cells Cause Long-Term Neurological Impairment after Traumatic Brain Injury in Mice. *Cell Reports* **29**, 1178-1191.e6 (2019).

80. Rossi, S. *et al.* Activation of Melanocortin Receptors MC_1 and MC_5 Attenuates Retinal Damage in Experimental Diabetic Retinopathy. *Mediators of Inflammation* **2016**, 1–13 (2016).

81. Huang, Q.-H., Hruby, V. J. & Tatro, J. B. Systemic α-MSH suppresses LPS fever via central melanocortin receptors independently of its suppression of corticosterone and IL-6 release. *American Journal of Physiology-Regulatory, Integrative and Comparative Physiology* **275**, R524–R530 (1998).

CHAPTER FIVE

FUTURE RESEARCH EVALUATING MELANOCORTIN RECEPTOR SIGNALING FOLLOWING EXPERIMENTAL TRAUMATIC BRAIN INJURY

Adapted from submitted R21 grant and the Pediatric Education Research Training grant from Loma Linda University Pediatric Department

Introduction

Traumatic brain injury (TBI) is a major health concern in the United States resulting in a substantial number of hospitalizations and deaths [1]. TBI causes subsequent morbidity and long-term effects that are influenced by age, sex, injury severity, and inflammatory status [2,3]. Several studies show persistent neuroinflammation following TBI, lasting as long as 17 years after injury[4–6]. However, it is unclear which components of the inflammatory response are indicators of repair and which continue to drive pathology and brain vulnerability [6]. Clinically, neuroinflammation following TBI is associated with increased intracranial pressure, increased mortality, poor functional outcomes [7], reduced processing speed [4], and is a risk factor for the development of epilepsy and neurodegenerative disorders [6,8,9]. Glial cell activation has been evaluated through positron emission tomography (PET) with radiotracers for translocator protein 18 kDa (TSPO). TSPO expression increases upon microglia activation and TSPO radioligands have been used to evaluate the inflammatory status of National Football League players and TBI patients, demonstrating widespread, chronic glial activation [4,5]. *These findings illustrate the imperative need for a more thorough understanding of the multifaceted endogenous neuroinflammatory response to TBI and the therapeutic mechanisms of immune-modulatory compounds.*

Melanocortins (MCs) are a family of peptides endogenously derived from pro-opiomelanocortin precursors [10]. MCs include compounds such as adrenocorticotropic hormone (ACTH) and alpha-melanocyte stimulating

hormone (α-MSH), both of which are agonists for melanocortin receptors [10,11]. There are five MC receptor subtypes with tissue-specific expression, including melanocytes (MC_1), peripheral immune cells ($MC_{1,3,5}$), endothelial cells (MC_1), the adrenal cortex (MC_2) and the central nervous system ($MC_{3\text{-}4}$). In the CNS, MC receptor distribution is ubiquitous [12]. Due to their widespread expression in CNS tissue and cell type, melanocortins induce diverse behavioral and neuroinflammatory responses (see chapter 1 for overview of functions). Briefly, behavioral alterations include increased grooming, improved memory, and modulation of both erectile function and feeding behavior. Of relevance to acquired brain injury, melanocortin signaling is also involved in energy homeostasis [13], steroidogenesis [14,15], CNS immune modulation [16–18], neurogenesis and neuronal survival [19–21], synaptic plasticity [22,23] and peripheral immune cell trafficking [24,25]. Due to the heterogeneity of the secondary response to TBI, the multifaceted nature of melanocortin agonists provides an intriguing and attractive therapeutic research area. However, very little research has been conducted on the effect of melanocortin agonists following acquired brain injury.

Below we describe four future research areas that would enhance our understanding of melanocortin agonists following TBI through Aim 1) evaluation of dosage effects for clinically relevant melanocortin agonists, Aim 2) use of *in vivo* imaging of inflammation following administration of anti-inflammatory compounds, Aim 3) quantification of the effect of melanocortin agonists on peripheral immune cell infiltration following TBI and, finally, Aim 4)

the potential contribution of MC4R in microglial phenotype and immune response in normal and injured brains. *Our overall hypothesis is that MC4R signaling reduces neuroinflammation and improves functional recovery via microglia phenotype modulation following experimental TBI.*

General Methods for Future Research

Model of Traumatic Brain Injury

Adult 3-month-old C57BL/6J male mice (Jackson Laboratory, Bar Harbor, ME) will be randomly assigned to TBI or sham groups. TBI will be induced through the well-recognized controlled cortical impact (CCI) model as previously described [26]. The location of injury results in damage to the primary motor cortex, the medial and lateral parietal association cortex and septal pole of the hippocampus resulting in behavioral deficits [27]. Sham groups will experience the entire procedure except the final impact.

CoSyn Administration

CoSyn is being supplied by *West Therapeutic Development, LLC*, (Grayslake, IL) Dosing was chosen based on literature and previous work in our lab [28–31]. The first dose of CoSyn or setmelanotide will be administered subcutaneously 3 hours after CCI and then given once per day for seven days. The most effective dose will be determined via Aim 1. For Aims 2-3, dosage and drug selection will be dependent on Aim 1 data. However, to date, our lab currently has shown immune modulatory and behavioral effects of CoSyn with a dosage of 60U/kg/day and Aim 2-3 will be based on this previous research.

Cortical, Hippocampal and Serum Cytokine Expression

Cytokine expression will be evaluated through the use of a 29-plex mouse cytokine panel developed by Meso Scale Discovery (Piscataway, NJ, USA). The cytokine panel evaluates the expression of 29 cytokines including both pro and anti-inflammatory compounds (e.g. IFN-γ, IL-1β, IL-6, IL-10, IL-12p70, MCP-1, MIP-1α and TNF-α). Principal component analysis of cytokine expression will be completed as previously described [32]. Perilesional, hippocampal and serum cytokine levels will be quantified using this method.

Microglia Phenotype

Microglia activation will be assessed through colocalization of Iba1 (microglia/macrophage marker) with specific markers for M1 (CD86) and M2 (CD206) phenotypic states and morphological assessment [33,34]. To quantify morphology of microglia, Iba1-immunolabeled cells will be processed and analyzed with *FracLac for ImageJ* to produce morphological parameters (e.g. fractal dimension, lacunarity, density, perimeter) for individual microglia as described previously by Karperien and colleagues [35]**.** Using three-dimensional colocalization, we will correlate microglia morphology with M1/M2 markers to quantify individual microglia activation states. Cell-typing cluster analysis will be conducted to identify and quantify changes in subpopulations of microglia following experimental TBI [36]. Briefly, principal component analysis will be performed to identify correlation between different variables – including single-cell morphological parameters with M1 (CD86) and M2 (CD206) markers. To

detect subpopulations, hierarchical cluster analysis with use of the squared Euclidean distance metric will be performed, as previously described [33,36]. Thorndike's procedure will be implemented to determine number of clusters. Between-group differences in percentage of cells in each cluster will be analyzed with two-way ANOVA with post hoc testing.

Behavioral Assessments

Cognitive and affective deficits will be evaluated using open field testing to evaluate anxiety-like behavior, Morris Water Maze (MWM) to evaluate cognitive deficits and tail suspension testing to evaluate depression-like behavior [37,38]. Stress-inducing behavioral testing is scheduled outside the treatment window to reduce alterations in glucocorticoid levels during treatment. Furthermore, animals will be handled using the tunnel method to reduce handling-induced stress [39]. Behavior with repeated-measures (MWM) will be assessed using a mixed-design ANOVA to measure differences between groups. Assumptions of normality, homogeneity of variance and sphericity will be tested. Two-way ANOVA will be used to test differences between groups for open field and tail-suspension testing. When significance is reached, individual between-group comparisons will be performed with post hoc testing. Data analysis will be completed using GraphPad *Prism* software (GraphPad Software, Inc., San Diego, CA).

AIM 1: Melanocortin Agonists following Traumatic Brain Injury

Rationale & Preliminary Data

Several compounds have been evaluated as MCR agonists (Table 1). These include both endogenous (□-MSH and ACTH) and synthetic analogs (cosyntropin, NDP-□-MSH). Of interest, two MC4R agonists have recently been tested for their clinical efficacy in the treatment of hyposexual desire disorder and rare genetic disorders of obesity, bremelanotide and setmelanotide, respectively. Setmelanotide has anti-inflammatory and macrophage phenotype modulating effects [40]. Furthermore, Setmelanotide is an attractive compound as it is currently in Phase 3 clinical trials resulting in the possibility of drug repositioning. A majority of research on the benefits of melanocortins following neuroinflammatory insult and acquired brain injuries have investigated MC4R-signaling via synthetic variants of α-MSH with no research on the effects of Setmelanotide following acquired brain injury. In favor of the use of a MC4R-selective agonist, it has been proposed that MC4R-selective agonists could reduce the peripheral immune side effects produced by MC1R, MC2R, and MC5R signaling [40]. However, MC4R-selective agonists also do not modulate inflammation through the other melanocortin receptors, including the stimulation of glucocorticoid production, which could reduce their efficacy. Unlike α-MSH and Setmelanotide, ACTH is the only endogenous MC that activates MC2R in the adrenal cortex, stimulating corticosteroid (CS) production [41]. In favor of the use of an ACTH analog, both the natural and synthetic variants

Table 1. Examples of melanocortin agonists currently available for pre-clinical research use

Agonist		Notes
□-MSH	**+**	Can cross BBB
	-	Short half-life
	R	Agonist for MC1R, MC3R-5R; Greater ligand affinity for MC5R and MC1R compared to ACTH
	G	Does not have steroidogenic effects
Long Acting Cosyntropin	**+**	Cheaper, less immune reactive than full length ACTH, safety testing for non-bound ACTH (1-24)
	-	Not currently FDA approved
	R	High ligand affinity for all receptor types, lower ligand affinity compared to □-MSH for MC1R and MC5R
	G	Has steroidogenic effects
Setmelanotide	**+**	Currently in Phase 3 clinical trials, demonstrated immune modulation in MS model
	-	Limited data
	R	Potent MC4R agonist
	G	Data unavailable, not proposed
NDP-□-MSH	**+**	Longer half-life than natural □-MSH analog
	-	Limited research of effectiveness
	R	MC4R agonist
	G	Does not have steroidogenic effects
Acthar Gel	**+**	FDA approved, human safety testing completed
	-	Expensive, can initiate an immune response
	R	High ligand affinity for all receptor types, lower ligand affinity compared to □-MSH for MC1R and MC5R
	G	Has steroidogenic effects
Bremelanotide	**+**	FDA approved
	-	Possible enhancement and specificity for modifying sexual functioning, no anti-inflammatory effects data
	R	Proposed as an MC4R agonist
	G	Data unavailable, not proposed

Information from Catania et al., 2004 and U.S. Food and Drug Administration

of ACTH stimulate all subtypes of the melanocortin receptors resulting in a multifaceted response including increases in circulating glucocorticoid levels [41].Along with the potential anti-inflammatory and neuroprotective effects of MC4R signaling, glucocorticoids have been shown to reduce inflammation andinflammation-induced toxicity [42,43]. However, the benefits of glucocorticoids following TBI are controversial as a large, randomized, multi-center TBI clinical trial (CRASH study) evaluating the effect of early administration on death and disability indicate that high-dose methylprednisolone increases mortality following significant head injury and therefore suggests that synthetic glucocorticoids should not be used for the treatment of TBI [44,45]. It is unclear if glucocorticoids are the predominant mechanism of action for ACTH analogs. No studies have directly compared the efficacy of both an ACTH analog with an MC4R-selective agonist following brain injury. Our lab has demonstrated the anti-inflammatory effects of a long acting synthetic ACTH analog (CoSyn, ACTH 1-24) following TBI but have not evaluated dose response. As a result, we propose a dose response study evaluating the immune modulatory and behavioral effects of CoSyn and Setmelanotide following experimental TBI.

Experimental Design

To evaluate the dose response of CoSyn and Setmelanotide, we will use the CCI model to induce injury in adult male mice as described in the general methods (Figure 1A-C). Our experimental design is composed of three sub-aims. Aim 1.1 addresses the acute inflammatory response and will inform our dose

A **Aim 1.1 Acute Immune Modulation of CoSyn and Setmelanotide**

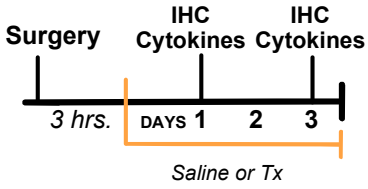

Experimental Groups
1. Naive
2. Sham + Saline
3. TBI + Saline
4. TBI + CoSyn 15 U/kg/day
5. TBI + CoSyn 30 U/kg/day
6. TBI + CoSyn 60 U/kg/day
7. TBI + Setmelanotide 20 µg/kg/day
8. TBI + Setmelanotide 40 µg/kg/day
9. TBI + Setmelanotide 80 µg/kg/day

B **Aim 1.2** Behavioral outcomes following CoSyn and Setmelanotide treatment

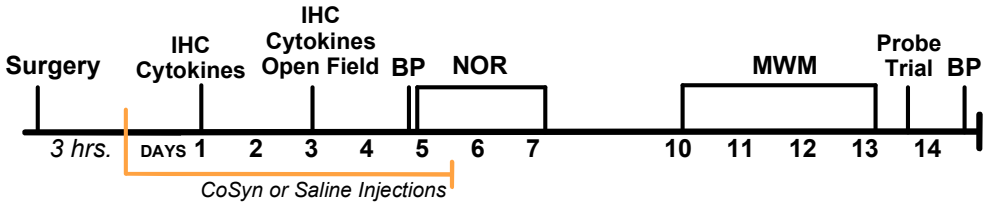

Experimental Groups
1. Naive
2. Sham + Saline
3. TBI + Saline
4. Sham + CoSyn [Selected from Aim 1.1]
5. TBI + CoSyn [Selected from Aim 1.1]
6. Sham + Setmelanotide [Selected from Aim 1.1]
7. TBI + Setmelanotide [Selected from Aim 1.1]

C **Aim 1.3** Role of MC4R signaling in behavioral and immune modulatory effects of melanocortin receptor agonist

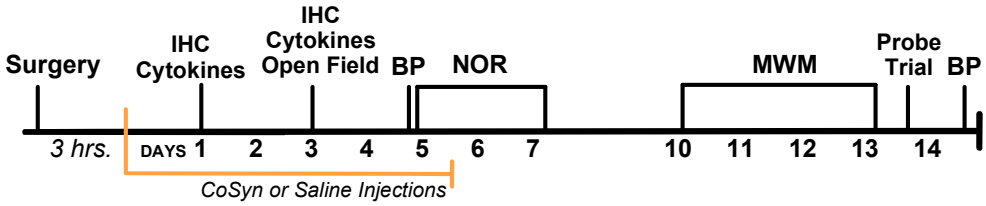

Experimental Groups
1. Sham + Saline
2. Sham + SHU9119
3. TBI + Saline
4. TBI + Tx [Selected from Aim 1.2]
5. TBI + Tx [Selected from Aim 1.2] + SHU9119

Figure 1. Experimental design for Aim 1

selection for Aim 1.2 (Figure 1A). Aim 1.2 will be a head-to-head comparison of CoSyn and Setmelanotide with evaluation of microglia/macrophage density and neutrophil infiltration via immunohistochemistry (IHC), cytokine expression and behavioral outcomes (Figure 1B). Aim 1.3 will evaluate the role of MC4R signaling in treatment through the use of an MC4R antagonist (SHU9119). Information gathered from Aim 1.2 will be used to inform selection of treatment for Aim 1.3. Methods used in Aim 1.1-2 will be repeated for Aim 1.3 (Figure 1C). A 3-hour treatment window was selected to balance the need for early intervention with the desire to choose a clinically relevant time-point. According to the CRASH study, over half of TBI patients were treated within 3-hours [44,46]. A literature search of studies using ACTH revealed that 60U/kg/day fell within the range of multi-day treatments. Therefore, our dosage range will be 15-60 U/kg/day (See table 3 in Chapter 1). Previous data from our lab has demonstrated that 120 U/kg/day resulted in signs of distress in mice following surgeries. Relying on clinical trial data, we have selected dosages ranging from 20-80 µg/kg/day for setmelanotide. Extended use of ACTH in the clinic results in side effects that include Cushing's syndrome, hypertension, ulcers and mood disturbances [47]. As a result, blood pressure (BP), behavioral tests for anxiety-like behavior, food consumption and weight will be monitored throughout the study.

Anticipated Results and Interpretation

We anticipate that both CoSyn and Setmelanotide will result in acute suppression of the inflammatory response (Aim 1.1) with dose-dependent

effects. Acute suppression will be evidenced through reduction in pro-inflammatory cytokine expression and reduced microglia/macrophages and neutrophils in the brain parenchyma and hippocampus. We anticipate no alterations in anxiety-like behavior with setmelanotide but increased anxiety-like behavior with CoSyn-treatment in both sham and TBI mice (Aim 1.2). We anticipate improved memory performance in the treated TBI mice in both the NOR and MWM compared to saline-treated TBI mice. Aim 1.3 will evaluate MC4R as a mechanism of action. We expect SHU9119 to diminish the treatment-induced improvements in memory as well as increase microglia/macrophage and neutrophils in the brain parenchyma compared to treated TBI mice.

Potential Pitfalls, Alternative Approaches, and Future Directions

Our lab has previously demonstrated the immune suppressive effects of CoSyn following TBI and therefore anticipate replication of this data. If we are unable to replicate our previous research, the use of Acthar Gel is an alternative approach an ACTH compound (Table 1). One potential pitfall is in the head-to-head comparison of Setmelanotide as this compound has never been tested as an anti-inflammatory following brain injury. If Setmelanotide does not show immune modulatory effects, several other MC4R agonists are available including Bremelanotide and NPD-□-MSH (Table 1). Future directions include the evaluation of alternative dosage regimens, quantification of neuronal cell death and synaptic plasticity, inhibition of other melanocortin receptors and the use of

adrenalectomized mice to evaluate the role of glucocorticoids in melanocortin agonist treatment following TBI.

AIM 2: Microglia Phenotype and In Vivo imaging of Glial Activation

Rationale & Preliminary Data

TBI is associated with a rapid and robust neuroinflammatory response followed by chronic microglia activation and inflammation [4,5]. We hypothesize that CoSyn results in reduced neuroinflammation and promotion of an M2 microglia phenotype thus conferring a neuroprotective effect following TBI (Figure 2A). Recent work in our lab using a mouse CCI model of TBI showed that at DPI three, daily injection of CoSyn (60U/kg/dose) attenuated TBI-induced microglia morphology changes as well as decreased number of microglia/macrophages at DPI three and 21 between treated and untreated groups (Figure 2B-C, n=6-8 per group). Analysis was completed under blinded conditions. The ImageJ plug-in *FracLac for ImageJ* was used to quantify morphology of microglia, as previously described [33,35]. Both injury groups showed increased microglia density consistent with microglia activation (Figure 2C). Treatment reduced injury-induced morphological changes compared to untreated-injured group and suggests CoSyn as a potential modulator of microglia activation and downstream neuroinflammatory responses.

Experimental Design

To test the hypothesis that CoSyn is anti-inflammatory following experimental TBI, 3-month old C57/Bl6 mice will undergo CCI injury followed

by saline or CoSyn delivery through subcutaneous injections. MRI and PET imaging along with immunohistochemistry will be conducted to evaluate microglia phenotype and *in vivo* glial activation. Techniques described in General Methods will be employed to evaluated microglia phenotype.

To evaluate the *in vivo* neuroinflammatory response with a translationally relevant and non-invasive technique, we will employ PET imaging using a 2nd generation translocator protein (TSPO) radioligand, [18F]DPA-714. TSPO is substantially upregulated predominantly in activated microglia and has been used to depict the inflammatory state [48,49]. Mice will be imaged at DPI 7 and 21 to evaluate the robust, initial microglia activation, temporal change and the chronic inflammatory state [50,51]. [18F]DPA-714 has been synthesized in the LLU radiochemistry laboratory in the Center for Imaging Research and will be used for our preclinical studies in mice. A 20 minute dynamic list mode acquisition will then be taken using a microPET scanner (Rodent R4, Concorde Systems). PET images will be reconstructed using a OSEM2D algorithm after scatter, decay and attenuation correction. MR images will be acquired separately (11.7T Bruker MR scanner) and co-registered with ^{18}F-DPA-714 PET reconstructed images using VivoQuant™ software (InVicro Inc.) An automated rigid transformation of InVicro's 3D mouse brain atlas to the co-registered images will be used to obtain quantitative standard uptake values (SUV) in up to 13 bilateral brain regions, including the hippocampus, thalamus and cortex. These measurements will be used to detect increased microglial activation in TBI mice compared to controls

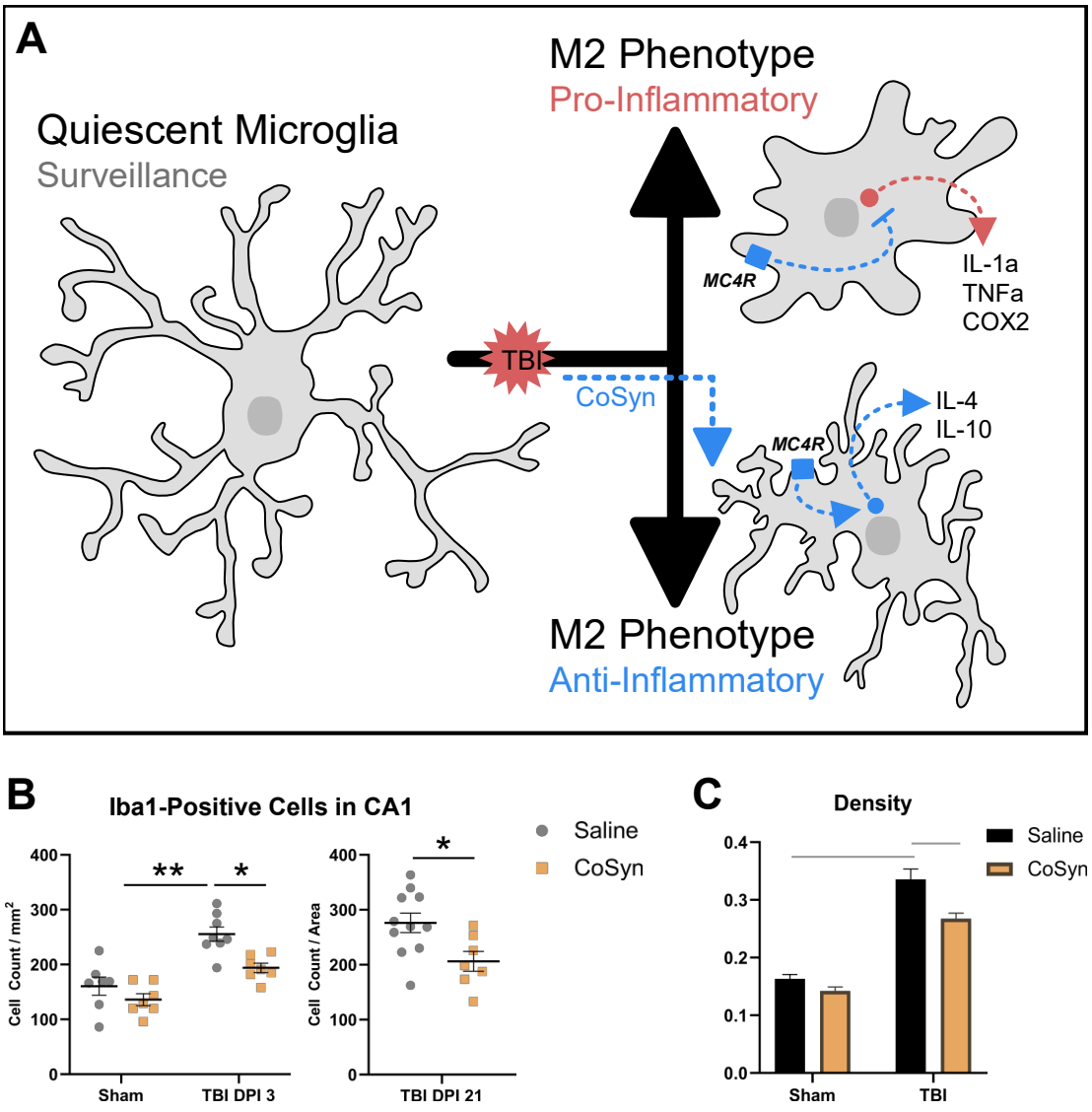

Figure 2. Preliminary data for Aim 2. (A) Diagram of morphological and phenotypic changes in microglia following TBI. (B) CoSyn administration reduced Iba1-positive cells in CA1 at DPI three and 21. (C) CoSyn administration reduces injury-induced increase in density. Statistical analysis was completed with Two-way ANOVA (B) or Levene's test (C). Post hoc Tukey test revealed between-group differences. Lines and * $p<0.05$, ** $p < 0.01$.

in areas of the brain distant from the lesion. Since the model produces variable injury, manual ROI's will also be drawn in areas of highest ^{18}F-DPA-71 uptake representing highest microglia activation and a second ROI in an area of lowest uptake representing lowest microglia activation. A High/Low Activation ratio will be calculated. These areas will be compared to MR T2 weighted images for lesion detection. In addition, an ROI will be placed in the cerebellum and used as a relative reference region as previously validated in a TBI model [48]. A ratio of highest ^{18}F-DPA-714 uptake (Lesion) to cerebellum will be calculated (Lesion/Cerebellum ratio). A statistical comparison of the High/Low and Lesion/Cerebellum ratios at each time point will be tested for statistical significance between groups by one-way analysis of variance (ANOVA) with post-hoc Bonferroni test. A sensitivity power analysis (two-way repeated measure ANOVA: ($\alpha = 0.05$ and $\beta = 0.2$) shows that 12 mice per group is sufficient to reveal minimum effect sizes of 0.30 (*G*Power* 3.1.9.2) for PET imaging.

Anticipated Results and Interpretation

As previous work in our lab has suggested, we anticipate that CoSyn will reduce microglia activation as demonstrated by morphology that is consistent with a more ramified morphology and will enhance expression of M2 markers compared to M1 markers. This suggests a phenotype consistent with enhanced resolution of the inflammatory response and would correlate with reduced lesion size and edema as indicated by MR imaging. We further anticipate that CoSyn

will alter the kinetic profile of inflammatory resolution resulting in quicker returns to baseline in CoSyn-treated compared to the saline-treated TBI animals, particularly at DPI seven when microglial activation is resolving [51].

Potential Pitfalls, Alternative Approaches, and Future Directions

A potential pitfall in our decision to inject CoSyn subcutaneously is that it may not cross the BBB. Subcutaneous injection is clinically relevant and the BBB is disrupted following TBI allowing for enhanced drug infiltration into the brain parenchyma [52]. An alternative approach is to bypass the BBB by intrathecal or intraventricular deliver of CoSyn. Both methods are invasive, less clinically relevant and could worsen TBI severity. Our current research methods also do not directly address the influence of peripheral immune cell infiltration which does affect the inflammatory response following TBI and may be modulated by CoSyn [53]. Flow-cytometry analysis is a potential future direction to better distinguish infiltrating immune cells but loses the spatial distribution characteristic and therefore was not chosen for this study [54]. Other melanocortins without steroidogenic effects could also be evaluated, including NDP-alpha-MSH or Setmelanotide [55]. Further research is needed on the BBB permeability as well as the long-term consequences of CoSyn treatment following TBI.

AIM 3: Peripheral Immune Cell Infiltration

Rationale and Preliminary Data

Peripheral immune cell infiltration following TBI exacerbates the inflammatory response and reduces functional outcome following TBI [53,56,57].

Following brain injury, peripheral immune cell recruitment is modulated by CCL22 and CCL17, ligands for CCR4. CCR4 is expressed in monocytes and CCR4-positive monocytes increase following TBI in human serum [58]. While CCL22 has previously been associated with an M2 phenotype, only one study has evaluated the role of CCL22 in experimental TBI showing an association between lower levels of CCL22 and improved functional outcomes suggesting a deleterious effect of CCL22 after injury [59]. Preliminary data from our lab shows that CoSyn treatment following TBI reduces injury-induced CCL22 expression (Figure 3A) and overall expression of CCL17 expression in sham-CoSyn and TBI-CoSyn treated groups (Figure 3B). CoSyn also decreased neutrophil infiltration and microglia/macrophage (Iba1+) cell count the brain parenchyma (Figure 3C). Furthermore, in humans, ACTH and steroid treatment lowers expression of CCL22 [60]. The role of CCR4-ligands (CCL22, CCL17) in leukocyte recruitment and their reduced expression following CoSyn treatment provide a strong rationale for evaluating the role of CoSyn adhesion molecule expression and peripheral immune cell invasion following TBI. We hypothesize that administration of CoSyn following TBI results in reduced macrophage accumulation.

Experimental Design

To test the hypothesis that CoSyn reduced peripheral macrophage infiltration following experimental TBI, 3-month old genetically modified mice will undergo CCI injury followed by saline or CoSyn delivery through

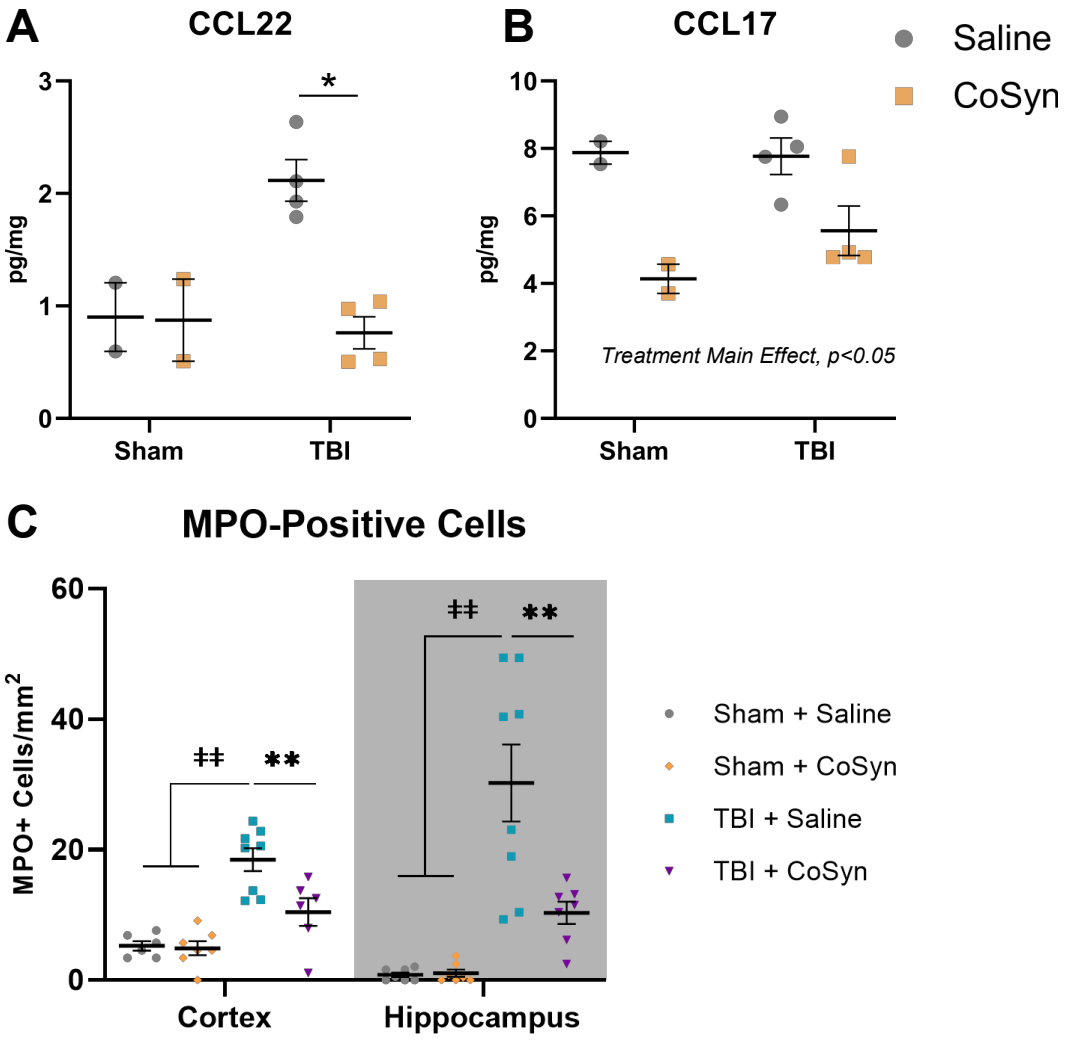

Figure 3. Preliminary data for Aim 3. (A) CoSyn ameliorated injury-induced CCL22 in cortical tissue at DPI seven (B) CoSyn administration reduced CCL17 expression in cortical tissue at DPI seven in both sham and TBI groups. (C) CoSyn attenuates injury-induced neutrophil (MPO+) infiltration. Statistical analysis was completed with Two-way ANOVA. Post hoc Tukey test revealed between-group differences. Lines and * $p<0.05$, ** $p < 0.01$, ‡‡ $p< 0.001$.

subcutaneous injections. To differentiate between tissue-resident macrophages and peripheral immune cell infiltration, we propose using a Cx3Cr1-GFP / CCR2-RFP reporter mouse line with use of mouse lines developed by Jackson Laboratory (Jackson Lab, Sacramento, CA). A homozygous reporter line with red-fluorescent protein (RFP) under the control of the CCR2 promoter will be bred with a homozygous reporter line with green-fluorescent protein (GFP) under the control of the Cx3Cr1 promoter to produce heterozygous $Cx3Cr1^{GFP/+}$, $CCR2^{RFP/+}$ mice (Figure 4C). CCR2 has been previously used as a reporter of peripheral monocytes while Cx3Cr1 is highly expressed in microglia [61]. To determine if morphology can distinguish between microglia and peripheral macrophages, *FracLac for ImageJ* will be used to assess 12 different morphological parameters and comparisons between microglia and macrophages, sham and injured as well as saline and CoSyn-treated will be conducted, as described in General Methods. To emulate Aim 1-2 design, microglia/macrophage quantification will be conducted for DPI 3, 7 and 21. Furthermore, to correlate blood brain barrier breakdown with macrophage infiltration, we will conduct inject Evans blue via the tail vein to evaluate blood brain barrier integrity.

Anticipated Results

We anticipate that CoSyn will reduce peripheral macrophage accumulation in the CNS following TBI. We further anticipate that distinct clustering will occur for peripheral macrophages compared to tissue-resident MG when combining morphology with MG and peripheral macrophage

markers. We also anticipate that CoSyn will increase BBB integrity exhibited as a reduction in Evans blue permeability into the brain parenchyma.

Potential Pitfalls, Alternative Approaches, and Future Directions

A potential issue is the development of the dual-reporter line. Currently, both reporter lines are established by Jackson Lab and homozygous lines are able to breed. Flow-cytometry analysis is a potential alternative approach to better distinguish infiltrating immune cells from MG but loses the spatial distribution and morphology of immune cells. We may also include analysis of neutrophil invasion in the future. Future directions include perturbation of CCL22 and CCL17 through anti-CCL22, siRNA or CCL22 or CCR4 knockouts [62].

AIM 4: Melanocortin Receptor 4 Signaling in Microglia following TBI

Rationale

The proposed study will evaluate the role of microglia-specific MC4R signaling on the neuroprotective effect of CoSyn following experimental TBI. To modulate MC4R signaling specifically in microglia, we will establish an inducible microglia-specific MC4R knockout line using already established MC4R-floxed and tamoxifen-inducible Cre lines (Jackson Lab, Sacramento, CA). Regardless of the effect of CoSyn, no studies have evaluated CNS or microglia-specific MC4R knockout mice and therefore the contribution of microglia MC4R signaling on the neuroinflammatory response following brain injury. The use of

microglia-specific inducible knockout lines are vital for identifying the unique and diverse responses of microglia to brain injury.

Experimental Design

To evaluate the role of MC4R signaling in microglia, a Cre-LOX system will be used (Figure 4). A tamoxifen-inducible Cre-recombinase with enhanced yellow fluorescent mouse line that is directed to CNS microglia and Cx3cr1-expressing myeloid cells under the control of Cx3cr1 promoter ($CX3CR1^{YFP\text{-}creER}$) will be bred with an MC4R floxed line (MC4rtm2.2Lowl/J) to produce an MC4R tamoxifen-inducible line with CNS microglia expression of Cre ($MC4R^{Cx3cr1}$; $CX3CR1^{YFP\text{-}creER}$ and MC4R-floxed mice available through Jackson Lab, Sacramento, CA). Three weeks prior to injury, $MC4R^{flox/flox}$::$CX3CR1^{YFP\text{-}creER}$ mice will be administered 75 mg/kg of tamoxifen dissolved in corn oil intraperitoneally daily for five consecutive days to induce Cre recombination via the CX3CR1 promoter, as previously reported (Figure 4) [63]. Previous research has demonstrated induction of genomic modification in both peripheral myeloid cells and microglia with the use of a $CX3CR1^{creER}$ line followed by re-population of peripheral myeloid cells without genomic modification [64]. Re-population of non-modified microglia did not occur [64]. To reduce the effect of MC4R knockout in peripheral myeloid cells and take advantage of endogenous re-population of peripheral myeloid cells, CCI induction will take place three weeks following final tamoxifen injection. To evaluate MG-specific Cre-expression and MC4R-KO efficiency, IHC will be used to identify MC4R+ and EYFP+ microglia number

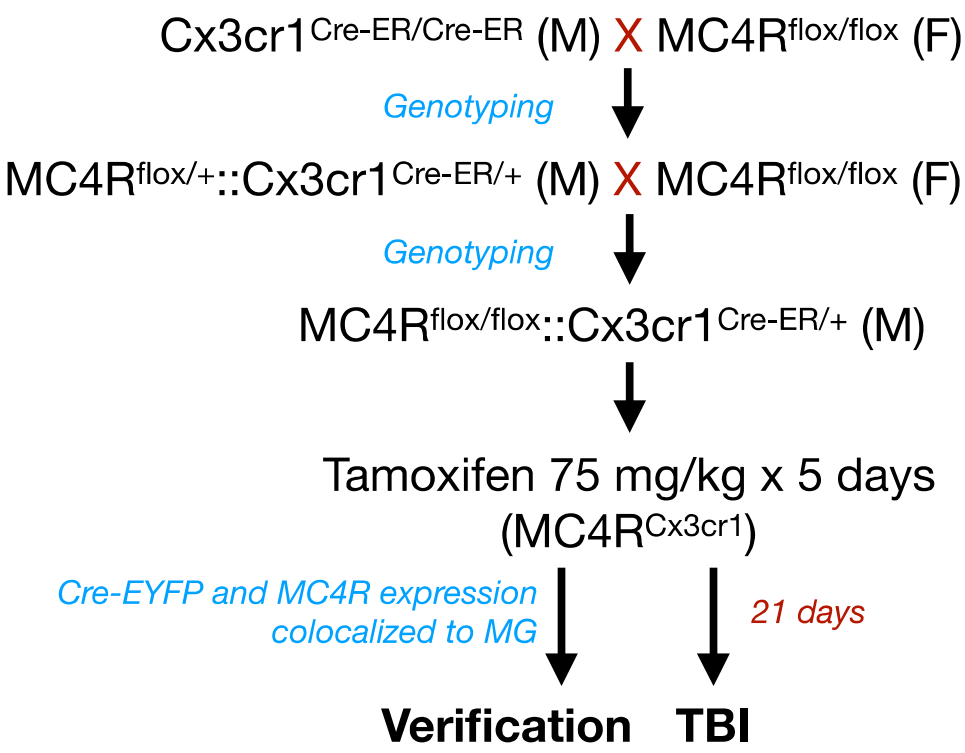

Figure 4. Overview of plan for generation and verification of Cre-Lox model.

using unbiased stereology methods (*Stereologer* from SRC, Tampa, FL). Genotyping of target and non-target tissue will be performed (Figure 4). Methods described in General Methods will be used to evaluate the neuroinflammatory (cytokine quantification and microglia phenotype) and behavioral outcomes.

Anticipated Results and Interpretation

We anticipate that microglia-specific MC4R KO will have increased and prolonged peripheral and brain inflammation along with increased microglia activation, specifically enhancing the M1 phenotype and increasing the M1/M2 ratio. This would suggest a phenotype consistent with reduced resolution of the inflammatory response and would correlate with increased lesion size and edema and enhanced behavioral deficits. Poorer outcomes in microglia-specific MC4R KO would suggest an important role of MC4R-signaling in modulating the microglial response following TBI and a potential therapeutic target.

Potential Pitfalls, Alternative Approaches, and Future Directions

While the MC4R floxed and Cx3cr1-Cre mouse lines are provided by Jackson Laboratory, a potential pitfall is the establishment of the MC4R inducible mouse line. While we acknowledge this potential issue, the use of the Cxcr1-Cre/MC4R inducible mouse line is the most efficient and direct way to assess the role of *in vivo* MC4R signaling in microglia. Both the CX3CR1$^{YFP\text{-}creER}$ and MC4rflox/flox mouse lines have been used to evaluate microglia-specific Cre expression and cell-specific Cre-induced MC4R KO, respectively [63,65].Alternative

approaches to evaluating the role of MC4R signaling in CoSyn therapy are the use of MC4R antagonist (HS024) or siRNA. However, both antagonists and siRNA are not cell-specific resulting in the ability to modulate MC4R but not identify the specific cells in which this signaling is beneficial. Along with MC4R, MC3R receptors are also expressed in the CNS and may contribute to the neuroprotective effects [66]. Previous research has indicated that melanocortins produce alterations in AMPK phosphorylation that may contribute to the alterations in glucose metabolism and neuroinflammation (Figure 4) [24]. An alternative mechanism of actions could be alterations in metabolic activity or mitochondrial functioning, both of which are dysfunctional following TBI [48,67,68]. Metabolic activity of microglia is also associated with activation state and both ROS-creation and ROS-scavenging, producing another potential explanation for the neuroprotective effect of melanocortin agonists following TBI [69,70]. Melanocortin agonists may also modulate the inflammatory response by inhibiting peripheral immune cell infiltration or through astrocyte modulation [40,71]. Research is needed to explore the central and peripheral immune melanocortin signaling treatment following TBI.

Overall Summary

By completing this research, we will provide evidence for the endogenous-based pro-resolving capacity of melanocortin receptor agonists following TBI and the role of MC4R signaling in altering microglia phenotype and attenuation of neuroinflammation. Our work will provide additional

evidence supporting the role of melanocortins as neuroinflammatory modulators with the goal of treating patients who are suffering from the long-term consequences of a TBI.

References

1. Flanagan, S. R. Invited Commentary on 'Centers for Disease Control and Prevention Report to Congress: Traumatic Brain Injury in the United States: Epidemiology and Rehabilitation'. *Arch Phys Med Rehabil* **96**, 1753–5 (2015).

2. Simon, D. W. *et al.* The far-reaching scope of neuroinflammation after traumatic brain injury. *Nature Reviews Neurology* **13**, 171–191 (2017).

3. Scherbel, U. *et al.* Differential acute and chronic responses of tumor necrosis factor-deficient mice to experimental brain injury. *Proc Natl Acad Sci U S A* **96**, 8721–6 (1999).

4. Ramlackhansingh, A. F. *et al.* Inflammation after trauma: Microglial activation and traumatic brain injury. *Annals of Neurology* **70**, 374–383 (2011).

5. Johnson, V. E. *et al.* Inflammation and white matter degeneration persist for years after a single traumatic brain injury. *Brain* **136**, 28–42 (2013).

6. Cherry, J. D. *et al.* Microglial neuroinflammation contributes to tau accumulation in chronic traumatic encephalopathy. *Acta Neuropathologica Communications* **4**, (2016).

7. Lindolfo da Silva Meirelles, Daniel Simon & Andrea Regner. Neurotrauma: The Crosstalk between Neurotrophins and Inflammation in the Acutely Injured Brain. *International Journal of Molecular Sciences* **18**, 1082 (2017).

8. Appleton, R. E. Post-traumatic epilepsy in children requiring inpatient rehabilitation following head injury. *Journal of Neurology, Neurosurgery & Psychiatry* **72**, 669–672 (2002).

9. Faden, A. I. & Loane, D. J. Chronic Neurodegeneration After Traumatic Brain Injury: Alzheimer Disease, Chronic Traumatic Encephalopathy, or Persistent Neuroinflammation? *Neurotherapeutics* **12**, 143–150 (2015).

10. Gallo-Payet, N. 60 YEARS OF POMC: Adrenal and extra-adrenal functions of ACTH. *Journal of Molecular Endocrinology* **56**, T135–T156 (2016).

11. Bertolini, A., Tacchi, R. & Vergoni, A. Brain effects of melanocortins☆. *Pharmacological Research* **59**, 13–47 (2009).

12. Kishi, T. *et al.* Expression of melanocortin 4 receptor mRNA in the central nervous system of the rat. *The Journal of Comparative Neurology* **457**, 213–235 (2003).

13. Krashes, M. J., Lowell, B. B. & Garfield, A. S. Melanocortin-4 receptor–regulated energy homeostasis. *Nature Neuroscience* **19**, 206–219 (2016).

14. Chen, M., Aprahamian, C. J., Kesterson, R. A., Harmon, C. M. & Yang, Y. Molecular Identification of the Human Melanocortin-2 Receptor Responsible for Ligand Binding and Signaling †. *Biochemistry* **46**, 11389–11397 (2007).

15. Goverde, H. J. M. & Smals, A. G. H. The anomalous effect of some ACTH-fragments missing the amino acid sequence 1-10 on the corticosteroidogenesis in purified isolated rat adrenal cells. *FEBS Letters* **173**, 23–26 (1984).

16. Montero-Melendez, T. *et al.* The Melanocortin Agonist AP214 Exerts Anti-Inflammatory and Proresolving Properties. *The American Journal of Pathology* **179**, 259–269 (2011).

17. Huang, Q. & Tatro, J. B. a-melanocyte stimulating hormone suppresses intracerebral tumor necrosis factor-a and interleukin-1b gene expression following transient cerebral ischemia in mice. *Neuroscience Letters* 5 (2002).

18. Bitto, A. *et al.* Protective effects of melanocortins on short-term changes in a rat model of traumatic brain injury*. *Critical Care Medicine* **40**, 945–951 (2012).

19. Lisak, R. P., Nedelkoska, L., Bealmear, B. & Benjamins, J. A. Melanocortin receptor agonist ACTH 1–39 protects rat forebrain neurons from apoptotic, excitotoxic and inflammation-related damage. *Experimental Neurology* **273**, 161–167 (2015).

20. Giuliani, D. *et al.* Treatment of cerebral ischemia with melanocortins acting at MC4 receptors induces marked neurogenesis and long-lasting functional recovery. *Acta Neuropathol* **122**, 443–453 (2011).

21. Spaccapelo, L. *et al.* Melanocortin MC4 receptor agonists counteract late inflammatory and apoptotic responses and improve neuronal functionality after cerebral ischemia. *European Journal of Pharmacology* **670**, 479–486 (2011).

22. Shen, Y. *et al.* Stimulation of the Hippocampal POMC/MC4R Circuit Alleviates Synaptic Plasticity Impairment in an Alzheimer's Disease Model. *Cell Reports* **17**, 1819–1831 (2016).

23. Shen, Y., Fu, W.-Y., Cheng, E. Y. L., Fu, A. K. Y. & Ip, N. Y. Melanocortin-4 Receptor Regulates Hippocampal Synaptic Plasticity through a Protein Kinase A-Dependent Mechanism. *Journal of Neuroscience* **33**, 464–472 (2013).

24. Chen, S. *et al.* Activation of melanocortin receptor 4 with RO27-3225 attenuates neuroinflammation through AMPK/JNK/p38 MAPK pathway after intracerebral hemorrhage in mice. *Journal of Neuroinflammation* **15**, (2018).

25. Getting, S. J., Christian, H. C., Flower, R. J. & Perretti, M. Activation of melanocortin type 3 receptor as a molecular mechanism for adrenocorticotropic hormone efficacy in gouty arthritis. *Arthritis & Rheumatism* **46**, 2765–2775 (2002).

26. Romine, J., Gao, X. & Chen, J. Controlled Cortical Impact Model for Traumatic Brain Injury. *Journal of Visualized Experiments* (2014) doi:10.3791/51781.

27. George Paxinos & Franklin, K. *Paxinos and Franklin's the Mouse Brain in Stereotaxic Coordinates*. (Academic Press, 2012).

28. Chachua, T., Yum, M.-S., Velíšková, J. & Velíšek, L. Validation of the rat model of cryptogenic infantile spasms: Validation of the Infantile Spasms Model. *Epilepsia* **52**, 1666–1677 (2011).

29. Velíšek, L., Jehle, K., Asche, S. & Velíšková, J. Model of infantile spasms induced by *N* -methyl-D-aspartic acid in prenatally impaired brain. *Annals of Neurology* **61**, 109–119 (2007).

30. Scantlebury, M. H., Chun, K.-C., Ma, S.-C., Rho, J. M. & Kim, D. Y. Adrenocorticotropic hormone protects learning and memory function in epileptic Kcna1 -null mice. *Neuroscience Letters* **645**, 14–18 (2017).

31. Rindler, T. N. *et al.* Knockout of the Na,K-ATPase α_2 -isoform in the cardiovascular system does not alter basal blood pressure but prevents ACTH-induced hypertension. *American Journal of Physiology-Heart and Circulatory Physiology* **301**, H1396–H1404 (2011).

32. Helmy, A., Antoniades, C. A., Guilfoyle, M. R., Carpenter, K. L. H. & Hutchinson, P. J. Principal Component Analysis of the Cytokine and

Chemokine Response to Human Traumatic Brain Injury. *PLoS ONE* **7**, e39677 (2012).

33. Fernández-Arjona, M. del M., Grondona, J. M., Granados-Durán, P., Fernández-Llebrez, P. & López-Ávalos, M. D. Microglia Morphological Categorization in a Rat Model of Neuroinflammation by Hierarchical Cluster and Principal Components Analysis. *Frontiers in Cellular Neuroscience* **11**, (2017).

34. Donat, C. K., Scott, G., Gentleman, S. M. & Sastre, M. Microglial Activation in Traumatic Brain Injury. *Frontiers in Aging Neuroscience* **9**, (2017).

35. Karperien, A., Ahammer, H. & Jelinek, H. F. Quantitating the subtleties of microglial morphology with fractal analysis. *Frontiers in Cellular Neuroscience* **7**, (2013).

36. Schweitzer, L. & Renehan, W. E. The use of cluster analysis for cell typing. *Brain Research Protocols* **1**, 100–108 (1997).

37. Bajwa, N. M. *et al.* Mild Concussion, but Not Moderate Traumatic Brain Injury, Is Associated with Long-Term Depression-Like Phenotype in Mice. *PLOS ONE* **11**, e0146886 (2016).

38. Zhao, Z., Loane, D. J., Murray, M. G., Stoica, B. A. & Faden, A. I. Comparing the Predictive Value of Multiple Cognitive, Affective, and Motor Tasks after Rodent Traumatic Brain Injury. *Journal of Neurotrauma* **29**, 2475–2489 (2012).

39. Gouveia, K. & Hurst, J. L. Reducing Mouse Anxiety during Handling: Effect of Experience with Handling Tunnels. *PLoS ONE* **8**, e66401 (2013).

40. Kamermans, A. *et al.* Setmelanotide, a Novel, Selective Melanocortin Receptor-4 Agonist Exerts Anti-inflammatory Actions in Astrocytes and Promotes an Anti-inflammatory Macrophage Phenotype. *Front. Immunol.* **10**, 2312 (2019).

41. Catania, A. Targeting Melanocortin Receptors as a Novel Strategy to Control Inflammation. *Pharmacological Reviews* **56**, 1–29 (2004).

42. Golde, S., Coles, A., Lindquist, J. A. & Compston, A. Decreased iNOS synthesis mediates dexamethasone-induced protection of neurons from inflammatory injury in vitro. *Eur J Neurosci* **18**, 2527–2537 (2003).

43. Dinkel, K., MacPherson, A. & Sapolsky, R. M. Novel glucocorticoid effects on acute inflammation in the CNS: Glucocorticoids and CNS inflammation. *Journal of Neurochemistry* **84**, 705–716 (2003).

44. Roberts, I, Yates, D & Sandercock, P. Effect of intravenous corticosteroids on death within 14 days in 10008 adults with clinically significant head injury (MRC CRASH trial): randomized placebo-controlled trial.

45. Edwards, P., Arango, M., Balica, L., Cottingham, R. & El-Sayed, H. Final results of MRC CRASH, a randomised placebo-controlled trial of intravenous corticosteroid in adults with head injury—outcomes at 6 months. *The Lancet* **365**, 1957–1959 (2005).

46. Mohamadpour, M., Whitney, K. & Bergold, P. J. The Importance of Therapeutic Time Window in the Treatment of Traumatic Brain Injury. *Frontiers in Neuroscience* **13**, (2019).

47. Food and Drug Administration. H.P. Acthar Gel (repository corticotropin) Injection. (2010).

48. Israel, I. *et al.* Combined [18F]DPA-714 micro-positron emission tomography and autoradiography imaging of microglia activation after closed head injury in mice. *Journal of Neuroinflammation* **13**, (2016).

49. Dupont, A.-C. *et al.* Translocator Protein-18 kDa (TSPO) Positron Emission Tomography (PET) Imaging and Its Clinical Impact in Neurodegenerative Diseases. *International Journal of Molecular Sciences* **18**, 785 (2017).

50. Wang, G. *et al.* Microglia/macrophage polarization dynamics in white matter after traumatic brain injury. *Journal of cerebral blood flow and metabolism : official journal of the International Society of Cerebral Blood Flow and Metabolism* **33**, 1864–74 (2013).

51. Jin, X., Ishii, H., Bai, Z., Itokazu, T. & Yamashita, T. Temporal Changes in Cell Marker Expression and Cellular Infiltration in a Controlled Cortical Impact Model in Adult Male C57BL/6 Mice. *PLoS ONE* **7**, e41892 (2012).

52. Thal, S. C. & Neuhaus, W. The Blood–Brain Barrier as a Target in Traumatic Brain Injury Treatment. *Archives of Medical Research* **45**, 698–710 (2014).

53. Lagraoui, M. *et al.* Controlled Cortical Impact and Craniotomy Induce Strikingly Similar Profiles of Inflammatory Gene Expression, but with Distinct Kinetics. *Frontiers in Neurology* **3**, (2012).

54. Serhan, C. N. *et al.* Resolution of inflammation: state of the art, definitions and terms. *The FASEB Journal* **21**, 325–332 (2007).

55. Tao, Y.-X. The Melanocortin-4 Receptor: Physiology, Pharmacology, and Pathophysiology. *Endocrine Reviews* **31**, 506–543 (2010).

56. Kenne, E., Erlandsson, A., Lindbom, L., Hillered, L. & Clausen, F. Neutrophil depletion reduces edema formation and tissue loss following traumatic brain injury in mice. *Journal of Neuroinflammation* **9**, (2012).

57. Makinde, H. M., Cuda, C. M., Just, T. B., Perlman, H. R. & Schwulst, S. J. Nonclassical Monocytes Mediate Secondary Injury, Neurocognitive Outcome, and Neutrophil Infiltration after Traumatic Brain Injury. *The Journal of Immunology* **199**, 3583–3591 (2017).

58. Cadosch, D. *et al.* Immune response deviation and enhanced expression of chemokine receptor CCR4 in TBI patients due to unknown serum factors. *Injury* **41**, e4–e9 (2010).

59. Chio, C.-C. *et al.* Exercise attenuates neurological deficits by stimulating a critical HSP70/NF-κB/IL-6/synapsin I axis in traumatic brain injury rats. *J Neuroinflammation* **14**, 90 (2017).

60. Pranzatelli, M. R., Tate, E. D., McGee, N. R., Colliver, J. A. & Ransohoff, R. M. CCR4 Agonists CCL22 and CCL17 are Elevated in Pediatric OMS Sera: Rapid and Selective Down-Regulation of CCL22 by ACTH or Corticosteroids. *J Clin Immunol* **33**, 817–825 (2013).

61. Parillaud, V. R. *et al.* Analysis of monocyte infiltration in MPTP mice reveals that microglial CX3CR1 protects against neurotoxic over-induction of monocyte-attracting CCL2 by astrocytes. *J Neuroinflammation* **14**, 60 (2017).

62. Dogan, R.-N. E. *et al.* CCL22 regulates experimental autoimmune encephalomyelitis by controlling inflammatory macrophage accumulation and effector function. *Journal of Leukocyte Biology* **89**, 93–104 (2011).

63. Appel, J. R. *et al.* Increased Microglial Activity, Impaired Adult Hippocampal Neurogenesis, and Depressive-like Behavior in Microglial VPS35-Depleted Mice. *The Journal of Neuroscience* **38**, 5949–5968 (2018).

64. Wolf, Y., Yona, S., Kim, K.-W. & Jung, S. Microglia, seen from the CX3CR1 angle. *Frontiers in Cellular Neuroscience* **7**, (2013).

65. Sohn, J.-W. *et al.* Melanocortin 4 Receptors Reciprocally Regulate Sympathetic and Parasympathetic Preganglionic Neurons. *Cell* **152**, 612–619 (2013).

66. Muceniece, R. *et al.* The MC3 receptor binding affinity of melanocortins correlates with the nitric oxide production inhibition in mice brain inflammation model. *Peptides* **27**, 1443–1450 (2006).

67. Brabazon, F. *et al.* [^{18} F]FDG-PET Combined with MRI Elucidates the Pathophysiology of Traumatic Brain Injury in Rats. *Journal of Neurotrauma* **34**, 1074–1085 (2017).

68. Kato, T. *et al.* Statistical Image Analysis of Cerebral Glucose Metabolism in Patients with Cognitive Impairment following Diffuse Traumatic Brain Injury. *Journal of Neurotrauma* **24**, 919–926 (2007).

69. Ghosh, S., Castillo, E., Frias, E. S. & Swanson, R. A. Bioenergetic regulation of microglia. *Glia* **66**, 1200–1212 (2018).

70. Kalsbeek, M. J. T., Mulder, L. & Yi, C.-X. Microglia energy metabolism in metabolic disorder. *Molecular and Cellular Endocrinology* **438**, 27–35 (2016).

71. Scholzen, T. E. *et al.* α-Melanocyte Stimulating Hormone Prevents Lipopolysaccharide-Induced Vasculitis by Down-Regulating Endothelial Cell Adhesion Molecule Expression. *Endocrinology* **144**, 360–370 (2003).

APPENDIX A

IMAGEJ MACRO FOR RANDOM FRACTIONATION

```
//Open ROI file with ROI selected from original cropping protocol. Original
        ROI needs to be present or the program will not work.

roiManager("Add")
roiManager("Select", 0);

run("Select None");

saveSettings();
original=getTitle();
setForegroundColor(255,0,0);
width = getWidth()-30;   // width of the randomly placed ROI
height = getHeight()-30; // height of the randomly placed ROI
RoisN =6; // number of ROIs
trials=100 ; //maximum trials to avoid infinite loop

i=0;
j=0;

xa=newArray(RoisN);
ya=newArray(RoisN);

run("Duplicate...", "title=Reference");

selectWindow("Reference");
 run("8-bit"); //makes it greyscale
 run("RGB Color"); //RGB to display colours
 run("Restore Selection");
 run("Make Inverse");
 run("Fill");
 run("Select None");

while (i<RoisN && j<trials){
      w = 350;
      h = 350;
      x = random()*width;
      y = random()*height;
      j++;
      //Check for pixels with value (255,0,0):
```

```
      flag= -1;
      makeRectangle(x, y, w, h);
      //Scanning the rectangle perimeter should be faster than scanning the
        whole box.
      //This is slower, as checks all the points in the box:
      for (xs=x;xs<x+w;xs++){
        for (ys=y;ys<y+h;ys++){
          if (getPixel(xs,ys)==-65536) // pixel is (255,0,0)
            flag=0;
        }
      }
      if (flag==-1){
        xa[i]=x;
        ya[i]=y;
        run("Fill");
        i++;
      }
  }

  close();
  selectWindow(original);
  setForegroundColor(255,255,0);
  for (j=0;j<i;j++){
    makeRectangle(xa[j], ya[j], w, h);
     roiManager("Add");
  }
 restoreSettings();
 run("Select None");

roiManager("Set Color", "cyan");
roiManager("Set Line Width", 3);
run("Flatten");

roiManager("Select", newArray(0,1,2,3,4,5,6));
roiManager("Delete");

myDir = _____
saveAs("tiff", myDir+ "CA1-ROIs" + File.separator + "ROI_" + getTitle);


run("Close");
run("Close");
```